IN VITRO ASSEMBLY OF AN INFECTIOUS cDNA CLONE OF INFECTIOUS BRONCHITIS VIRUS AND ITS APPLICATION AS A GENE TRANSFER VECTOR

A Dissertation

by

SOONJEON YOUN

Submitted to the Office of Graduate Studies of
Texas A&M University
in partial fulfillment of the requirements for the degree of

DOCTOR OF PHILOSOPHY

December 2003

Major Subject: Veterinary Microbiology

IN VITRO ASSEMBLY OF AN INFECTIOUS cDNA CLONE OF INFECTIOUS BRONCHITIS VIRUS AND ITS APPLICATION AS A GENE TRANSFER VECTOR

A Dissertation

by

SOONJEON YOUN

Submitted to Texas A&M University
in partial fulfillment of the requirements
for the degree of

DOCTOR OF PHILOSOPHY

Approved as to style and content by:

Ellen W. Collisson (Chair of Committee)	Julian Leibowitz (Member)
Judith M. Ball (Member)	Karen-Beth Scholthof (Member)
	Ann Kier (Head of Department)

December 2003

Major Subject: Veterinary Microbiology

ABSTRACT

In vitro Assembly of an Infectious cDNA Clone of Infectious Bronchitis Virus and Its Application as a Gene Transfer Vector. (December 2003)

Soonjeon Youn, B.S.; M.S.; D. V. M., Konkuk University

Chair of Advisory Committee: Dr. Ellen W. Collisson

An infectious cDNA clone of Vero cell adapted Beaudette strain of IBV was constructed using *in vitro* assembly of cDNA fragments. The entire genome of IBV was RT-PCR amplified into seven fragments, with each piece overlapping about 10 nucleotides. The fragments were ligated and transcribed to synthesize RNA, which was transfected into BHK-21 cells. These cells were then overlaid onto IBV susceptible Vero cells. After five days transfection, the virus was successfully rescued from the transfected cells. The cDNA clone from our laboratory strain has a five nucleotide insertion not present in the originally sequenced virus, resulting in total genome size of 27,613 nucleotides. The infectious cDNA clone was further manipulated to demonstrate its potential as a gene transfer vector, by replacing the ORF5a open reading frame with enhanced green fluorescent protein. The recombinant infectious cDNA clone was also successfully rescued after three days transfection of BHK-21 cells followed by co-culturing with Vero cells. This study showed that the 5a protein, whose function is not known, is not necessary for *in vitro* IBV replication. This study also showed that the 5a ORF is a good candidate for an insertion site of recombinant genes for the development of IBV infectious cDNA clone as a gene transfer vector.

ACKNOWLEDGEMENTS

I thank Dr. Ellen W. Collisson for her trust and enthusiasm toward my study. I also appreciate her giving me the wonderful opportunity to work with her at Texas A&M University.

I thank Dr. Ann Kier for her financial support that helped me to complete my study in department of Veterinary Pathobiology in Texas A&M University.

I thank Dr. Julian Leibowitz for his guidance, encouragement and advice.

I thank Dr. Karen Scholthof for her encouragement and careful proofreading of this dissertation.

I thank Dr. Tres Camacho for his constant encouragement, inspiration, patience and tremendous help with my English.

I thank Jyothi Jayaram for her help with my English and friendship.

I thank Tootie Youn for her patience and being such good company during hard times.

TABLE OF CONTENTS

CHAPTER Page

LIST OF TABLES

LIST OF FIGURES

FIGURE Page

CHAPTER I

INTRODUCTION

INFECTIOUS BRONCHITIS

Avian infectious bronchitis is one of the most important poultry diseases in the world, causing great economic losses to the poultry industry (39). It is also considered the most common disease in both broilers and layers. Its causative agent is infectious bronchitis virus (IBV). IBV was first described in 1931 by Schalk and Hawn in North Dakota as an "apparently new respiratory disease of baby chicks" (158) and then subsequently isolated by Beaudette and Hudson in 1937 (14). Initially IBV caused respiratory disease in chickens but later additional types of IBV emerged. IBV can be divided into three different forms based on the primary symptoms in infected birds. The respiratory form of IBV primarily results in respiratory illness such as gasping, tracheal rales, coughing and nasal discharge (6). This form is caused by IBV strains that include Massachusetts, Arkansas, and Connecticut. Second is the nephropathogenic form of IBV, which causes not only respiratory illness but also causes nephritis by certain stains of IBV such as Gray, Holts, Australian T strain and PA/Wolg/98 (1, 208). Often the respiratory form is more severe in young chicks and the nephritic form is predominantly seen in older chicks up to 10 weeks of age. The third form of IBV is a reproductive form

---

This dissertation follows the format of Journal of Virology.

in which the virus directly affects the reproductive organs of birds such as ovaries and reproductive tracts (41). The reproductive form of IBV infection causes not only poor egg production in infected birds but also poor egg quality. The most economically detrimental consequences for the poultry industry of infection of IBV are poor egg quality and markedly poor growth in chicks that survive causing vast economic loss in the poultry industry (14). Chicks infected with IBV show varying mortality depending on strains of virus that infect flocks, illness ranges from asymptomatic infection to very high mortality with no lesions because of rapid disease progression (39). A problem in controlling of IBV is the increased susceptibility to bacterial infection, such as E. *coli* and this complication exacerbating chronic respiratory disease and airsacculitis (6).

The incubation time of the virus is dose dependent and ranges from 18 to 36 hours after transmission by inhalation. The virus is not vertically transmitted through eggs (39). In experimental infection studies, IBV can be isolated from the trachea, lungs, kidney, and bursa of chickens from 24 hr to the 7th day after aerosol exposure (76).

The control of IBV depends mainly on vaccination. However, concurrent infection of the flocks with more than one serotype and vaccine breaks by field strains differing from the vaccine have been reported. With live vaccines, it may be possible to prevent disease but not prevent infection (65, 87). Usually a vaccine regimen requires using an inactived IBV strain given as an oil-in-water emulsion to chickens that have already been primed by vaccination with a live attenuated IBV vaccine.

CLASSIFICATION

Avian infectious bronchitis virus is a member of the *Coronaviridae* family that belongs to the order of *Nidovirales*. Nidovirales contains four families, the *Toroviridae*, *Arteriviridae*, *Roniviridae* as well as *Coronaviridae* (34, 168). The classification is based on polycistronic genome organization and regulation of gene expression from a nested set of subgenomic mRNAs, despite significant size differences between genuses ranging from 13 to 32 kb. Coronaviruses, as well as the other nidoviruses, have a unique, discontinuous transcription strategy that produces several subgenomic mRNAs, as well as the genomic RNA packaged into its virions. The subgenomic mRNAs form 3' co-terminal nested sets in which each mRNA contains a common 3' untranslated region and 5' leader sequence (90).

Coronaviruses infect various animal species, causing respiratory, gastrointestinal, cardiovascular, and neurological disease (126). Human coronaviruses have been associated with mild common colds, diarrhea, possibly multiple sclerosis, as well as severe acute respiratory syndrome (SARS) (70). Coronaviruses have been divided into three distinct groups by antigenic cross-reactivity and sequence analysis of structural protein genes. Group I coronaviruses include human coronavirus 229E (HCoV-229E), transmissible gastroenteritis virus (TGEV), canine coronavirus (CCV), feline coronavirus (FECV), and feline infectious peritonitis virus (FIPV). Group II includes human coronavirus OC43 (HCoV-OC43), murine hepatitis virus (MHV), and bovine coronavirus (BoCV). Group III includes IBV with some turkey coronaviruses (TCV) and pheasant coronavirus. The recently identified coronavirus that is the causative agent of

severe acute respiratory syndrome (SARS) in humans is distinct from other coronaviruses based on its genomic organization and structural genes (186). However, there was a report that SARS is a Group II coronaviruses based on phylogenetic study comparing the replicase gene with other coronaviruses and torovirus (167).

MOLECULAR BIOLOGY OF CORONAVIRUS

Morphology

Coronavirus virions are pleomorphic in shape with a diameter of 80 to 160 nm and are composed of four major structural proteins, which include the nucleocapsid protein (N), the integral membrane protein (M), the spike protein (S) and the small envelope protein (E) (90). Petal-like spikes that appear as a corona give the virus its name and have a distinct morphology by electron microscopy (EM) (15). These prominent surface projections of up to 20 nm in length cover the entire virion surface (15). Some species of coronaviruses, such as TCV, have smaller spikes on the virion surface. The N proteins interact with viral genomic RNA to form helical ribonucleoprotein complexes (RNP) that are similar in morphology to paramyxovirus RNPs (49). Not only genomic RNA but also every subgenomic RNA interacts with N protein forming RNP in the infected cells. In the case of TGEV, an icosahedral core shell structure has been shown by EM (142). One report indicated that two different forms of IBV virions could be made in infected cells (119). One form is the infectious virus particle, which has viral RNP, the other form has a lower density and has no RNP. This finding is consistent with the observation

that co-expression of E and M protein produce virus like particles (VLPs) without internal virion structures (193).

Genome Organization

The genomes of the coronaviruses ranging from 27.6 to 32 kb are the largest genomes of all the known RNA viruses. Coronaviruses have a linear, positive sensed polyadenylated RNA that is infectious when transfected into susceptible cells (112, 161). In infected cells, coronaviruses produce from five to eight subgenomic RNAs in addition to genomic RNA depending on the virus (165). Each RNA is numbered according to its size. Genomic and subgenomic RNA organization of IBV is illustrated in Figure 1. IBV has six subgenomic RNAs including its genomic RNA with RNA 1 being the largest, and RNA 6 being the smallest (35). The genomic RNA, as well as every subgenomic RNA, is 5’ end capped and has a polyadenylated tail of about 100 nucleotides (nts) at the 3’ end (112, 113, 161, 196). Subgenomic RNAs range from 2 to 8 kb and with genomic RNA share a common 3’ terminus forming a nested set (172, 173). Genomic and subgenomic RNAs have 3’ and 5’ untranslated regions (UTR) believed to contain *cis*-signal sequences for viral replication and transcription (48). The 5’ end of each mRNA has leader sequence about 60 to 72 nts (91, 92, 171). Most coronavirus ORFs are preceded by an untranslated region of varying length containing a conserved sequence, which has been given the term intergenic sequence (IG) or transcription regulatory sequence (TRS) (28, 90).

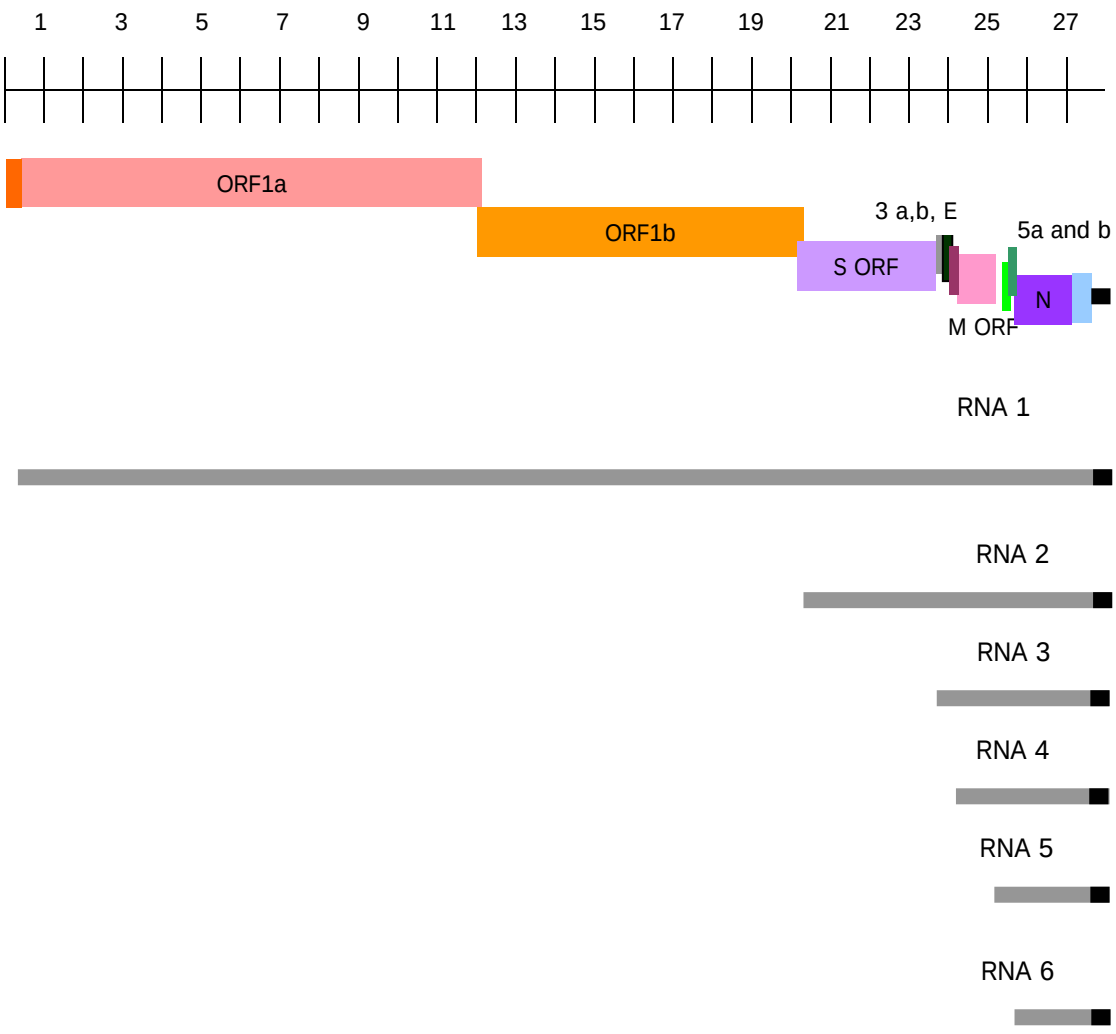

FIG. 1. Schematic of the IBV genomic and subgenomic RNA organization. S represents the spike glycoprotein; M, the membrane protein; E, the small envelope protein; N, the nucleocapsid protein. RNA1 encodes replicase gene, pp1a and pp1ab; RNA2 encodes S protein, RNA3 encodes 3a, 3b and the E proteins, RNA4 encodes the M protein, RNA5 encodes 5a and 5b whose functions are not known and RNA6 encodes the N protein. The black box represents poly (A) tails.

The overall IBV genome organization is similar to other prototype coronaviruses such as MHV and TGEV, having the “replicase gene-S-E-M-N” gene order. ORFs encoding small nonstructural group specific proteins, such as 3a, b and 5a, b of IBV lie between the structural genes (103). Comparisons of the different genomic organizations of coronaviruses are illustrated in Figure 2. However, with a smaller genome size of 27.6 kb compare to other coronaviruses, such as MHV with a genome of 31 kb, IBV genomic usage is more compact. ORFs of IBV are overlapped. For example, the 3’ end of the 1b genome overlaps with the S ORF by about 50 nts (30).

IBV RNA 1, which encodes the replicase gene, is indistinguishable from genomic RNA and contains the ORF for replicase genes, pp1a and pp1ab, and ORFs for the structural proteins. Like most coronaviruses, every subgenomic RNA of IBV only expresses the extreme 5’ ORF except for RNA 3 and RNA 5, which encode 3a, 3b, 3c (E), 5a and 5b ORFs respectively. IBV has several nonstructural proteins of which functions are not well understood. The exception is gene 3c, which encodes an important structural membrane protein, E protein (104, 203). Two thirds of RNA 1, about 20 kb, of IBV genome encoding two large ORF1a and 1b, that express polyproteins of pp1a, 441 kDa and pp1b, 300 kDa, respectively. pp1ab is produced via -1 ribosomal frame shifting upstream of a psuedoknot structure between ORF1a and ORF1b (25, 26). Polyproteins encoded by gene 1 are cleaved by viral proteinases during posttranslational processing (57).

RNA 2 encodes the spike (S) protein of IBV. As mentioned previously, the 3’ end of 1b ORF overlaps with the ORF of S by about 50 nts in the Beaudette strain. It is

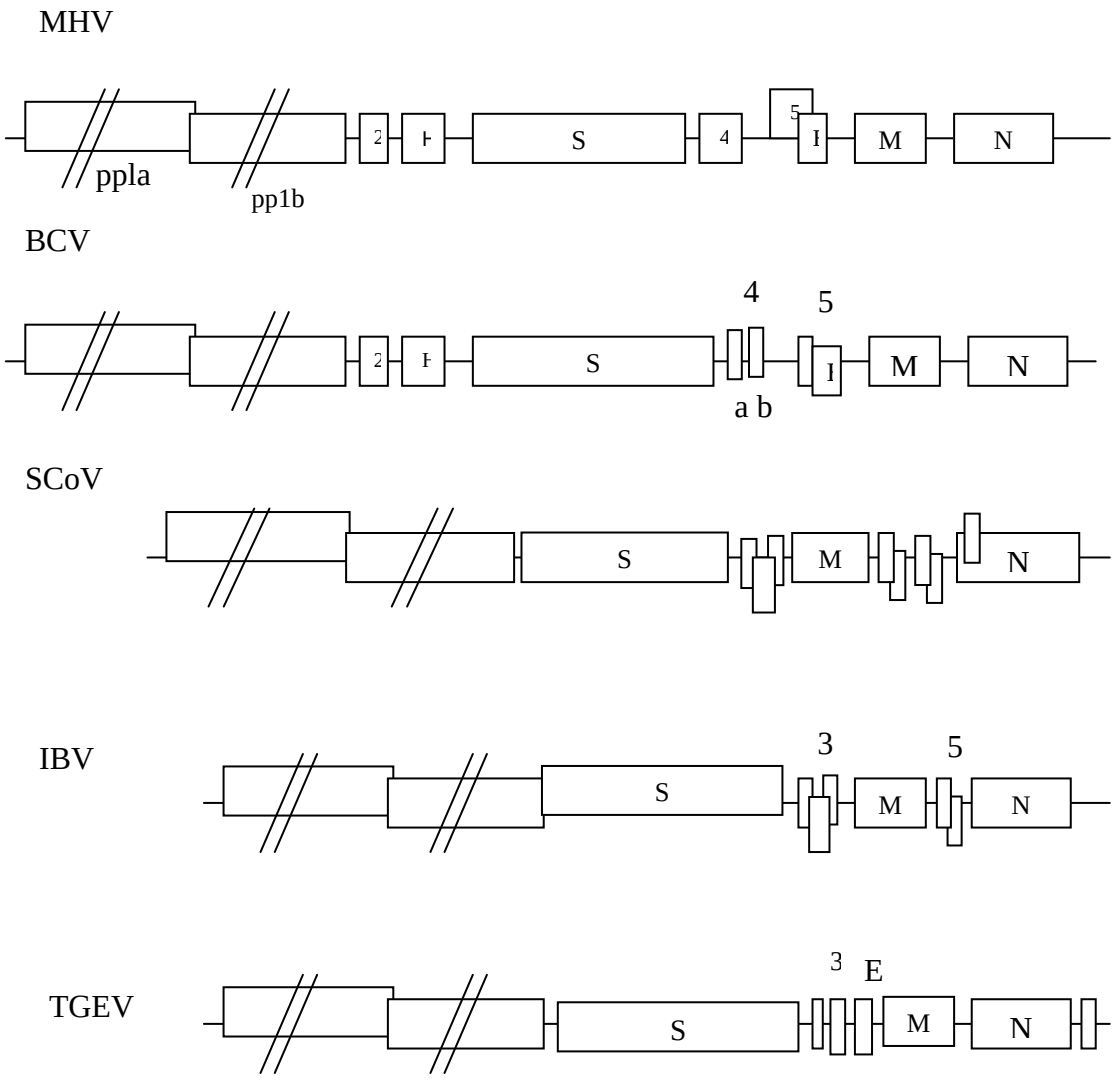

FIG 2. Comparison of genome organization of coronaviruses. ORF1a and ORF1b are interrupted and shortened to highlight the remaining genes. Boxes represent ORFs.

not certain if this is a common feature of IBV. RNA 3 encodes three ORFs, 3a, 3b, and 3c. Nucleotide sequencing and expression studies indicated that gene 3 was tricistronic and that ORF3a and 3b produced proteins in small amounts in IBV infected cells (103), but their functions are a subject of further study. The ORF3c encodes the small envelope protein (103, 104). An unusual folding region (UFR) of 265 nts containing the 3a and 3b coding region upstream of the E ORFs was noticed (95). This UFR consists of five RNA stem-loops that could be modeled into a superstructure by the interaction of two putative pseudoknots. It was predicted that this region could serve as an internal ribosomal entry site (IRES) for the cap independent expression of E protein. RNA 4 of IBV encodes M protein. Just as RNA 3 is multicistronic, nucleotide sequencing and expression studies showed that RNA 5 is dicistronic and encodes two nonstructural proteins, 5a and 5b. Expression of these two proteins has been shown in IBV infected cells, but the function of these proteins and mechanism of expression also needs to be determined (105). RNA6, the smallest but the most abundant RNA in IBV infected cells encodes the N proteins.

Coronavirus Non-Structural Proteins

RNA 1 encodes the coronavirus replicase gene. The schematic of genomic RNA organization of coronaviruses is illustrated in Figure 3. The replicase genes of coronaviruses consist of two large open reading frames, ORF1a and ORF1b, the latter of which is expressed by ribosomal frame shifting (26). The ORF1a and ORF1ab translation products are large nonstructural polyproteins encoding polyproteins pp1a and

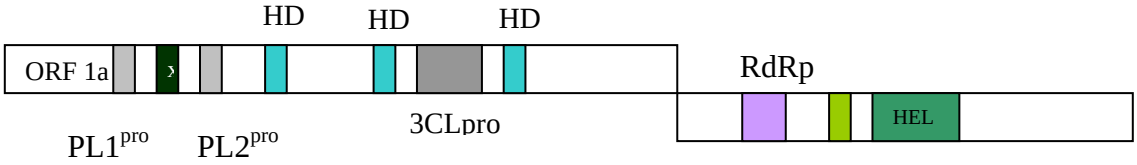

FIG. 3. Schematic of coronavirus gene 1 organization. PL1 ^{pro} represents a papain-like proteinase 1; PL2 ^{pro}, a papain-like proteinase 2; 3CL^{pro}, a 3C-like proteinase; MP1 and MP2 represent the hydrophobic domains; RdRp, RNA-dependent RNA polymerase; HEL, helicase and the black box indicates a domain with an unknown function in coronaviruses. The small green box between RdRp and HEL represent a cysteine-rich domain. IBV and SCoV have only one PL2 ^{pro} domain instead of two PL ^{pro}.

pp1ab, respectively. Polyprotein precursors of the nidovirus ORF1a and ORF1ab translation products are cleaved by viral proteinases at a minimum of 13 sites (207). ORF1b encodes RNA dependent RNA polymerase (RdRp), helicase (HEL) and methyltransferase (56). Functions of the ORF1a-encoded polyproteins include proteinases that process viral nonstructural proteins and proteins that are membrane associated (100-102, 133). Most nidovirus replicase subunits are thought to assemble into an RNA-protein complex, which is presumably held together by protein-protein and /or protein-RNA interactions. Some of replicase genes have been shown to co-localize with viral RNA (19, 20, 133, 159, 164, 192). Putative hydrophobic domains in the ORF1a protein have been proposed to mediate the membrane association of this complex (19, 164). The N terminal half of the ORF1a protein encodes multiple papain-like cysteine protease domains (PL^{pro}). The proteolytic activity of PL^{pro} has been demonstrated and characterized in detail (73, 97, 99, 207). Compared to group I and group II coronaviruses that encode two PL^{pro}, IBV has two overlapping PL^{pro} and only the first PL^{pro} is functional. SARS also encodes only one $PL2^{pro}$ (97, 186). Another functional coronaviral proteinase, the 3C-like cysteine protease ($3CL^{pro}$) is located in the central region of the ORF 1a polyprotein (114). This $3CL^{pro}$ belongs to the chymotrypsin-like protease superfamily and is flanked by hydrophobic domains (207). Proteolytic activity of the protein has been demonstrated and characterized in detail in MHV, HCoV and IBV (69, 74, 115, 206). Several studies have shown that this proteinase cleaves pp1ab fusion polyprotein at the QS dipeptide bonds to the 100-kDa protein species in IBV (101, 102, 107).

Compared to other positive strand RNA viruses, distinct features of a coronavirus replicase include a helicase domain downstream of the RdRp motif in ORF1b and the classic GDD core motif in the RdRp is substituted by an SDD (68). In addition, compared to a putative catalytic triad, such as cysteine, histidine and glutamic acid, for the proteinase activity, cysteine and histidine are sufficient enough for coronavirus $3CL^{pro}$ protease activity (102).

Coronavirus Structural Proteins

Coronaviruses have four essential structural proteins. These include spike glycoprotein (S), small envelope protein (E), integral membrane protein (M), and nucleocapsid protein (N). In addition to these elements, some strains of group I and II coronaviruses have an additional glycoprotein, the hemagglutinin/esterase (HE) protein which is assumed to be acquired from influenza virus C and is not essential for viral replication *in vivo* or *in vitro* (4, 16, 37, 119).

The S protein is the most prominent virion protein that can be seen by EM, forming a corona around the virions. This type I glycoprotein passes through the host derived lipid bilayer membrane once, with most of the molecule forming an amino-terminal ectodomain (18). The S protein can be divided into three different parts other than the signal sequence that targets the proteins to the ER (117). The first part is the ectodomain of S, which is largely exposed outer surface of the virion. The second part is the transmembrane domain (TM), which consists of hydrophobic amino acids that are embedded in the virus envelope. The third part of the S protein is the endodomain that

has a C terminal tail inside of the virions. The TM and endodomain are believed to confer the stability of the S proteins on the virion.

S proteins form homotrimers (33) and are co-translationally N-glycosylated, after which the carbohydrates are processed in the endoplasmic reticulum and in the Golgi apparatus (55, 134). The majority of the S protein in virus-infected cells localizes in the ER and Golgi intermediate compartment (ERGIC) but when the S protein is expressed by itself, it is transported to the plasma membrane. This implies that some other viral protein interacts with S protein and localizes to the budding sites. In addition, an excess amount of S protein expressed in infected cells is transported to the plasma membrane inducing cell-cell fusion of neighboring cells thus promoting virus spreading.

Newly synthesized proglycoprotein S is cleaved by carboxypeptidase-like activity *in vivo* or by trypsin *in vitro* into S1, the N-terminal product and S2, the C-terminal product. The cleavage site lies near the center of the protein at a cluster of basic amino acids (37). This cleavage has been shown to be required for the activation of viral infectivity and cell fusion in MHV {Sturman, 1985 #136, 181). IBV-Beaudette S1 and S2 are comprised of 514 amino acid residues (56.2 kDa), and 625 amino acid residues (69.2 kDa), respectively. The amino acid cleavage sites of IBV and MHV S1 and S2 were identified by partial amino terminal sequencing of spike polypeptide, S2, which was identified as RRFRR for IBV and RRAR(H)R for MHV (37, 117).

However, in the case of FIPV, TGEV and likely SARS, the S protein dose not have a cleavage site (78). Major neutralization epitopes, which determine the serotypes of IBV, map to the S1 protein (36). This protein interacts with cellular receptors, whereas the S2

is responsible for anchoring S1 into the viral envelope and for cell membrane fusion. Cellular receptors for several coronaviruses have been identified. Two cellular receptors have been identified for MHV. MHVRI and MHVR2, which are translated from the same mRNA through alternate splicing and are expressed in different tissues (46) (58).

Integral membrane glycoprotein (M) is the most abundant envelope glycoprotein of coronaviruses (152). It is composed of 225 amino acids in IBV. Its predicted molecular weight, based on amino acid sequence data is about 25 kDa. However, the actual molecular weight in infected cells is about 30 kDa. M protein expressed in infected cells or expressed from cDNA transcripts has several isotypes. The MHV has five different isotypes that can be distinguished electrophoretically ranging from M_0 to M_5 (83, 150, 191. This molecular weight discrepancy is based on different glycosylation of the M protein depending on the location of the protein in different intracellular compartments {Locker, 1992 #332)(106). M proteins of coronaviruses also differ in glycosylation and localization. MHV has O-linked glycosylation and targets to the *trans*-Golgi apparatus (110, 135, 178) whereas IBV has N linked glycosylation (32, 108) and targets to *cis*-Golgi (118).

The M protein spans the membrane bilayer three times, having a short glycosylated amino terminal domain on the exterior of the virus and a large carboxyl terminus, containing more than half the mass of the molecule, in the virion interior (5, 111, 151). In contrast to other viral glycoproteins, M protein doesn't have a signal sequence at its N terminal but has internal signal sequence in the membrane-spanning hydrophobic regions (148). In IBV, the first transmembrane domain appears to be sufficient for

retention of the protein in the Golgi (182), whereas the cytoplasmic tail and at least one transmembrane domain of the MHV-M protein are necessary for viral retention at the *trans*-Golgi (109).

The M protein is an important viral structural protein. Its interaction with S protein is important for the incorporation of S protein into a virus particle. S protein can be expressed on plasma membranes without the presence of M protein expression, however if the S protein is co-expressed with M protein, it localizes to the ER-Golgi intermediate compartment which is suggested as a virus budding site (118, 149) (189). M and S protein interaction in MHV has been shown (137). Transmembrane domains and amphipathic domains of the M protein are necessary for interaction with S in MHV (52). Targeted mutagenesis of MHV and FIPV has shown that without the proper TM and endodomain of the S protein, the ectodomain of different species S protein cannot be incorporated into virus particles (53, 66). This study suggested that TM and endodomain of the S protein might interact with the M protein. The M protein is also important for virus budding and assembly with E protein. The M protein has been shown to have an affinity for RNA even though the domain of M that interacts with the RNA or RNP is not known (179). Recently, Narayanan et al. (128) suggested that M protein provides the specificity of viral genomic RNA packaging by interacting directly with the packaging signal sequence of MHV genomic RNA. Monoclonal antibodies specific for the M protein do not neutralize virus infectivity, suggesting that M protein is not involved in virus attachment to receptors.

The third glycoprotein on the virion surface is HE. It is present in BCV, TCV, HCoV, and some strains of MHV, but is not present in IBV or TGEV. It is also an N-linked glycoprotein. This glycoprotein shares some sequence homology with the hemagglutinin protein of influenza C virus, and it is proposed that HE protein of these coronaviruses is derived from the influenza virus by non-homologous recombination (116). HE protein of BCV exhibits hemagglutinin and esterase activity and some strains of MHV also show esterase activity. Monoclonal antibodies specific for the HE protein of BoCV can inhibit virus-induced hemagglutination and neutralize viral infectivity implying that at least in BoCV, HE is involved with S protein for viral attachment.

The E protein was recently recognized as a structural protein (104, 203). This protein in IBV is comprised of 108 amino acids are about 10 kDa molecular weight. In contrast to other coronavirus structural proteins, E protein is expressed by cap-independent translation from an IRES which is located in the ORF3a and 3b regions or in the 5a region in MHV (106, 188). E protein localizes in the perinuclear region with a small amount migrating to the cell surface (203). The E protein is anchored in the membrane by a sequence in the N-terminal half of the protein and is largely embedded within the viral membrane with only a hydrophilic C-terminus protruding inside the virion (121).

Co-expression of E and M proteins produces virus like particles (VLP) without viral RNP. However, expression of the E proteins of MHV or IBV produces vesicles that can be released from the cells in the absence of other viral proteins (47, 120). Co-expression of M and E are necessary in TGEV and bovine coronavirus (BoCV) to make virus-like particles (VLP) (13, 17, 193). E protein has been suggested to “pinch off the neck” of the

assembled virus particle from cells during the final stages of budding (193), implying that an E protein is essential for VLP formation in every coronavirus. However, Kuo et al. (85) has shown that an E deletion mutant of MHV is still viable, although it grow poorly and with delayed kinetics. The exact role of E protein in the virus assembly process and budding is not yet clear. Direct interaction between the E and M proteins has not been demonstrated. It is possible that such an interaction would serve to facilitate the budding of virus particles.

The N protein is the only phosphorylated structural protein in the coronavirus (198). N protein is composed of 409 amino acids having a molecular weight of about 50 kDa in IBV (22). Coronavirus nucleocapsid sequences vary among major antigenic groups but are highly conserved within groups (199). The N protein has basic residues that occur in clusters depending on the virus, serine residues account for 8 to 10% of the total amino acids in N proteins and the abundance of serine residues count for the specific phosphorylation on serine residues in MHV (170).

N protein is considered a multifunctional protein playing important roles not only as a structural protein but also as a protein involved in viral replication and transcription. N protein interacts with viral genomic RNA forming a helical nucleocapsid (RNP) and interacts with subgenomic RNAs in the cytoplasm. MHV N protein has been shown to interact specifically with the 5’ leader containing sequences (10). MHV and IBV-N proteins can be divided into three structural domains. The middle domain is an RNA-binding domain that binds to both coronavirus and non-coronavirus RNA sequences *in vitro* in MHV (125, 130). However, there is no known RNA binding motif in

coronavirus N protein. In the case of IBV, C terminal and N terminal regions of N protein but not the middle region interact with the 3' end of the non-coding region of IBV genomic RNA (43, 205). Antiserum raised against N protein inhibited the synthesis of the genome-sized RNA by 90% in an *in vitro* replication system implying N protein is involved in transcription or/and translation of the viral genome (45). Several reports implied that the phosphorylation status of the N protein might be involved in the control of viral transcription and replication.

REPLICATION OF CORONAVIRUSES

Coronaviruses replicate in the cytoplasm of infected cells, preferentially in epithelial cells. It has been shown that the MHV can replicate inside the enucleated cell implying that the host nucleus and/or nuclear factors are not involved in virus replication. However, studies with IBV and a human coronavirus have shown that the replication of these viruses is hindered by α-amanitin treatment or in enucleated cells (61). This suggests that maybe some host nuclear factor(s) are involved in virus replication, at least for IBV and HCoV. Coronavirus replication does not completely shut down the cell replication cycle and continuous host translation is necessary for viral replication (154). The replication complex of coronaviruses has been described to be associated with late endosomal membranes by colocalization of viral replicase and newly synthesized RNA with a late endosomal marker by immunofluorescence assay (IFA) and electron microscopy (EM) (166, 192). This replication complex translocates to the virus budding site, ERGIC, at late times post infection (20).

Coronavirus replication also needs continuous viral protein translation and N protein (45). Inhibitors of protein synthesis, such as cycloheximide, inhibit RNA synthesis (122). Dependency of RNA synthesis on protein synthesis continues throughout the viral replication cycle. The RNA polymerase or some cofactors have to be continuously synthesized. Negative-stranded and positive-stranded coronavirus RNA synthesis have different sensitivities to inhibition by cycloheximide (154), implying that the negative and positive-stranded RNAs are likely synthesized by two different polymerase activities. Two enzymatically distinct RdRp activities, one acting early and the other during late infection, have been described (24) even though there are some inconsistencies between studies (45, 122).

Coronaviruses employ several different strategies to translate their structural or non-structural proteins in infected cells. First, several subgenomic RNAs are produced that are functionally monocistronic, expressing only the extreme 5' ORF. Second, it exploits ribosomal frameshifting and post-translational cleavage of polyproteins. Finally, an IRES is used to translate proteins in a cap-independent manner from polycistronic ORFs.

Attachment and Penetration

Attachment and penetration are complex processes that have not been characterized in detail for most coronaviruses. The virion binds to the cell membrane receptors by either the S or HE glycoproteins (42). IBV entry into susceptible cells occurs at both at 4°C and 37°C (138). Conformational changes in either of the viral proteins S or HE may be induced by virus binding to the cellular receptor and lead to

fusion of the virus envelope with host cell membranes (46). MHV-A59-induced fusion is optimal at neutral or mildly alkaline pH (180). Other coronaviruses, such as HCV-229E, IBV or some strains of MHV do not fuse at neutral pH and the fusion occurs in endosomal membranes rather than the plasma membrane (64). Coronaviruses generally are highly species specific *in vivo* and *in vitro*. The species specificity appears to be mediated at the site of entry, since MHV genomic RNA is infectious and MHV replicates efficiently in nonpermissive hosts that express the MHV receptor. In addition, a recombinant FIPV with the MHV S protein can replicate in murine cell lines (71). Receptors for the MHV virus have been identified. MHV receptor (MHVR) is a member of the carcinoembryonic antigen-cell adhesion molecule (CEACAMs) family of glycoproteins (200). Subsequently, MHVR (2d) was found as a splice variant of MHVR (4d) (58). Membrane expression of this molecule renders MHV resistant cells, such as human and hamster cells, susceptible to MHV infection (58, 59). Aminopetidase N (APN), a membrane bound metalloprotease, has been identified as a receptor for TGEV and HCV-229E. In humans, hAPN is also known as CD13 (54). TGEV and HCV-229E both utilize only species-specific APN glycoproteins as receptors. This indicates that not only the attachment to receptors, but also possibly some other host factor(s) are involved in host specific virus infection (45). Several studies implicate the involvement of HE protein in virus attachment in MHV and even more so in BCV. However, these studies need to be expanded. After virion attachment onto its cellular receptor, virus will be internalized and targeted to the cellular organelles where the virus will replicate. Mechanisms of replication are not yet well studied in coronavirus.

Viral Transcription

Similar to most positive stranded RNA viruses, after the release of the genomic viral RNA into host cells, replication begins with the viral RNA serving as the messenger for RdRp synthesis. The polymerase transcribes the genomic RNA into a negative stranded full length RNA and the negative stranded subgenomic RNA serve as templates for the synthesis of subgenomic and genomic RNAs (93). The presence of multiple subgenomic mRNAs is a characteristic feature of coronaviruses. Depending on the coronavirus, five to eight subgenomic RNAs are transcribed in infected cells. They have 5' and 3' untranslated regions (UTR) and a poly(A) tail of about 100 nts. The extreme of 5' end of each subgenomic RNA has a stretch of 65-98 nucleotides, referred to as the leader sequence. The leader sequence is identical to the sequence at the 5' end of the genomic RNA and is not found elsewhere in the genome (89, 91). However, the sequences between each gene, termed the intergenic sequences (IG) or transcription regulatory sequence (TRS), have a sequence homology of 7 to 18 nucleotides with the 3' end of the leader sequence (28). The core sequence of the IG sequence for MHV is AAUCUAAAC, whereas the 3' end of the leader consists of several tandem repeats of UCUAA (88). The consensus sequence for IBV is CU(U/G)AACAA, AUCUAAAC is the consensus sequence for BoCV, and AACUAAAC is the consensus sequence for FIPV and TGEV (170). Because of the characteristics of coronavirus transcription that produces subgenomic RNAs, and function of leader sequences, several models have been proposed to explain the generation of subgenomic RNAs for coronavirus mRNA transcription. Two facts exclude splicing as the mechanism to produce subgenomic

RNA. First, in ultraviolet (UV) transcriptional mapping studies, the UV target size of each mRNA is equivalent to its physical size, indicating that each mRNA is transcribed independently, and is not derived from the process of a large precursor RNA (79, 174). Second, because coronaviruses replicate solely in the cytoplasm, the possibility of splicing as a mechanism for coronavirus transcription mechanism is excluded.

One coronavirus transcription model is the leader-primed model. This model is illustrated in Figure 4. According to this model, discontinuous transcription occurs during positive stranded RNA synthesis. Leader RNAs are transcribed at the 3' end of the negative stranded RNA template, before dissociating from the template, and subsequently binding to any IG or TRS on the negative stranded template. The leader RNA serves as the primer for subgenomic RNA transcription, resulting in a subgenomic RNA that contains a leader RNA fused to the mRNA. This model is based on the presence of free leaders in infected cells. Several small leader sequence-related RNA species have been detected in the cytoplasm of MHV-infected cells (11). These leader RNAs are distinct in size and reproducible in different cell types. However, most of these leader RNAs are either larger or smaller than the leader sequence present at the 5' end of the mRNAs, implying that additional processing of these leader RNAs may occur during mRNA transcription. A temperature-sensitive (ts) mutant has been isolated that synthesizes only the small leader-related RNAs, but not mRNAs, at the nonpermissive

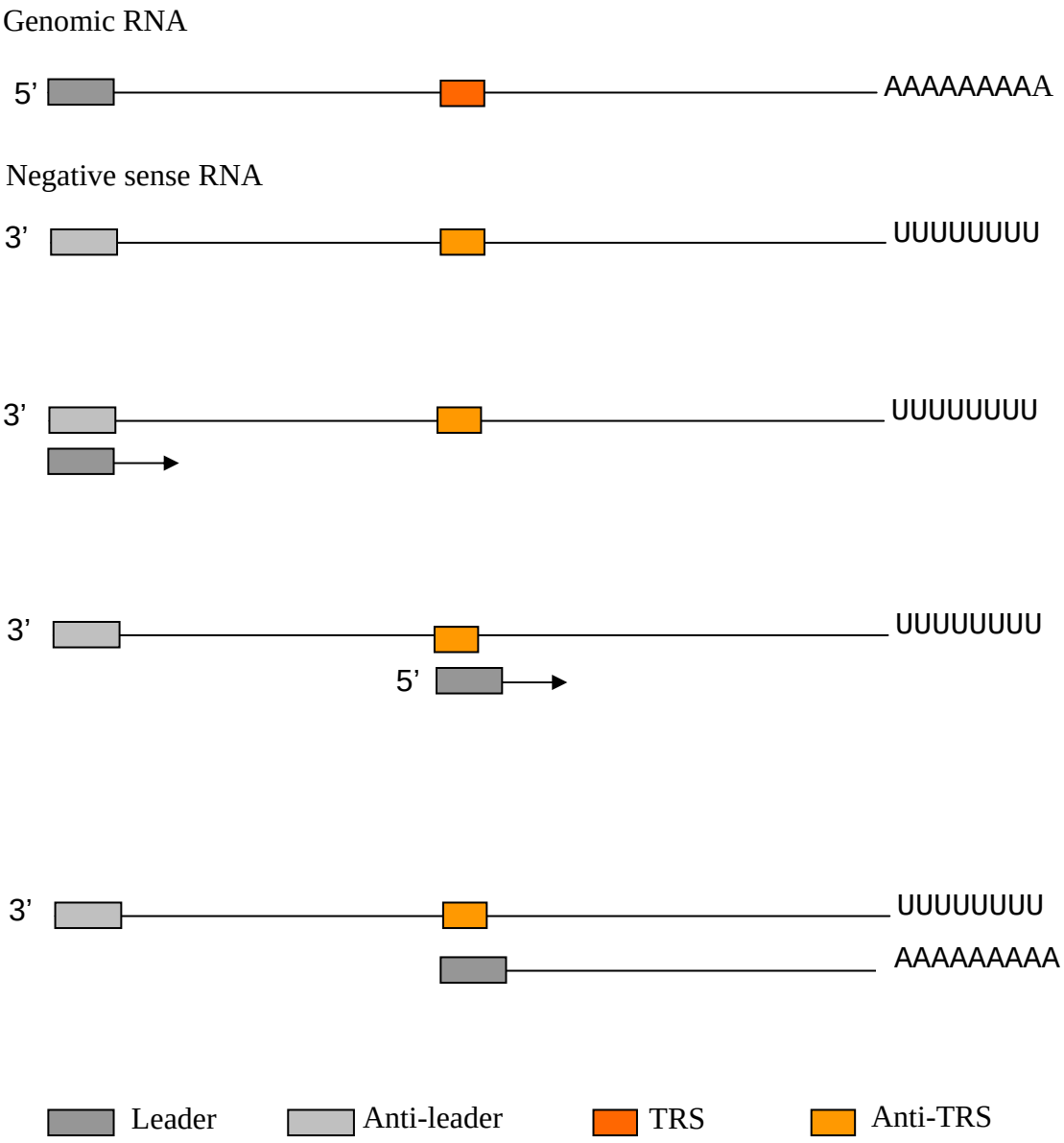

FIG. 4. The leader-primed model of coronavirus transcription

temperature (11). Thus, the possibility that the synthesis of the leader RNA and mRNAs are two separate and discontinuous events is supported by *in vivo* and *in vitro* studies. When different strains of MHV were coinfected into cells or exogenous leader RNA was introduced into virus infected cells, heterologous MHV leader sequence was incorporated *in trans* into subgenomic mRNAs at the precise leader-mRNA junction sites (7). As mentioned before, seven nucleotides are conserved in the TRS in most coronaviruses.

The second model is the discontinuous extension of negative strand transcription (156). This model is illustrated in Figure 5. Discontinuous transcription could potentially occur during negative-strand RNA synthesis. During negative strand RNA synthesis from the full-length genomic RNA template, RdRp pauses at one of the IG or TRS sequences and then jumps to the 3' end of the leader sequence in the genomic RNA template, generating a subgenomic negative strand RNA with an antisense leader sequence at its 3' end. This subgenomic negative strand RNA then serves as a template for synthesis of mRNAs. Several studies have shown that both genomic and subgenomic sized negative stranded RNAs are present even though positive strand RNA is present at a higher amount (12, 155, 157, 162). All the negative strand RNAs were in double-stranded form and no free negative stranded RNA was detected.

Coronavirus RNA synthesis takes place on membranous structures associated with late endosomes. Colocalization of newly synthesized viral RNA and most of the gene 1 products have been shown. N protein involvement in RNA transcription has been suggested because antibody against N protein inhibits MHV RNA synthesis *in vitro*.

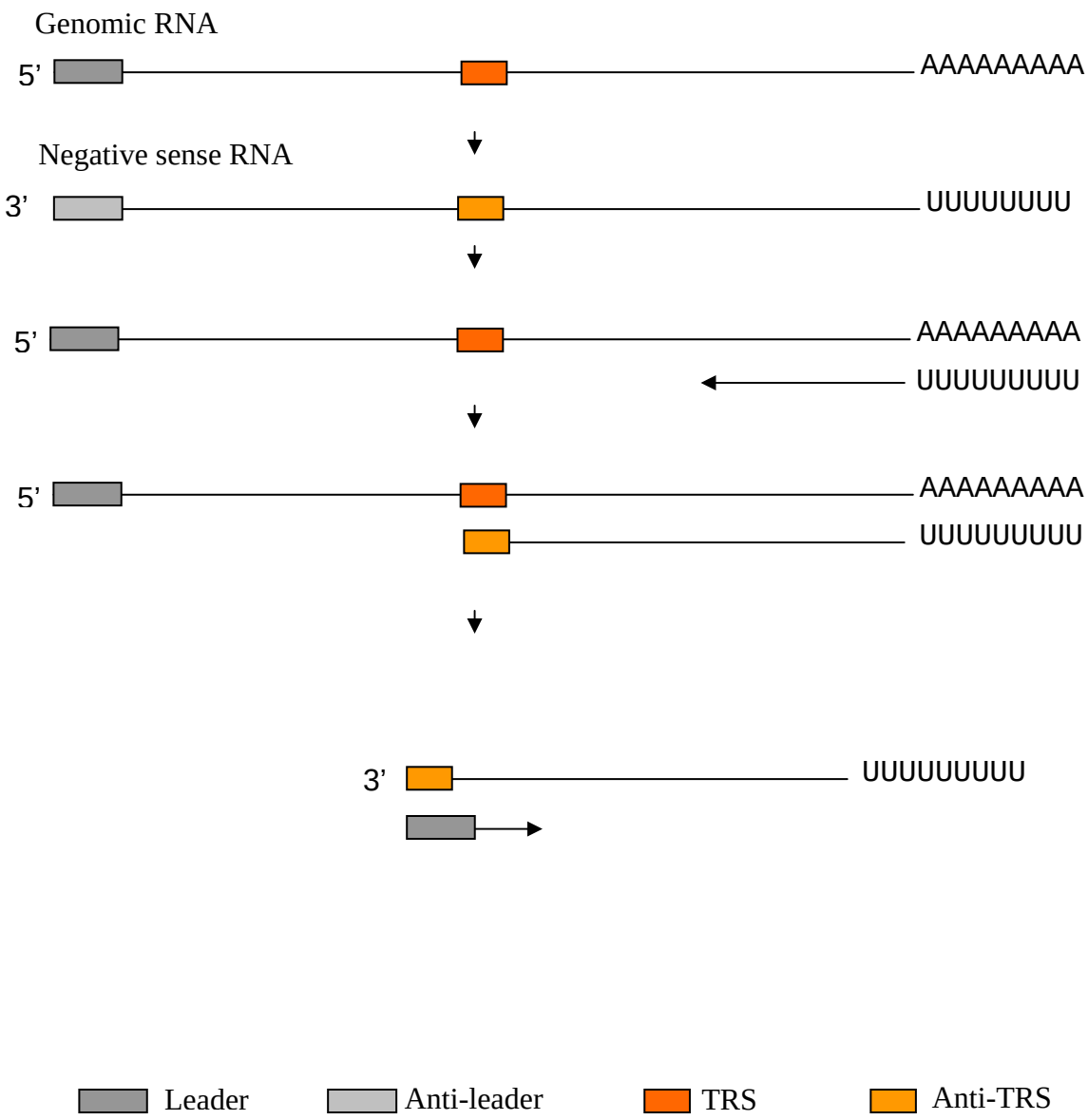

FIG. 5. Discontinuous extension of negative strands model of transcription

Recombination

One of unique features of coronaviruses is the high frequency of RNA recombination (123). The high rate of recombination in coronaviruses has been demonstrated not only experimentally in mixed infections, but also in infected animals and in natural infection (82, 86). A calculation of recombination frequencies suggests that the entire genome of MHV will have a recombination frequency of roughly 25% (9). The recombination frequency is so high that no selection pressure was needed for the isolation of recombinants (82, 123). The possible sites of recombination between different MHV strains appear to be distributed over the entire genome, even though a recombination hot spot was identified near a hypervariable region in MHV and IBV (8, 195). The high frequency of coronavirus recombination is probably caused by the nonprocessive nature of the coronavirus RNA polymerase. Coronavirus replication of the genome, except for the leader sequence, may proceed in a discontinuous and nonprocessive manner (11). RNA synthesis pauses at sites of extensive secondary structure of the RNA template and the incomplete RNA products dissociate from the template because of a nonprocessive nature of the coronavirus RNA polymerase. These dissociated RNA products then rebind to the RNA template to continue RNA synthesis (96).

Viral Assembly

The genomic RNA synthesis and encapsidation are coupled in MHV-infected cells. Because encapsidation requires N proteins, the accumulation of the N protein

could possibly tip the balance of RNA synthesis from transcription towards RNA replication. The binding of the N protein to RNA has been shown *in vitro* for many coronaviruses (10, 176). The encapsidation by N proteins is necessary, but not sufficient for RNA packaging into mature virions. The N protein binding to viral RNA could be a regulatory mechanism of RNA synthesis rather than a virion assembly process. Without viral infection, coexpression of the M, E, and S proteins results in the assembly of coronavirus-like particles that are released from cells (17, 193). The VLPs produced in this manner form a homogeneous population that is morphologically indistinguishable from normal virions. Thus, coronavirus virion assembly does not require the participation of the nucleocapsid, defining a new mode of virion budding. In addition, the reverse genetic approach was used to show that S protein is also dispensable in the viral assembly, only the M and E proteins without RNP are required for VLP. It has been suggested that in MHV, N protein interacts with viral genomic RNA producing helical nucleocapsids and then the M protein and packaging signal sequence of genomic RNA interact to confer specificity on packaging of the viral genomic RNA into the virion (128).

S protein and M protein interactions are important for assembly to produce infectious virus that can function in the virus and receptor interaction. Assembly of S protein into the coronavirus envelope is governed by the M and S protein interaction. S protein is expressed on the plasma membranes without M protein, but when it is co-expressed with M protein, it is localized in the ER-Golgi intermediate compartment, also known as *cis*-Golgi, where the virus obtains its lipid bilayer as it buds (83). The carboxyl-

terminal domain of the S, that includes the S transmembrane domain and an endodomain of 64 residues, is sufficient to interact with the M protein and draw the mature S protein into particles (66).

Coronaviruses are assembled at perinuclear membranes by budding into the ER-Golgi intermediate compartment. From there, the particles are transported in vesicles through the secretory pathway to the plasma membrane domain where they are released by exocytosis (190). TGEV enters and is released apically (146). MHV-A59 enters apically but is released both apically and basolaterally depending on the cell line (145, 147). HCoV-22E also infects the apical surface and is released apically (194). It is believed that polarity of the viral release from the infected cell can affect tropism and spread of the viruses whether it will cause systematic infection or local infection. It is interesting that coronaviruses causing local infection, such as gastroenteritis and upper respiratory disease, are released apically, but the MHV that causes more systemic disease such as hepatitis and encephalitis is released mainly basolaterally.

INFECTIOUS cDNA CLONES OF CORONAVIRUS

Because of its large size limitation, and regions toxic to *E. coli*, until recently there was no infectious cDNA clone of a coronavirus. Recently, several groups used different approaches to overcome the size limitation of coronaviruses and have cloned the approximately 30 kb entire genomes of several coronaviruses. The first breakthrough was by Almazan et al. (2), using bacterial artificial chromosomes (BAC) to construct an infectious cDNA clone of TGEV. Yount et al. (201) used a novel approach to produce an

infectious cDNA clone of TGEV. Instead of cloning the entire TGEV genome into a cloning vector, they used *in vitro* assembly using unique restriction enzyme systems. The type II restriction enzymes, such as BsmBI and SapI, recognize non-palindromic sequences, and digest the DNA outside of the restriction enzyme recognition sequence resulting in 3-4 nucleotide overhangs. These nucleotide overhangs are non-palindromic and have unique sequence composition. Each DNA fragment digested with these restriction enzymes can be religated with compatible overhangs produced by digestion with the same enzyme. Subsequently, Thiel and Casais (31, 185) made infectious cDNA clones of human coronavirus, HCoV 229E and IBV respectively using vaccinia virus as a cloning vector. The entire coronavirus genomes were cloned into vaccinia virus. The recombinant virus will infect cells and produce both coronavirus and vaccinia virus, but because of their size difference, recombinant vaccinia virus was filtered out.

Each approach used to develop infectious cDNA clones of coronaviruses has advantages and disadvantages. In addition to the large size of the genome being an obstacle developing infectious clones, regions in the polymerase genes are very unstable in bacterial plasmid vectors or BAC systems. These problems have been solved by adding an additional intron into the BAC system or by breaking down the coronavirus genome into smaller fragments for cloning into separate plasmids. These infectious cDNA clones have been used to express heterologous genes, demonstrating their potential as expression vectors or gene delivery systems (3, 169, 187). Using characteristics of coronaviruses, which produce several subgenomic RNAs to express several different proteins, Thiel et al. (187) has developed a multigene RNA vector with HcoV-229E. In this study, they

expressed three different proteins, chloramphenicol acetyltransferase (CAT), the firefly luciferase (LUC) and the green fluorescent protein (GFP) genes by using independent TRSs for each gene (187). This study shows the possibility of coronavirus infectious cDNA clones as an alternative for gene delivery systems or expression vectors.

CHAPTER II

SYSTEMATIC ASSEMBLY OF A FULL-LENGTH INFECTIOUS cDNA OF A BEAUDETTE STRAIN OF INFECTIOUS BRONCHITIS VIRUS (IBV)

INTRODUCTION

Infectious bronchitis virus (IBV) is one of the most economically important diseases in the poultry industry (39). The mortality of the disease varies, depending on the viral strain, but the acute and chronic effect of disease such as the retarded growth of broilers and a decrease in egg production in layers causes tremendous losses in the industry (6).

IBV belongs to the order of *Nidovirales*, genus *Coronavirinae*. The genomes of these viruses are 5' capped, 3' polyadenylated, and are positive sense RNA (34, 161). As with other positive strand RNA viruses, after infecting susceptible cells, the IBV genome is used as an mRNA to express its replicase. IBV expresses its proteins using subgenomic RNAs (sgRNA) and an internal ribosomal entry site (IRES) (95, 106). IBV sgRNAs are structurally polycistronic, but functionally monocistronic with the exception of RNA 3 and RNA 5. RNA 3 is a tricistronic mRNA which expresses 3a, 3b, and 3c proteins (103). Among these, 3c is a structural protein, the small envelope protein, E (104, 203). RNA 5 expresses two proteins, 5a and 5b. Even though expression of these proteins in infected cells has been shown (105), the function of these proteins have not been addressed. Expression of E protein from RNA 3 uses an IRES, but the mechanism

of 3b and 5b expression is speculated as a leaky scanning mechanism but has not yet been shown experimentally.

IBV can be classified into several different serotypes depending on the S1 protein of the virus (65). Since some vaccine strains of IBV cannot cross protect against IBV strains with distinct serotypes, problems in controlling the disease are continuing to arise in field situations. In addition, because of the innate nature of the polymerase gene in RNA viruses, the IBV polymerase does not have proof reading ability. In addition, frequent recombination between different strains of viruses causes the emergence of naturally occurring new types of recombinant viruses in the field causing vaccine breaks (86).

Molecular biology studies of many viruses, including both positive and negative strand viruses, have been accelerated by a reverse genetic systems (23, 62, 141). Infectious cDNA clones have been used to address mechanisms of viral replication, pathogenesis, virus packaging and in the development of vaccines not only for single stranded genomic RNA viruses, but also for segmented viruses, such as Influenza virus (72, 75, 131, 132).

Infectious cDNA clones of coronaviruses were difficult to generate because of their large genome size and the instability of its genes in bacterial plasmids. However, several groups have recently developed infectious cDNA clones of coronaviruses (2, 31, 201, 202). Several approaches were used to overcome the size limitation of the coronavirus genome to successfully clone the entire genomes. One of the first breakthroughs was by Almazan et al. (2) using bacterial artificial chromosomes (BACs) as a cloning vectors to construct an infectious cDNA clone of TGEV. Yount et al. (201) used a unique approach

to produce an infectious cDNA clone of TGEV. Instead of cloning the entire TGEV genome into cloning vectors, they used *in vitro* assembly of several cDNAs using a unique type II restriction enzyme system that recognize non-palindromic sequences and digested the DNA outside of the restriction enzyme recognition sequences. By using enzymes such as BglI and BsmBI, each DNA fragment was religated with neighboring fragments that had compatible sequence composition. Following this procedure, Thiel and Casais (31, 185) made infectious cDNA clones of human coronavirus, HcoV 229E and IBV respectively, using vaccinia virus as a cloning vector. Yount et al. also developed a new strategy to construct an MHV infectious cDNA clone (202). By introducing restriction enzyme recognition sequences in MHV genomes by RT-PCR that can be used for *in vitro* assembly without introducing nucleotide sequence changes, Yount et al. used the characteristics of the restriction enzyme and coined the term "no see'm technology". After digestion of the amplicons with the restriction enzyme and *in vitro* ligation, the restriction enzyme recognition sequences introduced by PCR disappear.

We used this *in vitro* assembly strategy to construct an infectious cDNA clone of IBV using restriction enzymes BsmBI and SapI. Our aim was to develop a rapid process to make IBV vaccines that can effectively control the outbreak of new IBV strains in the field. To develop an effective vaccine against IBV, it is critical to know the biology of the virus, especially with regards to the genes of the virus involved in viral attenuation and pathogenicity. As mentioned before, to understand the molecular biology of RNA viruses, the development of an infectious cDNA clone is very useful. In this study, we developed

an infectious cDNA clone of IBV using the cell adapted Beaudette strain which is easily manipulated in a short time frame.

MATERIALS AND METHODS

Viruses and Cells

A Vero cell adapted Beaudette strain of IBV was obtained from American Type Culture Collection (ATCC, Manassas, VA) and then plaque purified three times. The virus was propagated in the African green monkey kidney Vero cell line, obtained from the ViroMed Laboratory (Minnetonka, MN) and maintained in Dubecco's modified Eagle medium (DMEM) containing 5% fetal bovine serum (FBS) supplemented with penicillin G (100 unit/ml) and streptomycin (100 ug/ml). The baby hamster kidney cell line, BHK-21, was also obtained from Viromed and maintained in DMEM containing 10% FBS supplemented with antibiotics as described for the Vero cells.

RNA Preparation

Viral RNA was prepared from the supernatant of IBV infected Vero cells. Briefly, Vero cells were infected with IBV at 0.1 multiplicity of infection (m.o.i) and incubated in a CO_2 incubator at 37°C until the cells showed more than 80% cytopathogenic effect (CPE), such as syncytia formation. The cells showing extensive CPE were frozen and thawed three times and then cell debris was pelleted by

centrifugation at 3,000 rpm using a tabletop centrifuge (CR 412; Jouan Inc. Winchester, VA). The supernatants were then ultracentrifuged at 35,000 rpm for 2 hours at 4°C using an L7-55 ultracentrifuge (Beckman, Palo Alto, CA) with an SW55Ti swinging bucket rotor to pellet the virus. The viral pellet was re-suspended in small volumes of TEN (10 mM Tris-Cl, pH 8.0, 1 mM ethylendiaminotetraacetate (EDTA), pH 8.0 and 0.1 M NaCl) buffer.

TRIZOL reagent (Invitrogen, Carlsbad, CA) was used to extract the RNA from the re-suspended viral pellet following the manufacturer's instruction. Briefly, 1 ml of TRIZOL reagent was added into 200 ul of viral pellet suspension in TEN buffer and then mixed thoroughly by inverting the microfuge tube several times. The mixture was incubated for 5 minutes at room temperate and then 200 ul of chloroform was added before mixing thoroughly by inversion. The mixture was then incubated at room temperature for 3 minutes. To separate the aqueous and the organic phases, the mixture was centrifuged at 12,000 rpm for 15 minutes at 4°C using a microcentrifuge (5417 R ; Eppendorf, Hamburg, Germany). The upper (aqueous) phase was then transferred to a new nuclease free microfuge tube and 0.5 volume of isopropanol was added to precipitate the RNA. After 10 minutes incubation at room temperature, the RNA was pelleted by centrifugation at 12,000 rpm for 15 minutes at 4°C. Before suspending the RNA pellet in nuclease free-water, the RNA pellet was washed with 70% ethanol, and briefly air-dried. The RNA solution was quantified using a SmartSpec^{TM} 3000 spectrophotometer (BIO-RAD, Hercules, CA) and stored at –70°C until further use as a template for RT-PCR or as a size marker for electrophoresis.

Reverse Transcription (RT) Reaction

The cloning strategy for a full-length infectious cDNA clone of IBV is illustrated in Figure 6. This cloning strategy uses SapI or BsmBI restriction endonuclease to cleave at specific sequences (Figure 7) leaving highly variable three or four nucleotide overhangs that do not randomly self-ligate, but do ligate with the fragments containing the complementary nucleotide overhangs generated with the identical restriction enzyme.

The first cDNA reaction was done using the SUPERSCRIPT^{TM} First-Stranded Synthesis System for RT-PCR (Invitrogen, Carlsbad, CA) according to the manufacture's directions. Briefly, 1-2 ug of RNA in 8 ul of nuclease free water with 1 ul of 10 mM deoxynucleotide-triphosphate (dNTP) and 10 pmol of each reverse primer P1R, P2R, P3R, P4R and GNR (Table 1) were incubated in a 70°C water bath for 5 minutes. Reactions were chilled on ice for 5 minutes before adding 2 ul of 10X first strand buffer, 4 ul of 25 mM $MgCl_2$, 2 ul of 0.1 M dithiothreitol (DTT), 1 ul of recombinant RNase inhibitor (50 unit/ul, Invitrogen) and 1 ul of Superscript reverse transcriptase (50 Unit/ul) and then incubated at 42°C for 50 minutes. The reaction was terminated by incubating at 75°C for 15 minutes before degrading the RNA template with 1 ul of *E. coli* RNase H (2 Units/ul) with 20 minutes incubation at 37°C.

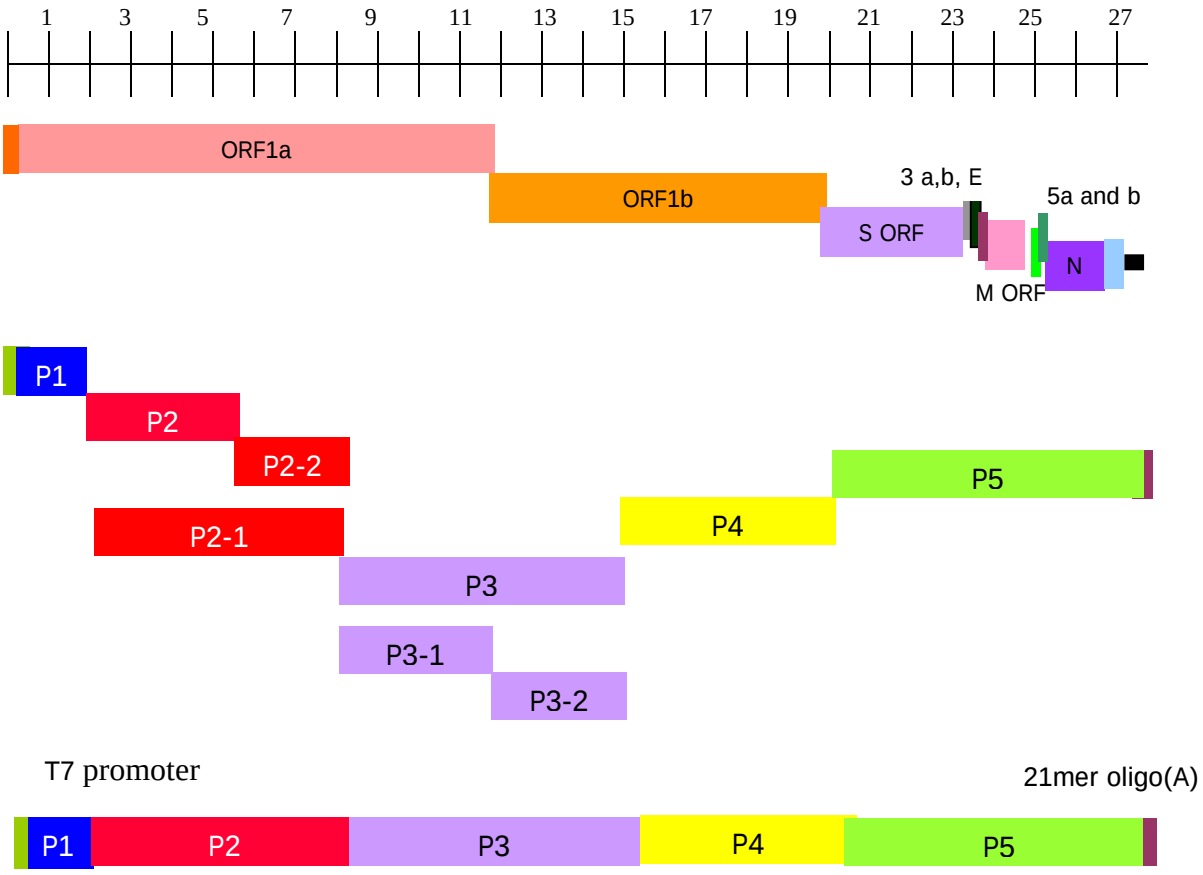

FIG. 6. Strategy for orderly assembly of an IBV infectious cDNA clone. Using RT-PCR and unique oligonucleotide primer mutagenesis, seven clones spanning the entire IBV genome were amplified using standard recombinant DNA techniques. Between P2-1 and P2-2, P3-1 and P3-2, unique BsmBI restriction sites were inserted at the 3' and 5' end of each junction. The approximate locations of each RT-PCR products is shown. T7 RNA polymerase promoter was inserted in front of the 5' end of P1 by PCR mutagenesis. In the same way, twenty nucleotides poly (A) tail was inserted at the 3' end of P5.

BsmBI restriction enzyme recognition sequence

5′...CGTCTC(N)$_1$ ⇓...3′
3′...GCAGAG(N)$_5$ ⇑...5′

Sequence of P2 between P2-1 and P2-2 junction

GCTAGTGTTAAGAGTGTTGTCGCTAGCTATAAGACCGTGTTATGTAAGGT
CGATCACAATTCTCACAACAGCGATCGATATTCTGGCACAATACATTCCA

NHE R

5′ GCTAGTGTTAAGAGTGTT GTCGCGAGACG 3′
3′ CGATCACAATTCTCACAACAGC GCTCTGC 5′

NHE f

5′ CGTCTCT
GTCGCTAGCTATAAGACCGTGTTA
3′ GCAGAGACAGC
GATCGATATTCTGGCACAAT

5′ GCTAGTGTTAAGAGTGTT GTCGCTAGCTATAAGACCGTGTTATGT
3′ CGATCACAATTCTCACAACAGC GATCGATATTCTGGCACAATACA

FIG. 7. No see'm technology using BsmBI restriction enzyme properties. Cloning and assembly strategy of P2-1 and P2-2 is illustrated. BsmBI site was inserted using PCR mutagenesis at the 3' end of P2-1, 5' end of P2-2. Cleavage with BsmBI restriction enzyme will create a novel four nucleotides overhang that specifically anneal with the complementary four nucleotides overhang generated by an identical BsmBI. Upon religation, BsmBI is deleted from the clone and reforms original sequence connecting two pieces intact.

TABLE 1. Primer pairs used for cloning of the individual IBV amplicons

Primer	Nucleotide Sequence	Genome location
T7P1F	5′-**TAATACGACTCACTATAGG**ACTTAAGATAGATATTAATATA-3′	1-22
P1R	5′-CCTTTCCAGAAGAGCAAATCTCC-3′	2254-2276
P1F	5′-GGAGATTTGCTCTTCTGGAAAGG-3	2254-2276
P2F	5′-GATCTTGCTGCGAAGAGCACTTTTG-3′	8611-8635
NHER	5′-CGTCTCGCGACAACACTCTTAACACTAGC-3′	5731-5753
NHEF	5′-CGTCTCTGTCGCTAGCTATAAGACCGTGTT-3′	5748-5771
P2R	5′-CAAAAGTGCTCTTCGCAGCAAGATC-3′	8611-8635
P3F	5′-GTAGTGATTCATTGAGACGTTTTG-3′	15508-15531
SACR	5′-CGTCTCGGGATCTACTGCAAATGAACATAG-3′	11926-11949
SACF	5′-CGTCTCGATCCCCGCGGACACATATTGTAAATATG-3′	11944-11971
P3R	5′-CAAAACGTCTCAATGAATCACTAC-3′	15508-11949
P4F	5′-CAGGCTCTTCATCAGGGTGTACTG-3′	20543-20566
P4R	5′-CAGTACACCCTGATGAAGAGCCTG-3′	20543-20566
GNR	5′-GCTCTAACTCTATACTAGCC-3′	27593-27613
GNRT	5′-TTTTTTTTTTTTTTTTTTTGCTCTAACTCTATACTAGCC-3′	27593-27613

Numbers followed the sequence data obtained from Vero cell adapted Beaudette sequence from our laboratory. Bold letter is T7 RNA polymerase promoter seq. Underlined letter is BsmBI restriction enzyme recognition sequence.

Polymerase Chain Reaction (PCR) for Amplification of Target Sequences

Two ul of each completed cDNA reaction was used to amplify the target DNA by PCR. PCR was done using the Expand Long Template PCR system (Roche, Indianapolis, IN) following the manufacturer's directions using a GeneAmp PCR system 2400 thermocycler (PerkinElmer, Boston, MA). Sequences of the primer pairs used for RT-PCR reaction are listed in Table 1.

cDNA synthesized with P1R primer was used as a template for P1 PCR amplification. A 50 ul reaction included 5 ul of 10X PCR buffer number 3, containing 22.5 mM $MgCl_2$, 2 ul of 10 mM dNTP, 1 ul of forward primer (T7P1F), 1 ul of reverse primer (P1R), 2 ul of a cDNA reaction and 0.75 ul DNA polymerase enzyme mix. Distilled waster was used to bring the total volume to 50 ul. Reaction conditions for the P1 PCR included an initial denaturation at 94°C for 2 minutes, followed by 30 cycles of denaturation at 94°C for 10 seconds, annealing at 55°C for 30 seconds and elongation at 68°C for 2 minutes. The final step was an elongation step at 68°C for 7 minutes.

P1F and NHER primers were used for P2-1 amplification. NHEF and P2R primers were used for P2-2 amplification. P2F and SACR primers were used for P3-1 amplification. SACF and P3R primers were used for P3-2 amplification. Because P2-1, P2-2, P3-1 and P3-2 have a similar target size of about 3.5 kb, the same reaction condition was used for these amplifications.

The conditions for P2-1, P2-2, P3-1 and P3-2 amplification included an initial denaturation at 94°C for 2 minute. First round PCR reaction conditions included 10 cycles at 94°C for 10 second, 58°C for 30 seconds and 68°C for 2 minutes 20 seconds.

Conditions for the second round of amplification were 20 cycles at 94°C for 10 seconds, 58°C for 30 seconds and 68°C for 2 minute 20 seconds, with a 20 second additional elongation time in every cycle. A final incubation of 10 minutes at 68°C was included for each reaction.

P3F and P4R primers were used for P4 amplification. Conditions for P4 were an initial denaturation at 94°C for 2 minutes followed by 10 cycles at 94°C for 10 seconds, 58°C for 30 seconds and 68°C for 4 minutes 20 seconds and the second round amplification conditions were 18 cycles at 94°C for 10 seconds, 58°C for 30 seconds and 68 °C for 4 minutes and 20 seconds, with 20 seconds additional elongation time added each cycle. This was followed by 10 minutes incubation at 68°C for final elongation.

P4F and GNR or P4F and GNRT primers were used for P5 amplification. PCR reactions included an initial denaturation at 94°C for 2 minutes. First round amplification reactions included 10 cycles at 94°C for 10 seconds, 58°C for 30 seconds and 68°C for 6 minutes 20 seconds and second round amplification, 18 cycles at 94°C for 10 seconds, 58°C for 30 seconds and at 68°C for 6 minutes and 20 seconds, with 20 seconds additional elongation time in every cycle. A final 10 minute 68°C elongation completed the amplification.

Cloning of Amplicons

Following amplification, 2 ul of each PCR product was electrophoresed in a 0.7% agarose gel, containing Tris-acetate-EDTA (TAE) buffer and ethidium bromide

(EtBr). The electrophoresis results were recorded using a FluoChem ™ gel analysis system (Alpha Innotech Corporation, San Leandro, CA). Each PCR product with the correct size was purified from a 0.7% agarose gel containing 100 ul of crystal violet (2 mg/ml) per 100 ml of agarose solution by electrophoresis. DNA bands were excised from the agarose gel and then purified using a QIAquick Gel Extraction Kit (QIAGEN Inc., Valencia, CA) following the manufacture's directions. The concentration of gel purified PCR products were measured with a SmartSpec 3000 spectrophotometer (BIO-RAD). Each PCR product was ligated into a cloning vector. P1 was ligated into a pSTBLUE vector (Novagen, Darmstadt, Germany) by incubating an equal molar ratio of vector and insert at 16°C for 2 hours. P2-1 though P3-2 were ligated into a pSMART HC vector (Lucigen, Middleton, WI) according to the manufacturer's instructions. Briefly, PCR products were treated with T4 DNA polymerase (Promega, Madison WI) filling in any 3' and 5' end nucleotide overhangs. After T4 DNA polymerase treatment, PCR products were treated with T4 Kinase (Promega) to phosphorylate the 5' ends. The products were further purified by phenol/chloroform extraction followed by ethanol precipitation. Equal molar ratios of PCR product and pSMART-HC vector were ligated for 2 hours at 16°C and then transformed into chemically competent NovaBlue (Novagen, Darmstadt, Germany) cells. P4 and P5 PCR products were directly ligated into pCR-XL-TOPO cloning vector (Invitrogen) for 5 minutes at room temperature and transformed into chemically competent Oneshot cells (Invitrogen). Transformed bacteria were plated on Luria-Bertani (LB) medium agar plates containing kanamycin (5 ug/ml) and grown overnight at 37°C.

Cloning of a Probe

To prepare a probe for northern and Southern blot analysis that was specific for the 3' end of IBV, a region containing the entire N ORF through the 3' UTR of IBV was RT-PCR amplified and cloned into a pGEM-3Zf(-) vector (Promega, Madison, WI). Briefly, the cDNA was prepared using the GNR primer and Superscript reverse transcriptase (Invitrogen) as described above. Two ul of a cDNA reaction was used for PCR. Taq polymerase (Promega) was used for PCR amplification following the manufacture's directions. 10 pM each of BNF (5' ATG GCA AGC GGT AAA GCA GC 3') and GNR (5' GCT CTA ACT CTA TAC TAG CC 3') oligos were added as the forward and reverse primer, respectively. The direction of N ORF cloned into pGEM-3Zf (-) vectors was determined by restriction enzyme digestion using BamHI (Promega), and confirmed by sequencing, using M13 forward and M13 reverse primers (Invitrogen). Both reverse and forward directions of ORF N were cloned as pGEBN-1 and pGEBN-2, respectively.

Nucleotide Sequencing

Each amplicon DNA was prepared from transformed *E. coli* cultures grown overnight in LB medium, and DNA templates were prepared using a QIAGEN mini prep kit (QIAGEN). PCR products purified with QIAquick PCR purification kit (QIAGEN, Santa Clarita, CA) were used for direct PCR product sequencing. Sequencing was performed using the ABI prism BigDye Terminator Cycle Sequencing Ready Reaction Kit (Applied Biosystems, Foster City, CA). The sequencing reaction included 350-500

ng of plasmid DNAs or 300 ng of PCR products mixed with 2 ul of BigDye mixture (ABI) and 10 pM of primers (synthesized by Integrated DNA Technologies, Inc, Coralville, IA) and the reaction mixtures were adjusted to 6 ul with distilled water. The conditions for the sequencing reactions included an initial denaturation at 96°C for 2 minutes followed by 30 cycles at 96°C for 30 seconds, 52°C for 15 seconds and 60°C for 4 minutes.

Three independent clones for each amplicon were isolated with plasmid mini-preparations as described above and sequenced using a panel of primers located about 400 nts apart on the IBV genome. Unincorporated nucleotides and primers were removed using micro Bio-spin chromatography columns (BIO-RAD, Hercules, CA) and the sequencing reaction was completely dried using a Speed-Vac Concentrator (Thermo Savant, Holbrook, NY). Completed sequencing reactions were sent to a core facility sequencing laboratory at the Department of Biology, Texas A&M University. Sequences were read using an ABI automatic sequencer 3100 (ABI).

Analysis of Sequences

Sequence data were analyzed using SDS Biology Workbench (http://workbench.sdsc.edu) (San Diego Supercomputer Center, University of California, San Diego, CA). For DNA and amino acid sequence comparisons, the LALIGN program was used. For cloning purposes, the TACG program was used to search for restriction enzyme digestion profiles. SIXFRAME was used to convert DNA sequences into amino acid sequences.

Assembly of a Full-length IBV Infectious Construct

Insert DNAs from each amplicon were digested with the appropriate restriction enzymes. P1 was digested with XhoI (Promega, Madison, WI) and then treated with calf intestine phosphatase (CIP) (Promega) to inhibit self-ligation. CIP treated DNA was phenol:chloroform extracted, ethanol precipitated and then digested with restriction enzyme SapI (New England Biolabs Inc., Beverly, MA). P2–1, P2-2 and P3-1 amplicons were double digested with restriction enzymes SapI and BsmBI. When the buffer conditions were not compatible, after one restriction enzyme digestion, the reactions were ethanol precipitated and then the DNA was reconstituted with the appropriate buffer and in the appropriate volume for the second enzyme digestion. Except for the BsmBI restriction enzyme digestion that needed to be incubated at 55°C, the restriction enzymes were incubated at 37°C. P3-2 and P4 replicons were single digested with restriction enzyme BsmBI. The P5 amplicon was digested with restriction enzyme EcoRI (Promega) then CIP treated and digested with BsmBI. Each DNA insert was run on a TAE agarose gel (0.8 to 1%) containing 2.4 ug/ml crystal violet to prevent UV-induced DNA damage that could impact subsequent manipulations of the DNA fragment. Target size inserts were excised from the agarose gel and the DNA inserts were extracted using a QIAquick Gel Extraction kit (QIAGEN Inc, Valencia, CA) following the manufacturer's instructions.

A high concentration of T4 DNA ligase (20 U/ul) was used to assemble infectious cDNA of IBV. Ligation reactions were incubated at 16°C overnight before inactivating the ligation reaction mixes by incubating at 65°C for 10 minutes. Aliquots

of the ligation reactions were electrophoresed on an agarose gel to confirm the ligation reaction and size of the ligation products. The correct sizes of larger ligation fragments were purified from agarose gel and then ligated step wise with other fragments. The final ligation reaction of P1 through P3-1 and P3-2 though P5 were pooled without further purification and then ligated overnight.

Northern Blot Analysis

Preparation of a random primed isotope labeled probe.

To prepare a random primed probe against the 3' end of IBV, pGEBN-2 was used as a template. The template DNA was digested with PstI restriction enzyme and then phenol:chloroform extracted followed by ethanol precipitation to remove contaminating RNase. One ug of template was used for an *in vitro* transcription and labeling reaction using T7 RNA polymerase (Promega). Briefly, 4 ul of 5X transcription buffer, 2 ul of 100 mM DTT, 1 ul of RNase inhibitor (Promega, 30 unit/ul), 4 ul of rNTP mix containing 2.5 mM rCTP, rATP, and rGTP, 1.2 ul of 200 uM rUTP, 5 ul of [α-^{32}P] rUTP (Perkin-Elmer), 1.3 ul of T7 RNA polymerase (20 unit/ul) were used in a 20 ul reaction. The reaction was incubated at 37°C for one hour and then ethanol precipitated. The probe was resuspended in deionized formamide and stored at –20°C. Activity of the probe was measured with a liquid scintillation system (Beckman Coulter Inc, Fullerton, CA) before using for hybridization reactions.

RNA transfer

To transfer RNA from an agarose gel to a nylon membrane for northern blot hybridization, 1 ul of each *in vitro* transcribed RNA was electrophoresed in a denaturing agarose gel containing formaldehyde following standard method (153) with modifications. RNA was denatured with sample buffer containing 1/10 v/v formaldehyde gel–running buffer (0.2 M 3-(N-norpholino) propanesulfonic acid (MOPS) (pH 7.0), 80 mM sodium acetate and 10 mM EDTA (pH 8.0)) with 1/5 v/v of formaldehyde, 1/2 v/v of deionized formamide, 2 ug of EtBr, and 1/10 v/v of formaldehyde gel-loading buffer (50% glycerol, 0.25% bromophenol blue, 0.25% xylene cyanol FF) per RNA sample containing total volume of 15 ul of reaction volume. RNA and sample buffer were mixed, denatured at 70°C for 5 minutes and chilled on ice. A 1% denaturing agarose gel containing formaldehyde was prepared with a 1/10 volume of 10X formaldehyde gel running buffer and formaldehyde to give final concentration of 2.2 M formaldehyde. Each RNA sample was loaded on the agarose gel and run at 90 V in 1X formaldehyde gel-running buffer. After every one hour, the buffer from each reservoir was mixed and returned to the gel apparatus for further electrophoresis. When the xylene cyanol dye front was at the bottom of the gel, electrophoresis was terminated. The gel was washed several times with distilled water and then soaked in 0.05 N NaOH for 20 minutes and exposed to long wavelength UV light for 60 seconds. The gel was then washed with distilled water and soaked for 20 minutes in 10 X sodium chloride sodium citrate (SSC) buffer. RNA from the gel was transferred to nylon membrane by capillary transfer in 10 X SSC overnight. RNA transfer was confirmed by EtBr staining

of the nylon membrane and molecular weight markers were indicated with pencil. The membrane was then fixed by UV cross-linking for 30 seconds using GS gene linker UV chamber (BIO-RAD).

Hybridization reaction

The membrane containing transferred RNA was hybridized with a probe against the 3' end of the IBV gene with specific activity of 2 x 10^7 cpm/ug that was labeled with α-^{32}P by random priming. Hybridization reactions were done using an autoblot hybridization oven (Bellco Glass Inc., Vineland, NJ). Hybridization conditions included incubation at 55°C for 12 hours in hybridization buffer containing 50% deionized formaldehyde, 2 X Denhardt's reagent, 5 X SSC and 0.1% SDS. After hybridization, excess probe was removed by washing with 1 X SSC, 0.1% SDS, followed by three washes for 20 minutes each at 68°C in 0.2 X SSC and 0.1% SDS. After hybridization, the nylon membrane was exposed to an image plate (IP) for 20 minutes to one hour, depending on signal intensity. The image was analyzed using a BAS-1800 II phosphoimage reader (Fusifilm Electronic Imaging Ltd. Tokyo, Japan) and analyzed using the Image Gauge V3.12 and L processor V1.72 program.

***In vitro* Transcription and Electroporation**

Capped runoff T7 transcripts were synthesized *in vitro* from *in vitro* ligated IBV cDNA template using an mMESSAGE mMACHINE ^{TM} T7 Ultra kit (Ambion, Austin,

TX) as described by the manufacturer with some modification. 20 ul of IBV RNA transcription reaction mixture was prepared containing 10 ul of 2 X NTP mixture, 3 ul of 30 mM GTP, 2 ul of 10 X transcription buffer, 2 ul of enzyme mixture and remainder was filled with nuclease free water and incubated at 37C° for 2 hours. Template DNA was removed by incubating the transcription reaction with 1 ul of DNase I (2 units/ul) for 20 minutes at 37 C°

To increase the efficiency of virus rescue after transfection, N transcript was also prepared and co-transfected with the IBV transcript. pGEMN-1 was used as a template for N transcripts. The amplicon was digested with a PstI restriction enzyme (Promega) to linearize the template and then phenol:chloroform extracted followed by ethanol precipitation to remove any RNase contamination. The DNA was resuspended with diethyl pyrocarbonate (DEPC) treated distilled water. 1 ug of the template was used for an *in vitro* transcription reaction using mMESSAGE mMACHINE ^{TM} T7 Ultra kit (Ambion, Austin, TX.). A poly (A) tail was added to the transcript with *E. coli* Poly(A) polymerase. Transcripts were precipitated with 7.5 M lithium chloride containing 50 mM EDTA before electroporation and transcripts were used with or without precipitation.

BHK-21 cells were grown to about 70% subconfluence before electroporation. BHK-21 cells were treated with trypsin to detach them from flasks. The cells were washed twice with ice cold DEPC treated PBS and then resuspended at 2 x 10^7 cells per ml in the cold PBS. One third of the transcription reaction using IBV template and one fifth of N transcript were mixed with 400 ul of BHK-21 cell suspension in a 1.5 ml

microcentrifuge tube. The cells and RNA mixture were immediately transferred to 2 mm gap electrophoration cuvettes (electroporation cuvettes plus model No. 620, BTX, Genetronics Inc., San Diego, California) and then elecrophorated at 850 V, 25 mΩ and at resistance 720 Ω using an electro-cell manipulator 600 (BTX, Genetronics, Inc. San Diego, California) with three consecutive pulses. After electroporation, cells were incubated at room temperature for 10 minutes and then the transfectant was diluted 1 to 20 in complete DMEM containing 10% FBS before resuspending with 1 x 10^6 Vero cells per 100 mm cell culture petridish.

Plaque Staining and Plaque Purification

Virus was serially diluted 10 fold with DMEM without FBS. Then, 200 ul of virus dilution was inoculated per well of six well cell culture plates that had been seeded with monolayers of Vero cells. After one hour incubation, residual virus was removed by washing the cells twice with PBS before overlaying the cells with 0.8% agarose containing 1X DMEM, 1% FBS and antibiotics. The cells were incubated until plaques were observed. For plaque staining, the agarose overlay was removed using a spatula, the cell monolayers were air dried briefly and overlaid with 2 ml of crystal violet staining solution per well. After 10 minutes, excessive crystal violet was removed and the cells were washed several times with PBS to remove residual crystal violet. For plaque purification, the agarose over plaques was picked with a 1000 lambda micropipette and suspended in 1 ml DMEM without FBS. The plaque suspension was

incubated at 4°C overnight and then the viral suspensions were inoculated onto Vero cell in 6 well plates as described before.

Kinetics of Viral Replication

Vero cells were infected with wild type IBV Beaudette strain and IBV Beaudette strain derived from an infectious cDNA clone and plaque purified three times. The Vero cells were seeded in 35 mm petridishes at a concentration of 10^6 per dish. The cells were infected with three plaques forming units per cell for an hour and then the media were replaced with DMEM containing 1% FBS with antibiotics, and 5, 10, 12, 19, and 21 hours after infection, the cells were harvested and stored at –70°C for subsequent plaque assays.

RESULTS

RT-PCR and Cloning of Amplicons

Fragments covering the entire genome of IBV Beaudette were amplified by RT-PCR. Each fragment overlapped by about 10 nucleotides. The RT-PCR products were cloned into cloning vectors and labeled as P1, P2, P3, P4 and P5 and their sizes are 2.2 kb, 6.3 kb, 6.8 kb, 5 kb and 7.2 kb, respectively, as shown in Figure 8. Some parts of the coronavirus genome have been reported to be toxic to bacterial host cells when they were transformed into bacterial host cells. This has also been reported during the process

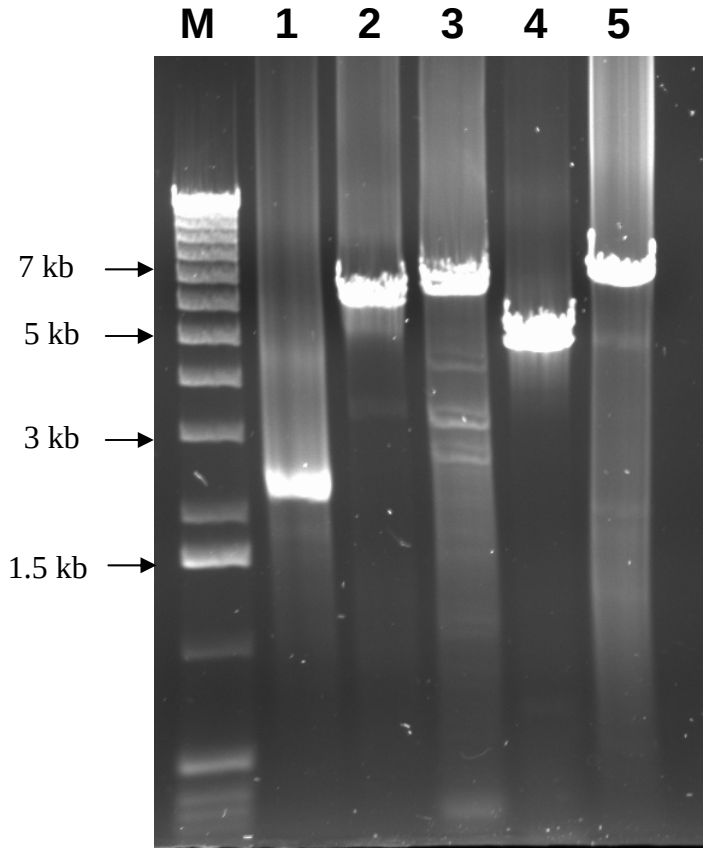

FIG. 8. RT-PCR amplification of the entire IBV genome. The entire genome of IBV was RT-PCR amplified into five pieces. The RT-PCR products were separated in a 0.8% agarose gel and stained with ethidium bromide. M, represents the 1 kb DNA ladder; Lane 1, RT-PCR product from nt 1 to 2269; Lane 2, RT-PCR product from nt 2269 to 8635; Lane 3, RT-PCR product from nt 8625 to 15520; Lane 4, RT-PCR product from nt 15520 to 20550; Lane 5, RT-PCR product from nt 20550 to 17613.

of construction of the infectious cDNA clones of TGEV, MHV and IBV (31, 201, 202). In this lab, several efforts were made to clone the large RT-PCR products of P2 and P3 into the pCR-XL-TOPO TA vector (Invitrogen) but without success. Since regions within these sequences of IBV were also reported to be toxic to *E. coli* (31), P2 and P3 were each divided into 2 smaller fragments. Because there was no SapI or BsmBI restriction enzyme recognition sequence inside these regions of the IBV genome, I decided to use the "no see'm technology" developed by Dr. Baric's laboratory (202) to insert the BsmBI restriction enzyme recognition sequences. The NHER, NHEF, SACR, and SACF primers were designed to hold a BsmBI restriction enzyme recognition sequence at the 5' or 3' end of each primer as shown in Table 1. In addition, to further overcome the toxicity of the IBV gene products in bacterial hosts after transformation, we used pSMARTHC-Kan vector (Lucigen) that was developed to avoid transcription of plasmid genes in bacterial hosts. The overall strategy used to develop an infectious cDNA clone of IBV is illustrated in Figure 6 and 7. After breaking down the P2 and P3 each into two fragments, these PCR products were successfully cloned into the pSMARTHC-Kan vector.

Compared to MHV amplicons that are known to be relatively unstable (personal communication, J. Leibowitz), IBV amplicons are considerably stable. After two or three rounds of 200 ml midi-culture preparations, and subsequent subcloning procedures, no mutations were found in P2, 3, and P5 amplicons. At nt 6385, nt 11137 and nt 13387, there were mutations that affected the amino acid sequence. At nt 6385, and nt 11137, a T to C transition resulted in a tyrosine to histidine substitution. At nt 13387, an A to G

transition resulted in a glutamic acid to glutamine substitution. These mutations were corrected by replacing the region containing the mutation with the same region in other clones having correct sequences.

At nt 25793 in ORF 5b, there was one nucleotide change from A to G resulting in an amino acid sequence change from glutamine to arginine. Since the function of the 5b is not known, this mutation was not changed to the wild type sequence and served as a marker for the infectious cDNA clone.

Sequencing Analysis

Each amplicon was sequenced from at least three independent clones to exclude inherent enzymatic errors that can occur from RT and PCR reactions. Several differences were identified in every amplicon. These aberrations were resolved by direct PCR product sequencing. Some of the sequence discrepancies were not corrected if the sequence differences did not result in a change in the amino acid sequence. If the nucleotide change resulted in amino acid sequence changes, these mutations were corrected using other amplicons that had the correct sequence. To replace these changes with the correct sequences, inserts from independent clones were swapped using unique restriction enzyme with correct amplicons. Some regions of the genome do not encode proteins but have important secondary structures. This is especially true for the 3'UTR region within P5. When there were sequence differences between independent clones for the same region, the sequence was corrected according to the direct RT-PCR sequencing.

Except for the sequence discrepancies between clones for the same amplicons, there were 76 genuine sequence differences from the published sequence data (22, 31). Sequence differences between the IBV strain used in this study, which has been passaged and adapted in Vero cells and the sequence published in 1987 (22) are summarized in Table 2. These changes occurred in the entire genome except for the RdRp region which was totally conserved indicating that it is critical for viral survival. An interesting observation in our study shows a 5 nts insertion in the intergenic region of ORF 4 and ORF 5. At this time, the relevance of the 5 nts insertion in the virus is unknown. Thus, the Beaudette strain of IBV in our study is 27613 nts instead of 27608 nts.

Systemic Assembly of Infectious cDNA by *In vitro* Ligation Reaction

To assemble a full-length cDNA of IBV, each amplicon was digested with appropriate restriction enzyme and insert DNAs from amplicons were purified by electrophoresis and gel purified as described in materials and methods (Figure 9).

Initially, ligation of all the fragments in a single reaction was attempted because each fragment, P1 through P5, has a different sequence overhang at the 3’ and 5’ ends after digestion with SapI or BsmBI. Theoretically, each fragment cannot be randomly ligated to each other, but only with the neighboring sequences, that share compatible ends. Therefore, it was hypothesized that it would be possible to connect each fragment into an infectious clone in one ligation reaction. However, with the random ligation and *in vitro* transcription reactions, only a shorter RNA transcript was obtained. To increase

TABLE 2. Summary of nucleotide and amino acid differences between IBV Beaudette used in this study and published sequence

	Location	**Nucleotide change**	**Amino acid change**	**Gene affected**
1	32	C-T	-	5’UTR
2	222	C-T	-	
3	282	G-A	-	
4	490	T-C	-	
5	841	C-T	S-P	pp1a
6	1374	G-A	-	
7	1845	T-C	-	
8	2000	C-T	A-V	
9	2015	A-G	C-G	
10	2439	A-T	G-E	
11	2651	C-T	T-M	
12	3169	A-T	-	
13	3210	A-G	-	
14	3283	A-G	K-E	
15	3322	C-A	L-I	
16	3428	C-A	A-D	
17	3926	T-C	L-S	
18	4481	C-A	T-N	
19	4791	A-G	-	

TABLE 2 continued

	Location	Nucleotide change	Amino acid change	Genes
20	5456	T-C	L-H	
21	5785	C-T	L-F	
22	5828	C-T	P-L	
23	6231	G-A		
24	7293	A-C		
25	7755	A-G		
26	9372	A-G		
27	10754	T-C	V-A	
28	10781	T-C	I-T	
29	11780	T-A	V-D	
30	12136	A-G	S-G	
31	13106	C-T		pp1b
32	13178	A-C	Q-H	
33	13646	A-G		
34	15302	A-G		
35	15594	C-A		
36	16286	C-T		
37	16718	A-G		
38	17546	T-C		

TABLE 2. Continued

	Location	Nucleotide change	Amino acid change	Genes
39	18195	T-C	Y-H	
40	20731	T-A	L-I	S
41	20755	C-T	L-F	
42	21149	A-C	N-T	
43	21357	A-T	K-N	
44	21457	A-G		
45	21459	A-T		
46	21628	A-C	N-H	
47	21711	G-A		
48	22347	T-C		
49	22433	A-G	K-R	
50	22415	A-C	N-T	
51	22441	C-G	L-V	
52	22492	A-G		
53	22535	T-C	F-L	
54	22590	C-T		
55	23402	G-T	S-I	
56	23724	T-A		
57	24338	T-C		

TABLE 2. Continued

	Location	Nucleotide change	Amino acid change	Genes
58	24508	C-T	P-S	
59	24661	A-G	I-V	
60	24716	C-T	T-I	
61	25342	G-T		
62	25426	G-A		
63	25458	T-C		
64	25465	C-T		
65	25793	A-G	Q-R	
66	25901	A-G		
67	25904	A-G		
68	25928	T-C		
69	26054	C-T		N
70	26208	G-T	D-Y	
71	26403	G-T	A-S	
72	26501	G-T	Q-H	
73	27048	T-G	Y-D	
74	27051	G-T	D-Y	
75	27069	A-G	N-D	
76	27466	A-C		

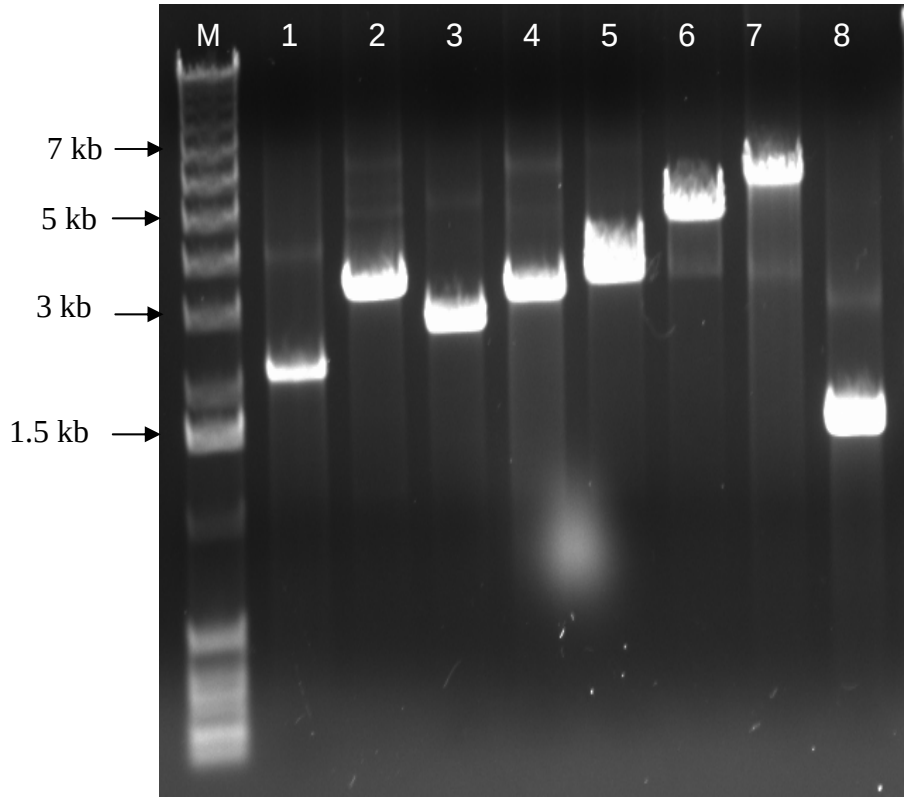

FIG. 9. Preparation of insert DNAs from each amplicon. Each amplicon was digested with appropriate restriction enzymes and inserts were separated from the vectors using agarose gel electrophoresis and DNA gel purification. M, 1 kb DNA ladder; lane 1, P1 insert prepared by XhoI digestion, CIP treated and then digested with SapI restriction enzyme to cut the insert out from the vector; lane 2, P2-1 insert digested with BsmBI and SapI; lane 3, P2-2 insert prepared by digestion with BsmBI and SapI restriction enzyme; lane 4, P3-1 prepared by BsmBI and SapI digestion; lane 5, P3-2 prepared by BsmBI digestion; lane 6, P4 insert prepared by BsmBI digestion; lane 7, P5 large fragment prepared by EcoRI digestion followed by BsmBI digestion; lane 8, small fragment of P5.

the possibility of ligations resulting in an entire genome of IBV infectious clone, each fragment was orderly ligated. P1 and P2-1 were ligated together and P2-2 and P3-1 were ligated. P3-2 and P4 were ligated and P5L, and P5S were ligated, and then the ligation products were extracted from agarose gels. The P1/P21-1 and P2-2/P3-1 were ligated together and P3-2/P4 and P5 were ligated. After verifying the ligation of each fragment by electrophoresis, without further purification, the two ligation reactions were pooled and ligated overnight at 16°C (Figure 10). To verify that the reaction contained the full-length IBV cDNA template, Southern blot analysis using the probe against the 3' UTR of IBV was done with the final product (data not shown). Only the orderly ligated about 30 kb cDNA could be hybridized with a probe against the 3' end of IBV whereas the randomly ligated cDNA template could not.

In vitro Transcription and Transfection of RNAs

After confirming that the cDNA template contained the full length IBV genome by Southern blot analysis, *in vitro* transcription reactions were performed using the purified template. The ligation template was extracted with phenol:chloroform and then ethanol precipitated to remove ligase and contaminating RNase. Approximately 0.2 pm of cDNA template was used for one *in vitro* transcription reaction. To confirm that the *in vitro* transcript had a full length RNA, northern blot analysis was performed using the same probe used for southern blot analysis. RNA transcribed from orderly ligated template only produce full-length in vitro transcript and could be hybridized with a

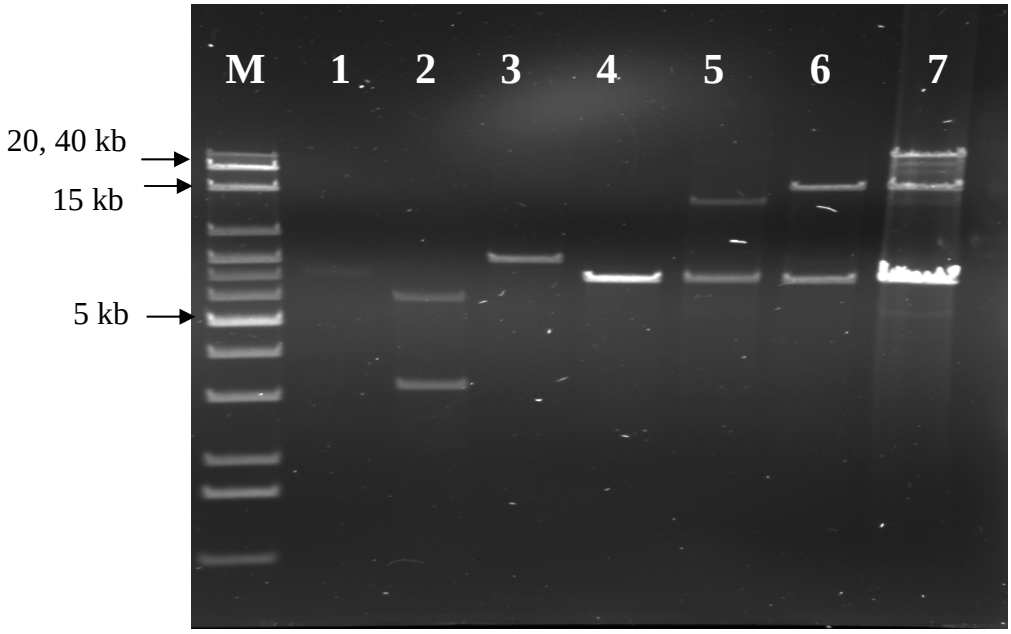

FIG 10. Systemic assembly of IBV full–length cDNA. Each amplicon was digested with the appropriate enzymes and inserts were purified from agarose gels. The inserts were orderly ligated and then larger ligated fragment were purified from agarose gels before ligated to neighboring fragments. M represents 1 kb DNA extension ladder, Lane 1 ligation reaction P1 with P2-1, lane 2, ligation of P2-2 and P3-1, lane 3, P4, purified ligation product P3-2 with P4, lane 4, purified ligation product P5, lane 5, ligation products from P1 to P3-1., lane 6, ligation products P3-2 through P5, lane 7, final ligation product P1 through P5.

probe against 3'UTR of IBV (Figure 11). Because it has been shown that the N transcript facilitates coronavirus transcription and increases the efficiency of virus rescue after viral RNA transfection (56, 184, 201), we co-transfected IBV N ORF transcripts with IBV transcript. Because we created clones of the N protein without a poly(A) tail, poly(A) was added using *E. coli* Poly (A)-polymerase after *in vitro* transcription. *In vitro* transcripts of IBV cDNA and the N ORF were elecrophorated into BHK 21 cells. Before using *in vitro* transcribed RNA, electroporation conditions were optimized using total cellular RNA extracted from IBV infected Vero cells. The transfection efficiency was higher when more than 2 ug of RNA and lower voltage was used with consecutive pulses rather than high voltage with a single pulse. Because BHK 21 cells are not susceptible to IBV infection, Vero cells were overlaid with electroporated BHK 21 cells. After 3 days transfection, the cells were overgrown and there was no evidence of CPE except apparent ballooning of some Vero cells. Subsequently, the cells were frozen and thawed three times and then passaged into new Vero cells. Cytopathogenic effect (CPE) was observed in the cells infected with supernatant from the cells transfected with IBV viral RNA 2 days after infection. CPE was noticed in the cells infected with supernatant from the cells transfected with *in vitro* transcribed RNA 3 days after infection. Both wild type IBV and molecularly cloned IBV showed the same syncytia morphologies.

To verify whether the virus was derived from the infectious cDNA clone or was just contamination, we did direct PCR product sequencing. The infectious cDNA clone has one nucleotide sequence difference from the wild type Beaudette strain in ORF 5b. Both the positive control, transfected with viral RNA, and a sample that is transfected

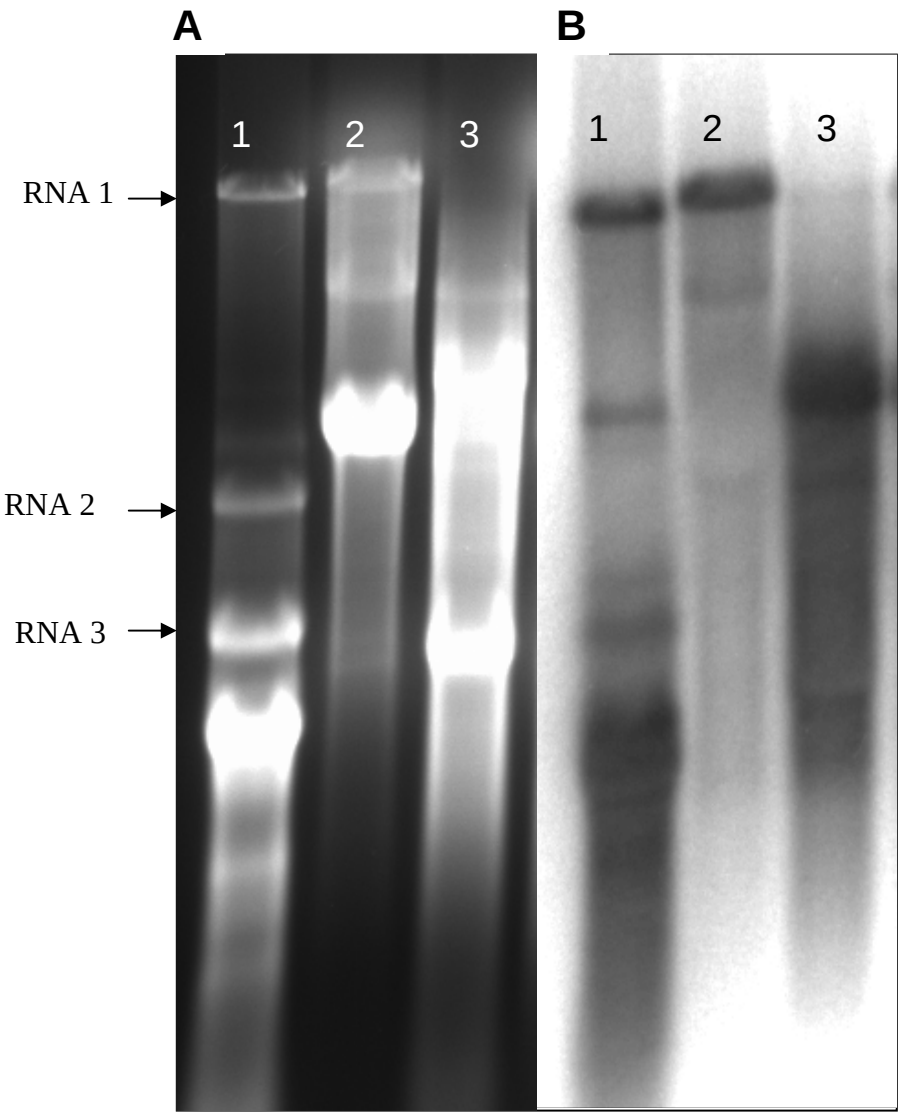

FIG. 11. *In vitro* transcribed RNA from *in vitro* assembled cDNA template encompassing the entire genome of IBV. (A) *In vitro* transcribed products and control RNA, total cellular RNA from IBV infected Vero cells were electrophoresed on denaturing agarose gel. (B) Northern blot of the RNA transferred to nylon membrane and then hybridized with a probe against 3' UTR of IBV. Lane 1 represents intracellular RNA from IBV infected Vero cells; lane 2, in vitro transcription reaction using orderly assembled in vitro ligation reaction, lane 3, *in vitro* transcription reaction

with *in vitro* transcribed cDNA's total cellular RNAs were extracted and used for RT-PCR. ORF5a region containing the mutation was RT-PCR amplified then the PCR products were used for direct PCR sequencing. As shown in Figure 12, wild type IBV and IBV rescued from the infectious cDNA clone showed sequence difference in the marker mutation.

Gross Plaque Morphology

To examine whether the virus from the infectious cDNA clone has the same properties as the wild type virus, we decided to look at plaque morphology. The virus derived form the infectious cDNA clone showed a higher titer than the control wild type virus prepared in the similar way. The gross morphology of each virus plaque, however, is similar (Figure 13).

Kinetics of Viral Replication

Vero cells were infected with wild type IBV Beaudette and molecularly cloned virus from the wild type IBV to compare its growth kinetics. As shown in Figure 14, wild type virus and cloned virus showed similar growth kinetics.

A

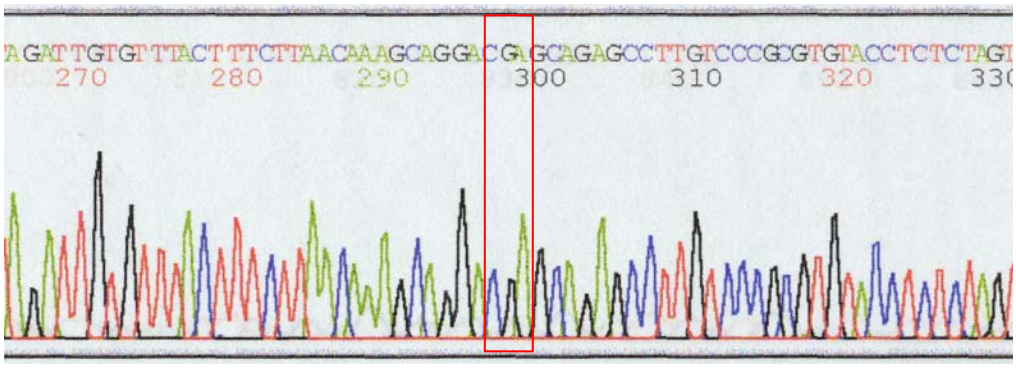

B

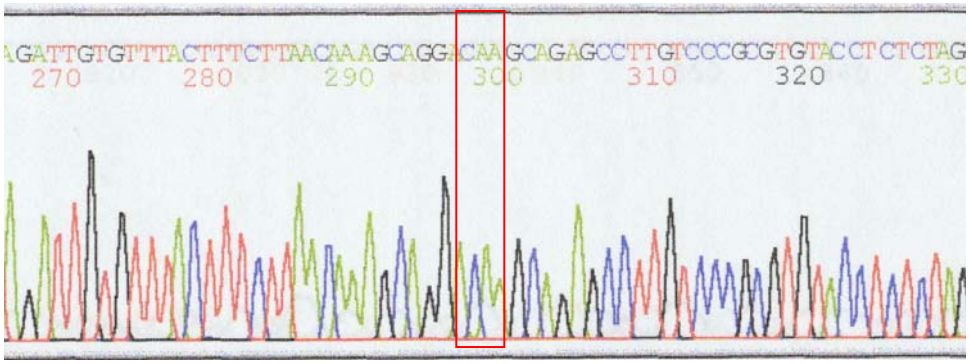

FIG. 12. Sequence comparison of (A) molecularly cloned IBV with (B) the wild type IBV Beaudette strain. One nucleotide change was made as a marker for the molecular clone of IBV in ORF5b changing the codon from CAA to CGA which confer the amino acid change from Gln to Arg. This mutation was confirmed by RT-PCR and direct PCR product sequencing.

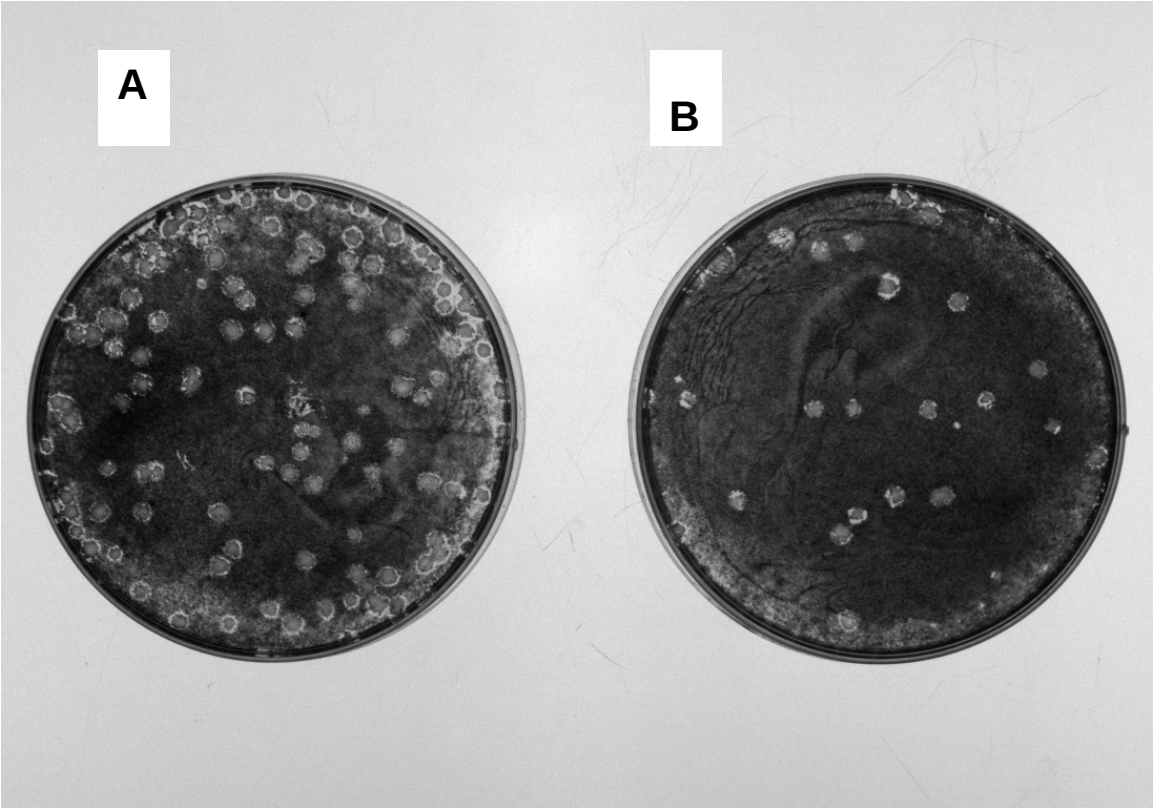

FIG. 13. Molecularly cloned virus plaque morphology. Cultures of BHK cells were electroporated with IBV full-length transcripts or total cellular RNA extracted from IBV infected Vero cells as a control and seeded with Vero cells in 100 mm cell culture dishes. Virus progeny was three time plaque purified and virus stocks were prepared in Vero cells. (A) plaque morphologies of molecularly cloned IBV, (B) wild type IBV virus plaque morphologies.

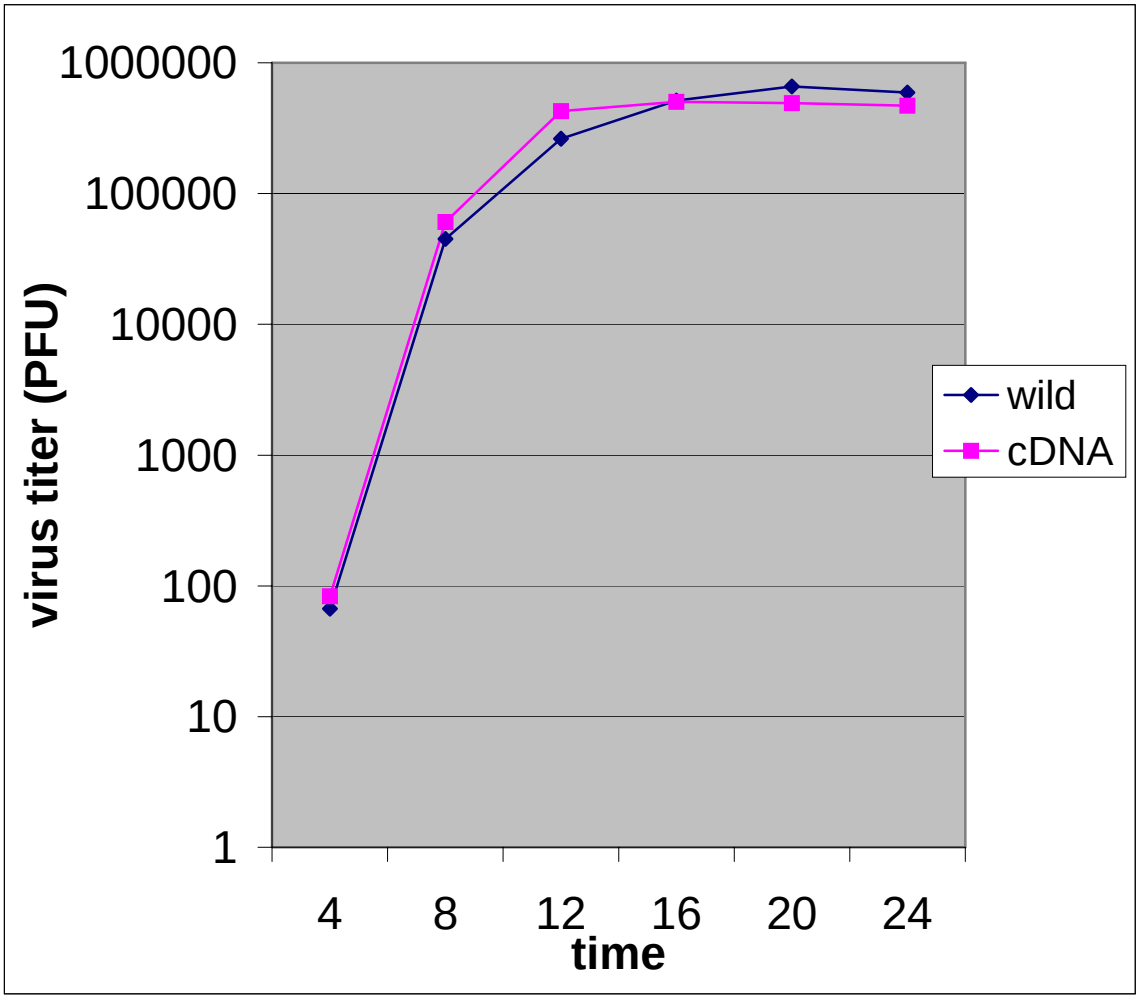

FIG. 14. Growth kinetic comparison of wild type IBV and molecularly cloned IBV. Wild type IBV and molecularly cloned IBV were infected to Vero cell with 3 PFU per cell and the cells were harvested in 4,8,12,16,20 and 24 hours after infection.

DISCUSSION

Toxicity and instability of the viral genes in bacterial plasmids and lack of the molecular biological techniques to clone large RNA genes into cloning vectors has been an obstacle for the development of the molecular clones of RNA viruses, especially for coronaviruses. However, the development of molecular biological techniques, such as RT-PCR, and further development of cloning vectors, such as bacterial artificial chromosome, have helped to solve these problems. Many properties of RNA viruses have been extensively studied using molecular clones of viruses. These studies include not only positive strand RNA viruses but also negative stranded RNA viruses and segmented RNA viruses (139).

Infectious cDNA clones of positive strand RNA and negative strand RNA viruses are useful tools for studying the functions of viral genes in viral replication and pathogenesis (139). Infectious cDNA clones can be especially helpful for the study of non-structural protein function in viral replication and assembly. In addition, infectious cDNA clones of RNA viruses can be used as vaccines against the virus from which it was derived or for a foreign gene(s) of another pathogen to induce humoral or cellular immunity against recombinant proteins. Viruses are themselves the most natural gene transfer vehicles.

Because of their large genomic size as compared to smaller RNA viruses, there was no coronavirus infectious cDNA clones. In the last few years, infectious clones of coronaviruses such as MHV, TGEV, HCoV and IBV have been generated. IBV infectious cDNA clones have been constructed using vaccinia virus as a cloning vector

(31). However, the vaccinia system is time consuming because of its selection process for the recombinant vaccinia virus containing infectious cDNA clones of coronaviruses. It is also cumbersome to produce mutations in coronavirus genes inside of vaccinia virus. Casai et al. mentioned that using the *in vitro* assembly technique with certain modifications was not successful in rescuing infectious cDNA clones of IBV in their study. However, in our study we showed that construction of an infectious cDNA clone of IBV using an *in vitro* assembly strategy is possible. We hypothesize that these differences are a matter of technique. The only technical difference is the use of unique restriction enzymes to inhibit self-ligation of each fragment instead of treating DNA fragments with phosphatase. Another factor may include protecting DNA from UV damage during the cloning process.

Furthermore, our study found several sequence differences between viruses even though a Vero cell adapted Beaudette strain of IBV was used by both ourselves and by Casai et al. These sequencing results are summarized in Table 2. Interestingly, our lab strain of IBV has five additional nucleotides compared to published sequence data (22) and an insertion between IG of E and M ORF that increases the genome size to 27613 nts without affecting any ORF. Therefore, as long as the virus genome maintains the TRS and start codon of the ORFs, certain small nucleotide changes in the viral genome can be tolerated. This might indicate one mechanism this large RNA virus has evolved to effectively survive notwithstanding its lack of polymerase proofreading ability.

Boursnell et al. (22) mentioned that IBV polymerase has a higher fidelity as compared to vesicular stomatitis virus (VSV) that shows several sequence differences

between independent cDNA clones of same region. In our study, we found several sequence differences between individual clones for the same regions amplified in the same condition at the same time. These sequence differences could occur during reverse transcription reactions or during PCR amplification. However, considering the polymerase properties of RNA viruses, it cannot be excluded that IBV polymerase produces quasi-species of genomic subgenomic RNA conferring viral evolution such as seen in retroviral replication. The study of the properties of coronavirus polymerases including fidelity and the discontinuous nature of the polymerase is an interesting area of investigation. It is possible that such studies could lead to the discovery of the mechanisms of evolution and survival when coping with a high rate of recombination and a lack of proofreading ability during the replication of a relatively large RNA genome.

In summary, an infectious cDNA clone of Vero cell adapted, attenuated Beaudette strain of IBV was constructed using *in vitro* assembly and no see'm technology that was previously used for the construction of TGEV and MHV. Compared to MHV for which individual amplicons are not completely stable during passage in the bacterial host, IBV amplicons are very stable after several passages and subsequent manipulations. The infectious cDNA clone of the Beaudette strain maintained in our laboratory is 5 nucleotides longer than the Beaudette strain of IBV originally sequenced. The virus rescued from the infectious cDNA clone showed the undistinguishable properties as parental wild type virus. As a marker, a single nucleotide change was made

in ORF5b region and the mutation was conserved in the virus rescued from the infectious cDNA clone.

CHAPTER III

EXPRESSION OF HETEROLOGOUS PROTEIN, GREEN FLUORESCENT PROTEIN USING INFECTIOUS cDNA CLONE OF INFECTIOUS BRONCHITIS VIRUS (IBV)

INTRODUCTION

Infectious bronchitis virus (IBV) is a long recognized problem for the poultry industry and has been identified as a causative agent of avian infectious bronchitis since 1937 (158). Problems controlling virus infection and disease include a high rate of mutation and high recombination frequencies causing new variants that cannot be protected with live vaccines. Therefore, it has been difficult to develop an efficient vaccine against IBV. Even though IBV is one of the fist described coronaviruses, there is little known about the molecular characteristics of the virus. In the past three years, however, there has been enormous advancement in coronavirus research. Among the major advancements is the development of several infectious cDNA clones of coronaviruses that include IBV, MHV-A59, TGEV and human coronavirus (HCoV) 229E (31, 185, 201, 202). Three different approaches have been used to produce infectious cDNA clones of coronaviruses.

The first approach uses bacterial artificial chromosomes (BAC) as a cloning vector that is used to construct the infectious cDNA clone of TGEV (2). This approach overcomes the cloning size limitation and stability of the genes in conventional cloning plasmid

vectors. However, the infectious cDNA in BAC is not stable in bacterial culture because some parts of viral sequences are known to be toxic to bacteria. To overcome this problem, an intron was inserted in the toxic region. Because cDNA transfected to the cells targets the nucleus, the intron will be spliced out when processed in the nucleus and then translocated into the cytoplasm (67). The cDNA has been used to express foreign proteins and green fluorescent protein and shown to induce lactogenic immunity in sows {Sola, 2003 #103). TGEV cDNA has also been engineered as a replication-competent, propagation-deficient virus vector by deleting E protein from the construct.

The second approach toward the creation of infectious cDNA constructs uses vaccinia virus as a cloning vector. By this method, IBV and HCoV infectious cDNA clones have been made (31, 185). Using this method, an infectious cDNA clone of IBV was constructed using vaccinia virus to show that S protein can confer host tropism by switching the S protein with other strains of IBV that have different cell tropism (30).

The third approach uses an *in vitro* assembly technique by which the entire genome of MHV and TGEV are cloned into plasmid vectors into several fragments and then the inserts are prepared by restriction enzyme digestion and ligated *in vitro* (201) (202). Using special characteristics of certain restriction enzymes such as SapI or BsmBI, non-palindromic sequences are recognized and cleaved outside of the recognition sequences leaving 3 to 4 nts overhangs at both 3’ and 5’ ends. These 3’ and 5’ ends can only be religated with the compatible sequences. By using the inherent properties of these enzymes, it is possible to introduce restriction enzyme recognition sequences in PCR products that can be cleaved out when digested.

Coronaviruses have several accessory proteins. Their genomic locations vary depending on the virus and most of their functions are not known. These proteins are referred to as group specific genes. MHV has four group specific genes including 2a, HE, ORF4 product and 5a. Only the function of HE protein has been described and is known as a structural gene, but it's presence is not necessary for viral replication or infection. Other group specific genes of MHV, except HE, also have been shown not to be necessary for viral replication *in vitro*, but they may function in the natural host. When these accessory proteins are deleted from MHV, the pathogenicity is significantly decreased. Therefore, these genes are good candidate genes for viral attenuation (51). IBV also has several group specific genes including 3a, 3b, 5a and 5b. Nucleotide sequence analysis has shown that 5a and 5b have the potential to encode two polypeptides of 7.4 and 9.5 kDa, respectively (21). Expression of these proteins has been shown in virus infected cells (105). Expression of 5a and 5b proteins has been detected throughout the cell with some apparent concentration at the perinuclear location (105). It has been reported that a natural IBV mutant with a premature termination codon in 3b expresses a truncated form of the viral protein that is not necessary for viral replication (163). These data suggest that IBV accessory proteins may also not be necessary for viral survival, at least *in vitro*.

In chapter II, I described a successful construction of an infectious cDNA clone of IBV-Beaudette, exploiting *in vitro* assembly and "no see'm technology". In this study, I wanted to answer the question whether IBV accessory proteins are necessary for viral replication *in vitro* using the infectious cDNA clone. For the following study, we sought to manipulate the cDNA clone of IBV for use as a gene transfer vector for the expression of

foreign protein in virus infected cells. In this study, we hypothesized that IBV 5a protein is not important for IBV survival *in vitro*. To resolve this issue, ORF5a ORF was replaced with enhanced green fluorescent protein (EGFP) ORF.

MATERIALS AND METHODS

Viruses and Cells

A Vero cell culture adapted Beaudette strain of IBV was obtained from American Type Culture Collection (ATCC, Manassas, VA) and then plaque purified three times in the laboratory before use. The virus was propagated in the African green monkey kidney, Vero cell line obtained from ViroMed Laboratory (Minnetonka, MN) and maintained in Dubecco's modified Eagle medium (DMEM) containing 5% fetal bovine serum (FBS) supplemented with penicillin G (100 unit/ml) and streptomycin (100 ug/ml). The baby hamster kidney cell line, BHK-21, was also obtained from Viromed and maintained in D-MEM containing 10% FBS supplemented with antibiotics as described for the Vero cells above.

PCR Amplification and Cloning

The overall cloning strategy is illustrated in Figure 15. Three regions were PCR amplified to replace ORF5a with enhanced green fluorescence protein ORF (EGFP).

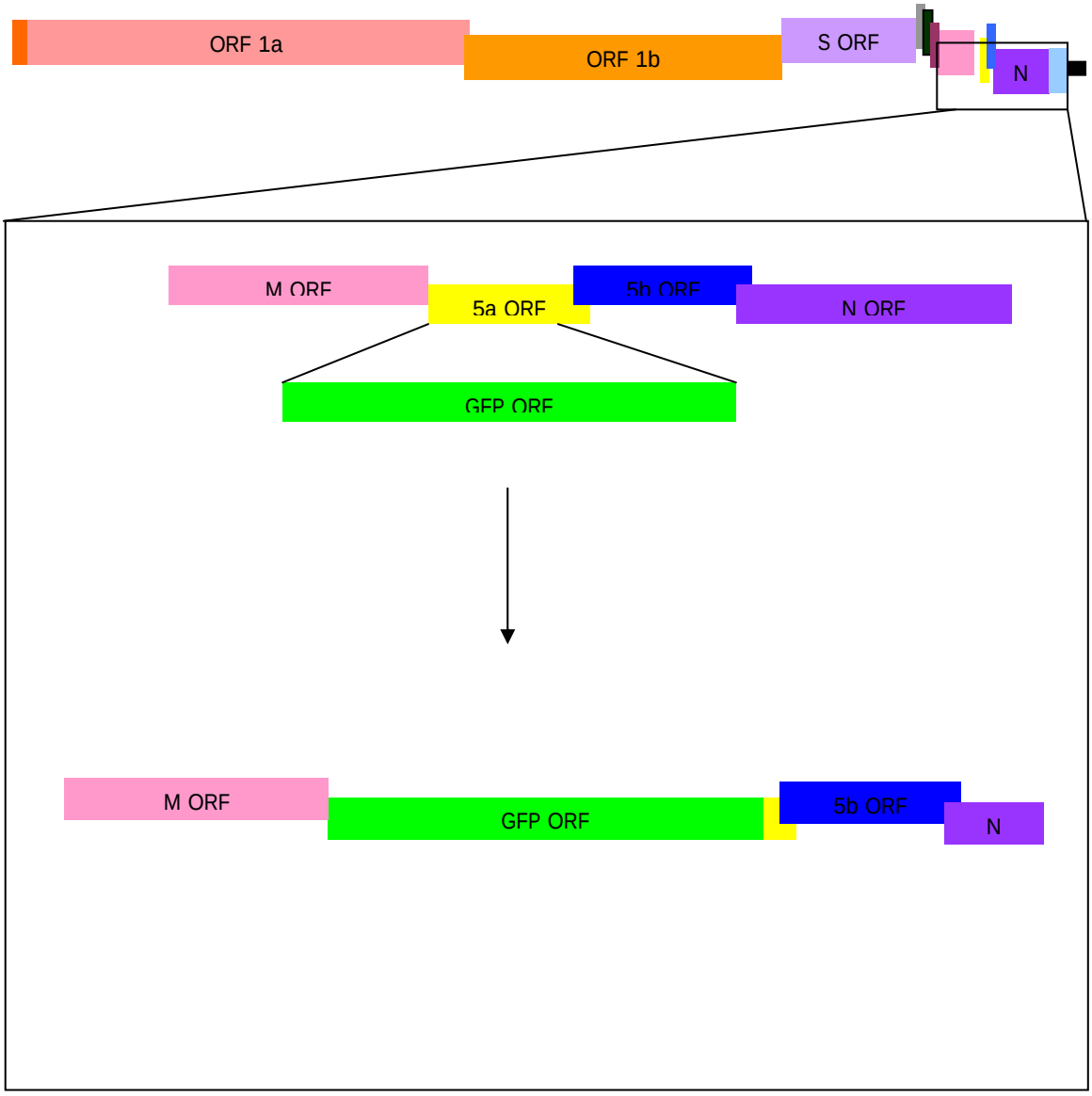

FIG. 15. Schematic of cloning strategy used to replace enhanced green fluorescent protein with ORF5a. From ORF 4 to the start codon of ORF5a, EGFP ORF, 3' end of ORF5a including a stop codon though 3' end of IBV genome will be cloned to produce three independent amplicons. These amplicons' inserts were cut out with BsmBI restriction enzyme and *in vitro* ligated to assemble an amplicon that has gene from ORF4 to 3' end of IBV. This was further subcloned using BamHI restriction enzyme to produce BPG5 amplicon that has all the structural genes of IBV except ORF5a that is replaced with ORF EGFP.

ORF M and the intergenic region of ORF M and 5a including the start codon of ORF 5a, and the 3' end of ORF 5a including stop codon through end of 3' UTR of IBV were PCR amplified using primer pairs listed on Table 3. EGFP was PCR amplified from pLEGFP-N1 vector (Clontech, Palo Alto, CA) as a template using a primer pair that has been designed to have BsmBI restriction enzyme recognition sequence at the each 3' and 5' ends. To replace EGFP with IBV 5a ORF, no see'm technology was employed (202). Neighboring genes of the 5a ORF have been engineered to be compatible with EGFP ORF using a BsmBI restriction enzyme as illustrated in Figure 16. For PCR amplification upstream and downstream of ORF5a, the P5 amplicon described in chapter II was used as a template.

For PCR amplification, the Expand High Fidelity PCR system (Roche, Indianapolis, IN) was used throughout the study and primer pairs used for PCR cloning though this study were listed in Table 3. For EGFP PCR amplification, 50 ng of pLEGFP-N1 vector (Clontech laboratories Inc., Palo Alto, CA), 10 pM of each forward and reverse primer (GFPSF and GFPER respectively), 1 ul of 10 mM deoxynucleotide triphosphate (dNTP), 5 ul of 10X PCR buffer number 3 (Roche), 8 ul of 25 mM $MgCl_2$, and 0.75 ul of thermostable DNA polymerase mixture were added into 200 ul PCR tubes and distilled water was added to bring the total reaction volume to 50 ul. Reaction condition for the EGFP PCR amplification includes an initial denaturation at 94°C for 2 minutes followed by 30 cycles of denaturation at 94°C for 10 seconds, annealing at 55°C for 30 seconds and elongation at 72°C for 30 seconds. The final step was an elongation at 72°C for 7 minutes.

TABLE 3. Sequences of primer pairs used for construction of IBVG

Primer	Nucleotide Sequence	Location in IBV genome
GFPSF	5′ **CGTCTC**ATGGTGAGCAAGGGCGAGGAG 3′	
GFPER	5′ **CGTCTC**CGCTTACTTGTACAGCTCGTCC 3′	
5ASR	5′ **CGTCTC**CACCATCGTCCGTATTTGTTAAGT 3′	25574-25592
5AEF	5′ **CGTCTC**TAAGCGTATACGCCCACCCA 3′	25658-25678
BMF	5′ ATGGCGGAAAATTGCACACTTGATTC 3′	24509-24535
GNRT	5′ TTTTTTTTTTTTTTTTTTTTGCTCTAACTCTATACTAGCC 3′	27593-27613

5a ORF and its neighboring sequence

CAAAAACTTAACAAATACGGACGATGAAA
GCGTATACGCCCACCCAATC
GTTTTTGAATTGTTTATGCCTGCTACTTT
CGCATATGCGGGTGGGTTAG

GFP sequences including start and stop codon

ACCATGGTGAGCAAGGGCGAGGAGCTG CTCGGCATGGACGAGCTGTACAAGTAAAGC
TGGTACCACTCGTTCCCGCTCCTCGAC GAGCCGTACCTGCTCGACATGTTCATTTCG

5ASR
5′ CAAAAACTTAACAAATACGGACGATGGTGGAGACG 3′
3′ GTTTTTGAATTGTTTATGCCTGCTACCACCTCTGC 5′

GFPSF
5′ CGTCTCATGGTGAGCAAGGGCGAGGAGCTGTTCAC 3′
3′ GCAGAGTACCACTCGTTCCCGCTCCTCGACAAGTG 5′

5a S and GFP S junction after ligation

CAAAAACTTAACAAATACGGACGA TGGTGAGCAAGGGCGAGGAGCTGTTCAC
GTTTTTGAATTGTTTATGCCTGCTACCA CTCGTTCCCGCTCCTCGACAAGTG

GFPE R
5′ CTCGGCATGGACGAGCTGTACAAGTAAGCGGAGACG 3′
3′ GAGCCGTACCTGCTCGACATGTTCATTCGCCTCTGC 5′

5a E F
5′ CGTCTCTAAGCGTATACGCCCACCCAATC 3′
3′ GCAGAGATTCGCATATGCGGGTGGGTTAG 5′

GFP stop codon and ORF5a 3’ end junction sequence after ligation

CTCGGCATGGACGAGCTGTACAAGT AAGCGTATACGCCCACCCAATC
GAGCCGTACCTGCTCGACATGTTCATTCG CATATGCGGGTGGGTTAG

FIG. 16. “No see’m technology” used to replace EGFP with ORF5a. Pink nucleotides denote BsmBI restriction enzyme sequence inserted primer pairs. Red nucleotides denote start codon or stop codon of EGFP and ORF5a. Underlined sequences are the primer used to amplified each gene by PCR.

The 5ASR and BMF were used as reverse and forward primers, respectively, for amplification upstream of ORF5a and ORF M. 50 ng of the template, amplicon P5, 10 pM of each forward and reverse primer, 1 ul of 10 mM of each deoxynucleotide triphosphate (dNTP), 5 ul of 10X PCR buffer number 3 (Roche), 8 ul of 25 mM $MgCl_2$, and 0.75 ul of thermostable DNA polymerase mixture were placed in 200 ul PCR tubes and distilled water was added to bring the total reaction volume to 50 ul. Reaction conditions for the PCR amplification includes an initial denaturation at 94°C for 2 minutes followed by 30 cycles of denaturation at 94°C for 10 seconds, annealing at 55°C for 60 seconds and elongation at 68°C for one minute. The final step was an elongation at 68°C for 7 minutes.

The 5AEF and GNRT were used as forward and reverse primers respectively for amplification downstream of ORF5a to the 3' UTR of IBV. 50 ng of template, amplicon P5, 10 pM of each forward and reverse primer, 1 ul of 10 mM deoxynucleotide triphosphate (dNTP), 5 ul of 10X PCR buffer number 3 (Roche), 8 ul of 25 mM $MgCl_2$, and 0.75 ul of thermostable DNA polymerase mixture were added into 200 ul PCR tubes and the total reaction volume was brought to 50 ul with distilled water. Reaction conditions for the PCR amplification includes an initial denaturation at 94°C for 2 minutes followed by 30 cycles of denaturation at 94°C for 10 seconds, annealing at 55°C for 30 seconds and elongation at 68°C for one minute 20 seconds. The final step was an elongation at 68°C for 7 minutes.

Following amplification, 2 ul of each PCR product was run on a 1% agarose gel in Tris-acetate-EDTA (TAE) buffer containing ethidium bromide (EtBr) and the results

were recorded using a FluoChem TM gel analysis system (Alpha Innotech, Corporation, San Leandro, CA). Each PCR product was purified from a 1% agarose gel containing crystal violet (2 ug/ ml). DNA bands were excised from the agarose gel and then purified using a QIAquick Gel Extraction Kit (QIAGEN Inc., Valencia, CA) following the manufacture's directions. The concentration of gel purified PCR products were measured with a SmartSpec 3000 spectrophotometer (BIO-RAD, Hercules, CA). Each PCR product was ligated into a cloning vector. EGFP and upstream of ORF5a were ligated into a pSTBlue-1 (Novagen, Darmstadt, Germany) according to manufacturer's directions. Briefly, equal-molar ratios of PCR product and pSTBlue vector were ligated for 2 hours at 16°C and then transformed into chemically competent NovaBlue cells (Novagen, Darmstadt, Germany). Final constructs of the EGFP ORF and the upstream region of ORF5a were named as pSTBGFP and pSTBM, respectively. The region beginning from downstream of ORF5a to 3'UTR of IBV was ligated into the pCR-XL-TOPO cloning vector (Invitrogen, Carlsbad, CA) for 5 minutes at room temperature and transformed into chemically competent Oneshot competent cells (Invitrogen). The final construct was named pCRB3'. Transformed bacteria were plated on Luria-Bertani (LB) medium agar plates containing kanamycin (5 ug/ml) and grown overnight at 37°C. Mini-prep cultures were prepared from the transformed colonies to confirm the insert size and direction using unique restriction enzyme recognition sequence in the inserts. The construct was confirmed with nucleotide sequencing using the universal primers SP6 and T7 primers synthesized in a commercial laboratory.

To assemble recombinant P5G amplicon, pSTBGFP, pSTBM and pCRB3' were digested with BsmBI. Appropriate inserts from each amplicon were gel purified as described above. Because pCRB3' has an internal BsmBI restriction recognition sequence other then BsmBI sites at 3' and 5' ends inserted by PCR mutagenesis, two DNA bands were prepared from pCRB3' BsmBI digestion reactions. Also, pCRB3' was used as a cloning vector after the restriction enzyme digestion because it has a pCR-XL-TOPO backbone. Equal-molar amounts of each insert were overnight ligated using T4 DNA ligase (3 units/ul, Promega) at 16°C and transformed into chemically competent one shot competent cells (Invitrogen) by heat shock at 45°C for 30 seconds. Subcloned recombinant P5G were confirmed by restriction enzyme digestion and sequencing.

Nucleotide Sequencing

Each amplicon DNA was prepared from transformed bacterial midi-cultures grown overnight and DNA templates were prepared using QIAGEN mini prep kit (QIAGEN). Sequencing was performed using the ABI prism BigDye Terminator Cycle Sequencing Ready Reaction Kit (Applied Biosystems Inv., Foster City, CA). For a standard sequencing reaction, 350-500 ng of plasmid DNA was mixed with 2 ul of BigDye mixture (ABI) and 10 pM of primers. The remainder of the reaction mixture was adjusted to 6 ul with distilled water. Sequencing reactions were performed using a GeneAmp thermocycler (PerkinElmer, Boston, MA) using conditions that included pre-denaturation at 96°C for 2 minutes and 30 cycles of 96°C for 30 seconds, 52°C for 15

seconds and 60°C for 4 minutes. Non-incorporated nucleotides were removed using micro Bio-spin chromatography columns (BIO-RAD, Hercules, CA) and completely dried using a vacuum drier. Completed sequencing reactions were sent to the Gene Technology Laboratory in the Department of Biology in Texas A&M University. Sequences were read using an ABI automatic sequencer 3100 (ABI).

Analysis of Sequence

Sequence data were analyzed using SDS biology workbench (http://workbench.sdsc.edu) (San Diego Supercomputer Center, University of California, San Diego, CA). LALIGN program was used for DNA and amino acid sequence comparison. The TACG program was used to search for restriction enzyme digestion profiles for cloning purposes. The SIXFRAME program was used to convert DNA sequence into amino acid sequence.

Assembly of a Full-length IBV Infectious Construct

Inserted DNAs from each amplicon were excised with the appropriate restriction enzymes. PI was digested with XhoI (Promega, Madison, WI) and then treated with calf intestine phosphatase (CIP) (Promega) to inhibit self-ligation. CIP treated DNA was phenol:chloroform extracted, ethanol precipitated and then digested with restriction enzyme SapI (New England Biolabs Inc., Beverly, MA). P2–1, P2-2 and P3-1 amplicons were double digested with restriction enzymes SapI and BsmBI. When the buffer

conditions were not compatible, after one restriction enzyme digestion, the reactions were ethanol precipitated and then the reaction was reconstituted with the appropriate buffer and in the appropriate volume before adding the second restriction enzyme. Except for the BsmBI restriction enzyme digestion that needed to be incubated at 55°C, the restriction enzymes were incubated at 37°C. P3-2 and P4 amplicons were single digested with restriction enzyme BsmBI. The P5 amplicon was digested with restriction enzyme EcoRI (Promega), then CIP treated and digested with BsmBI. Each DNA insert was run on a TAE agarose gel (0.8 to 1%) containing 2.4 ug/ml crystal violet rather than ethidium bromide to avoid UV-induced DNA damage that could impact subsequent manipulations of DNA fragments. Target size inserts were excised from the agarose gel and the DNA inserts were extracted using a QIAquick Gel Extraction kit (QIAGEN Inc, Valencia, CA) following the manufacturer's instruction.

A relatively high concentration of T4 DNA ligase (20 U/ul, Promega) was used to assemble infectious cDNA of IBV. Ligation reactions were incubated at 16°C overnight, before inactivating by incubating at 65°C for 10 minutes. An aliquot of the ligation reactions were run on an agarose gel to confirm the ligation. The appropriately sized larger ligation fragments were agarose gel purified and then ligated step-wise with other fragments. The final ligation reaction of P1 through P3-1 and P3-2 though P5 were pooled without further purification and then ligated overnight at 16°C.

RNA Preparation

Viral RNA was prepared from the supernatant of IBV infected Vero cells or recombinant IBVG rescued from transfection. Briefly, Vero cells were infected with 0.1 multiplication of infection (m.o.i) and incubated in a CO_2 incubator at 37°C until the cells showed more than 80% cytopathogenic effect (CPE) such as syncytia formation. The cells showing extensive CPE were frozen and thawed three times and then cell debris were precipitated by centrifugation at 3,000 rpm using a table top centrifuge (CR 412; Jouan Inc. Winchester, VA). The supernatants were then ultracentrifuged at 35,000 rpm for 2 hours at 4°C using an L7-55 ultracentrifuge (Beckman, Palo alto, CA) with an SW55Ti swing bucket rotor to pellet the virus. The viral pellet was re-suspended in small volumes of TEN (10 mM Tris-Cl, pH 8.0, 1 mM ethylendiaminotetraacetate (EDTA), pH 8.0 and 0.1 M NaCl) buffer.

TRIZOL reagent (Invitrogen, Carlsbad, CA) was used to extract the RNA from the re-suspended viral pellet following the manufacturer's instruction. Briefly, 1000 ul of TRIZOL reagent were added to 200 ul of viral pellet suspension in TEN buffer before mixing thoroughly by inverting the microfuge tube several times. The mixture was incubated for 5 minutes at room temperate, 200 ul of chloroform were added and then mixed thoroughly by inversion. This mixture was incubated at room temperature for 3 minutes. To separate the aqueous and the organic phases, the mixture was centrifuged at 12,000 rpm for 15 minutes at 4°C using a microcentrifuge (5417 R; Eppendorf, Hamburg, Germany). The upper phase was then transferred to a new nuclease free microfuge tube and a 0.5 volume of isopropanol was added to precipitate the RNA. After

a 10 minute incubation at room temperature, the RNA was pelleted by centrifugation at 12,000 rpm for 15 minutes at 4°C. Before suspending the RNA pellet with nuclease-free water, the RNA pellet was washed with 70% ethanol, then briefly air-dried. The RNA solution was quantified using a SmartSpec^{TM} 3000 spectrophotometer (BIO-RAD, Hercules, CA) and stored at –70°C until it was used for Northern blot analysis or RT-PCR.

Northern Blot Analysis

Preparation of a random primed isotope labeled probe.

To prepare a random primed probe against GFP and the 3' UTR, pGEGFP and pGEBN-2 were used as templates for *in vitro* transcription reactions. The template DNA was digested with PstI restriction enzyme and then phenol:chloroform extracted followed by ethanol precipitation to remove contaminating RNase. One ug of template was used for an *in vitro* transcription and labeling reaction using T7 RNA polymerase (Promega). Briefly, 4 ul of 5X transcription buffer, 2 ul of 100 mM DTT, 1 ul of RNase inhibitor (Promega, 30 units/ul), 4 ul of rNTP mix containing 2.5 mM rCTP, rATP, and rGTP, 1.2 ul of 200 uM rUTP, 5 ul of [α^{32}P] rUTP (Perkin-Elmer), 1.3 ul of T7 RNA polymerase (20 units/ul) were used in a 20 ul reaction. The reaction was incubated at 37°C for one hour and then ethanol precipitated. The probe was resuspended in deionized formamide and stored at –20°C. Radioisotope activity was measured with a liquid scintillation system (Beckman Coulter Inc., Fullerton, CA).

RNA transfer

To transfer RNA to nylon membranes, 1 ul of each *in vitro* transcribed RNA was run on a denaturing agarose gel containing formaldehyde following the standard methods (153) with modifications. RNA was denatured with sample buffer containing 1/10 v/v of 10X formaldehyde gel–running buffer (0.2M 3-(N-norpholino) propanesulfonic acid (MOPS) (pH 7.0), 80 mM sodium acetate and 10 mM EDTA (pH 8.0)) with formaldehyde, 1/2 v/v of formamide, 2 ug of ethidium bromide, and 1/10 v/v of formaldehyde gel-loading buffer (50% glycerol, 0.25% bromophenol blue, 0.25% xylene cyanol FF). RNA and sample buffer were mixed, denatured at 70°C for 5 minutes and chilled on ice. A 1% denaturing agarose gel containing formaldehyde was prepared with a 1/10 volume of 10 X formaldehyde gel running buffer and formaldehyde to give a 2.2 M final concentration. Each RNA sample was loaded on the agarose gel and run at 90 V in 1 X formaldehyde gel-running buffer. At one hour intervals, the buffer from each reservoir was collected, mixed and returned for electrophoresis. When the xylene cyanol dye front was at the bottom of the gel, electrophoresis was terminated. The gel was washed several times with distilled water and then soaked in 0.05 N NaOH for 20 minutes and exposed to long wavelength UV light for 60 seconds. The gel was then washed with distilled water and soaked for 20 minutes in 10 X sodium chloride sodium citrate (SSC) buffer. RNA from the gel was transferred overnight to a nylon membrane by capillary transfer in 10 X SSC. RNA transfer was confirmed by ethidium bromide staining of the nylon membrane and the molecular weight markers were indicated with pencil. The membrane was then fixed by UV cross-linking for 30 seconds.

Hybridization reaction

The nylon membrane was hybridized to random primed α-^{32}P labeled probes with an activity of 2 x 10^7 cpm. Hybridization reactions were performed using an autoblot hybridization oven (Bellco Glass Inc., Vineland, NJ). Hybridization conditions included incubation at 55°C for 12 hours in hybridization buffer containing 50% deionized formaldehyde, 2 X Denhardt's reagent, 5 X SSC and 0.1% SDS. After hybridization, excess probe was removed with 1 X SSC, 0.1% SDS, followed by three washes for 20 minutes each at 68°C in 0.2 X SSC and 0.1% SDS. After hybridization, the nylon paper was exposed to an image plate (IP) for 20 minutes to one hour, depending on the signal intensity. The image was analyzed using a BAS-1800 II phosphoimage reader (Fusifilm Electronic Imaging Ltd. Tokyo, Japan) and analyzed using the Image gauge V3.12 and L processor V1.72 programs.

***In vitro* Transcription and Electroporation**

Capped runoff T7 transcripts were synthesized *in vitro* from *in vitro* ligated IBV cDNA using an mMessage mMachine kit (Ambion, Austin, TX.) as described by the manufacturer with some modifications. Twenty ul of the IBV RNA transcription reaction mixture was prepared with three ul of 30 mM GTP stock and incubated at 37C° for 2 hrs.

To increase the efficiency of virus production, N transcript was also prepared for co-transfecting with the entire IBV transcript. pGEMN-1 was used as a template for N

transcripts. The plasmid was digested with a PstI restriction enzyme (Promega) to linearize the template and then phenol:chloroform extracted followed by ethanol precipitation to remove any RNase contamination. The DNA was resuspended with diethyl pyrocarbonate (DEPC) treated distilled water. One ug of the template was used for an *in vitro* transcription reaction using mMESSAGE mMACHINE ^{TM} T7 Ultra kit (Ambion, Austin, TX.). A poly(A) tail was added to the transcript with *E. coli* Poly(A) polymerase. Both transcripts were used, with or without precipitation with 7.5 M lithium chloride containing 50 mM EDTA.

BHK-21 cells were grown to subconfluence (about 70%) before electroporation. BHK-21 cells were treated with trypsin to detach them from flasks. The cells were washed twice with ice cold DEPC treated PBS and then resuspended in the cold PBS with 2 x 10^7 per ml infectious cDNA transcription reaction. N transcript was mixed with the cells in a 1.5 ml microcentrifuge tube. The cells and RNA mixture were transferred immediately to 2 mm gap electroporation cuvettes (electroporation cuvettes plus model No. 620, BTX, Genetronics, Inc. San Diego, California) and then electroporated at 850 V, 25 mΩ at resistance 720 Ω using an electro-cell manipulator 600 (BTX, Genetronics, Inc. San Diego, California) with three consecutive pulses. After electroporation, cells were incubated at RT for 10 minutes and the transfectant was diluted 1 to 20 in complete DMEM containing 10% FBS and resuspended with 1 x 10^6 Vero cell per 100 mm petri-dish.

Plaque Staining and Plaque Purification

Virus preparations were serially diluted 10-fold in DMEM lacking FBS. Then, 200 ul of each dilution was inoculated per well of six well cell culture plates that had been seeded with monolayers of Vero cells. After a one hour incubation, residual virus was removed by washing the cells twice with PBS before overlaying the cells with 0.8% agarose containing 1 X DMEM, 1% FBS and antibiotics. The cells were incubated until plaques were observed. For plaque staining, the agarose overlay was removed using a spatula, the cell monolayers were air dried briefly and overlaid with 2 ml of crystal violet staining solution per well. After 10 minutes, excessive crystal violet was removed and the cells were washed several times with PBS to remove residual crystal violet. For plaque purification, the agarose over the plaques were picked with a 1000 λ micropipette and suspended in 1 ml DMEM without FBS. Before inoculating, the plaque suspension, the viral suspension was incubated at 4°C overnight and inoculated to Vero cell in 6 well plates described before.

Kinetics of Viral Replication

Vero cells were infected with wild type IBV Beaudette strain and the IBV Beaudette strain derived from an infectious cDNA clone and plaque purified three times. The Vero cells were seeded in 35 mm petri dishes at a concentration of 10^6 per dish. The cells were infected with three plaque forming units per cell for an hour and then the media were replaced with DMEM containing 1% FBS with antibiotics, and 5, 10, 12, 19,

and 21 hours after infection, the cells were harvested and stored at –70°C for subsequent plaque assays.

RESULTS

PCR Cloning and Mutagenesis

To replace ORF5a with EGFP from the start codon of ORF5a, no see'm technology was used because there was no unique restriction enzyme recognition sequence at the start codon and the overall cloning strategy is illustrated in Figure 15 and 3-2. PCR mutagenesis was used to create a BsmBI restriction enzyme recognition sequences at the each junctions between EGFP and ORF5a. Three regions were amplified by PCR as shown in Figure 17. The sizes of each PCR product are ~700 nts for EGFP ORF, ~ 1.2 kb for M ORF though start codon of 5a, and ~2.5 kb for the end of 5a ORF through 3' UTR of IBV including 14 nts of poly(A) tail was amplified. These PCR products were gel purified as described in the Materials and Methods and ligated to pSTBlue or pCR-XL-TOPO vectors resulting in three amplicon, pSTBGFP, pSBM and pCRB3'. pSTBlue cloning vector was used for pSTBGFP and pSBM construction except for the pCRB3 that used the pCR-XL-TOPO cloning vector. Three amplicons were amplified by maxi prep culture. 10 ug of pSBM and pCRB3' were digested with XhoI restriction enzyme first and then ethanol precipitated for further digestion with BsmBI. pSTBGFP, pSBM and pCRB3' were digested with BsmBI enzyme. Because

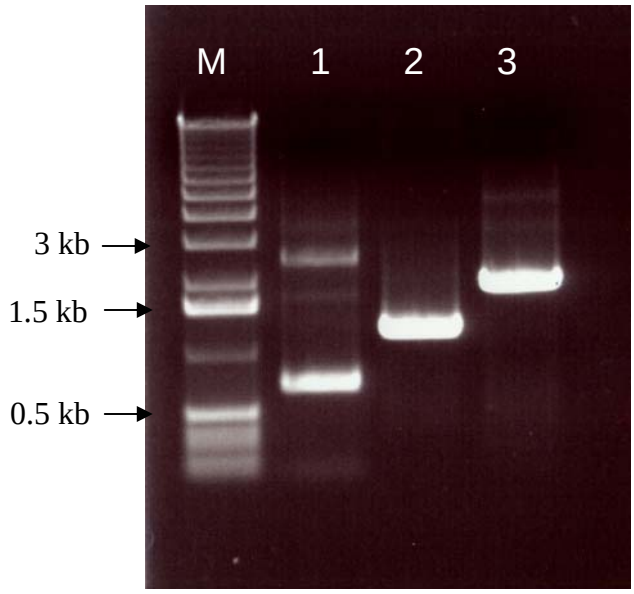

FIG. 17. Site-directed mutagenesis by PCR. To replace the enhanced green fluorescent protein (EGFP) gene with ORF5a, BsmBI restriction enzyme recognition sequences were created by PCR on the EGFP ORF and an ORF5a neighboring sequence. These restriction enzyme sites will be further used to religate EGFP with ORF5a neighboring gene.

M; 1 kb DNA ladder, lane 1; PCR product of EGFP, lane 2; PCR product from ORF M to start codon of ORF5a, lane 3; PCR product from 3' end of ORF5a to 3' UTR of IBV genome including the poly(A) tail.

pCRB3’ has an internal BsmBI recognition sequence, digestion of pCRB3’ with BsmBI produces two insert fragments. Inserts were separated from the vector by electrophoresis and purified from the gel after restriction enzyme digestion. These four fragments were ligated in one reaction. Because each BsmBI overhang has a unique sequence, theoretically the products can only be religated with the correct fragment. Furthermore, only the final ligation product with all the fragments having a pCR-XL-TOPO backbone can survive after transformation. Transformed plasmid constructs were verified by restriction enzyme digestion and the correct construct was named as pIBVG11.

Because the pIBVG11 construct only has the M ORF though 3’ UTR of IBV, further subcloning was performed using the pIBVG11 construct and amplicon P5 to produce P5 containing every structural genes as well as EGFP. Because pIBVG11 and P5 have the same orientation and M ORF has a unique BamHI restriction recognition sequence, both constructs were digested with BamHI. Then pIBVG11 was treated with phosphatase to prevent self-ligation. The larger fragment from P5 BamHI reaction containing the S ORF and part of the M ORF was replaced with a smaller fragment of pIBVG11 digested with BamHI. The ligation reaction was transformed into chemically competent cells and the recombinant GFP5 amplicon with EGFP instead of 5a were cloned. This GFP5 construct was sequenced using a primer upstream of 5a ORF to make sure there were no mutations during cloning. Sequences of EGFP and the upstream region of the ORF5a junction is shown in Figure 18. The EGFP ORF was replaced with ORF 5a exactly as intended. Furthermore, sequences, upstream of 5a and downstream of 5a did not have any unintentional mutations. This shows that IBV infectious cDNA is

ORF5a and GFP start codon junction after ligation

CAAAAACTTAACAAATACGGACGA TGGTGAGCAAGGGCGAGGAGCTGTTCAC
GTTTTTGAATTGTTTATGCCTGCTACCA CTCGTTCCCGCTCCTCGACAAGTG

A

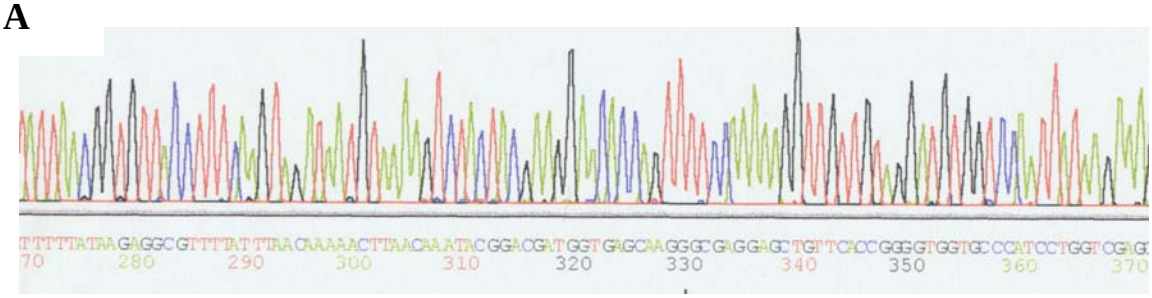

B

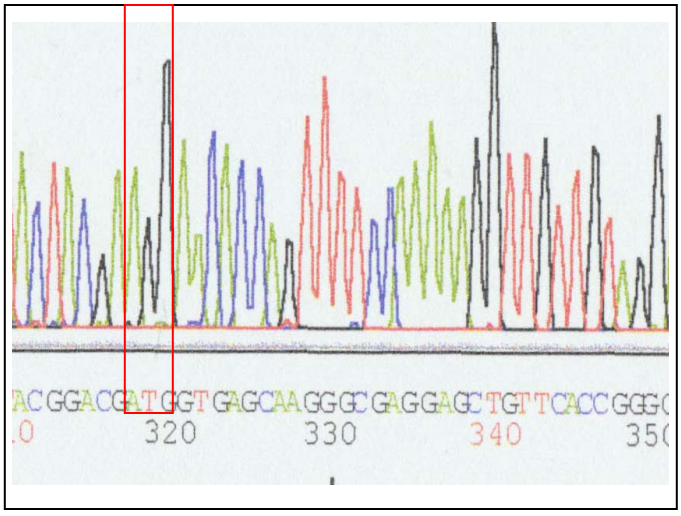

FIG. 18. Sequence verification of EGFP ORF and ORF5a replacement. The start codon was denoted in a red box. B is the enlargement of part of A containing start codon. Prior to the start codon, sequences are identical as the intergenic sequences between ORF5a, the start codon is from EGFP.

very stable for further manipulation and subsequent serial cultures compared to the MHV infectious cDNA.

Sequencing Analysis

After verifying sequences of the EGFP junction, it was assumed that there were no mutations introduced by PCR procedure because the PCR product was comparatively small and high fidelity thermostable polymerase developed for cloning of large PCR product was used to amplify the regions. After *in vitro* transcription and transfection, an infectious cDNA clone of IBV expressing EGFP could not be rescued. It was then decided to sequence the entire GFP5 amplicons and three nucleotide changes in 3' UTR introduced by PCR were identified. The region with mutations was replaced with the same region of amplicon P5 and used to produce the infectious cDNA clones of recombinant IBV with the EGFP.

***In vitro* Assembly**

Based on the experience acquired during development of the infectious cDNA clone of IBV, I used an orderly *in vitro* ligation approach for construction of the cDNA clone of IBV as described in chapter II. P1 and P2-1 were ligated and P2-2 and P3-1 were ligated then P3-2 and P4 were ligated together and GP5L, and P5S were ligated. The larger ligation products from each of the four ligation reactions were separated by electrophoreses on agarose gels. The ligation products of P1/P21-1 and P2-2/P3-1 were ligated and ligation products of P3-2/P4 and P5 were ligated separately and without

further purification, these two ligation reactions were pooled and ligated overnight at 16°C.

In vitro Transcription and Electroporation

Approximately 0.2 pM of cDNA template was used for an *in vitro* transcription reaction. To confirm that the *in vitro* transcript had a full-length RNA with the EGFP gene instead of ORF5a, a Northern blot analysis was performed using two different probes. One probe used was the same as that used for the 3'UTR of IBV for the infectious cDNA construction. The other probe was specific for EGFP. Because it has been shown that the N transcript increased the rescue of coronaviruses after transfection (56, 184, 201), N ORF transcripts were used as described in chapter II.

In vitro transcripts of IBVG cDNA and N ORF were electroporated into BHK-21 cells. Because BHK-21 cells are not susceptible to IBV infection, Vero cells were overlaid on the electroporated BHK-21 cells. Two days after transfection, apparent CPE was noticed in the cells transfected with total cellular RNA from IBV infected cell and three days after transfection, CPE was noticed in the cells transfected with recombinant IBVG infectious cDNA. To confirm whether this recombinant virus expressed EGFP, the cells were examined under the UV microscope. As shown in Figure 19, the recombinant IBVG expressed EGFP that 5a was replaced with EGFP. RT-PCR was used to confirm the size difference of ORF 5a region.

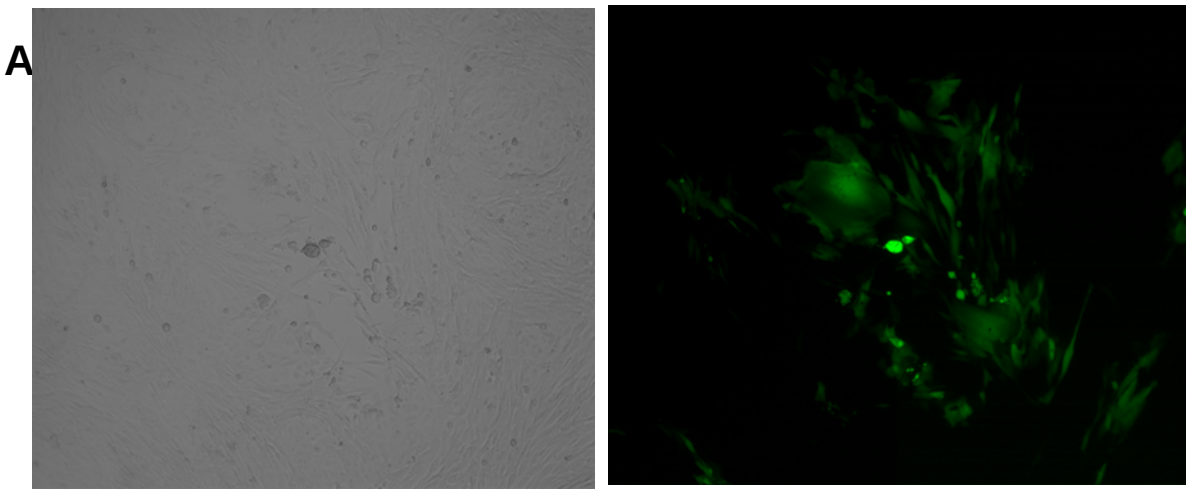

FIG. 19. Recombinant infectious cDNA clone which 5a ORF was replaced with EGFP ORF was viable in infected cells and expressed EGFP. Cells transfected with recombinant infectious cDNA expressing EGFP. (A) Cells 3 days after transfection with the recombinant EGFP IBV transcript as viewed under a phase contrast microscope (B) Cells transfected with recombinant EGFP IBV transcript after 3 days transfection under an UV microscope.

DISCUSSION

Infectious cDNA clones of RNA viruses are one of the most powerful tools to study the function of viral proteins, especially during viral replication and viral assembly. The availability of infectious cDNA clones for many small RNA viruses has resulted in a tremendous development of RNA virus research. With the development of molecular biological techniques, it has been possible to construct infectious cDNA clones of coronaviruses overcoming the difficulties the large genome size and toxicity of the coronavirus genome in bacterial hosts. Several groups used three different approaches to construct infectious cDNA clones of coronaviruses, including MHV, TGEV, HCoV and IBV. These infectious cDNA clones have been developed to express foreign genes for potential gene expression system, gene transfer vector, and as vaccine. Infectious cDNAs of coronaviruses can be used to study the molecular biology of the viruses. Many studies have been done using defective interfering (DI) particle or targeted recombination in MHV and FIPV before the development of infectious cDNA clones. However, it is hard to conclude the result of mutants, especially deletion mutation studies, because of the extremely high rate of recombination during viral replication and transcription and the multiple crossovers during the recombination process. Therefore, using infectious cDNA clones is a more reasonable approach compared to using a targeted mutagenesis approach to study coronaviruses.

Coronaviruses have several small ORFs, some of these ORF are expressed in virus infected cells. However, the exact functions of these genes are not well understood. These small genes, referred as group specific genes, are not necessary for viral

replication *in vitro* in MHV, even though deletion mutant viruses of the region were significantly attenuated. IBV has four small group specific antigens including 3a, 3b, 5a and 5b.

Previously, we were successful in constructing an infectious cDNA clone of the Vero cell adapted Beaudette strain of IBV. In this study, we wanted to use the infectious cDNA clone to resolve the issue of whether a small group specific antigen is necessary for the survival of IBV *in vitro*. One of the group specific genes, 5a ORF was replaced with green fluorescent protein. The C-terminal region of 5a protein was kept for the expression of 5b protein. After *in vitro* assembly and electroporation, a recombinant IBV 5a deletion mutant of IBV expressing EGFP was successfully rescued and the fluorescence was observed. By sequence analysis and northern blot analysis, it was confirmed that there was no unintentional mutations in the amplicons used to construct the recombinant clone. Based on this study, 5a protein of IBV is not necessary for survival of IBV *in vitro*, even though the function of the protein is not yet understood.

In our laboratory, group specific antigens of several different strains of IBV have been sequenced and shown that the proteins are conserved among different strains, especially putative 5a. Therefore, even though these proteins are not necessary for viral survival *in vitro*, it is possible that these proteins are important for viral replication in the natural host or maybe a protective protein against host defense mechanisms, such as cytokine mimicry molecules or anti-apoptotic proteins.

In summary, in this study, a recombinant infectious cDNA clone of IBV containing EGFP instead of 5a ORF was constructed. By sequence analysis of

amplicons, targeted mutagenesis was confirmed and the recombinant infectious cDNA was viable implying that the 5a protein is not necessary for IBV amplification in Vero cells. This also showed the possibility of using IBV as a gene transfer vector for poultry.

CHAPTER IV

RECOMBINANT SEMLIKI FOREST VIRUS REPLICON CAN BE PACKAGED INTO IBV VIRIONS WITHOUT IBV *CIS* ACTING SIGNAL SEQUENCE

INTRODUCTION

Infectious bronchitis virus (IBV) has been a recognized problem in the poultry industry since 1931 (158). IBV has been controlled by traditional attenuated live vaccine strategies. The high mutation rate and the high frequency of recombination of IBV, however, has made it necessary to seek alternative methods which can control the disease more effectively and to lower the possibility of emerging recombinant IBV originating from field and vaccine strains (reviewed in (39)).

IBV belongs to the order *Nidovirales* in the Coronaviridae family. Coronaviruses cause clinical disease in a number of animals, including humans (34, 126). Most coronaviruses cause disease only in the species from which they were isolated and, if they replicate in cell culture, predominantly replicate only in cell lines derived from their natural hosts (197). IBV has four known structural proteins, including the spike glycoprotein (S) that is post-translationally cleaved into S1 and S2, the integral membrane glycoprotein (M), the small membrane protein (E) and the nucleocapsid protein (N) (94). S, M, and E proteins are envelope proteins that are embedded in the host-derived bilipid layer of the viral envelope. The S protein is not required for virus budding process but is responsible for viral attachment and entry, determining host

specificity and creating the binding site for cellular receptors. Receptors for MHV, TGEV and HCoV have been identified (46, 54, 77, 136, 200). Determinants responsible for the generation of neutralizing antibodies also lie on N terminal of the S protein, especially S1 (40, 81, 84, 183).

Both M and E proteins localize in the *cis*-Golgi compartment and several studies have suggested that the M and E proteins are critical for intracellular viral budding (47, 50, 98, 118). Expression of the E proteins of MHV and IBV, in the absence of other viral proteins, produces vesicles that can be released from the cells (47, 120). However, co-expression of M and E are necessary in TGEV and bovine coronavirus (BoCV) to make virus like particles (VLP) (13, 17, 193). The N protein binds to the viral RNA genome, producing the ribonucleoprotein complex (10, 43, 125, 130, 144). The N protein is the only viral protein that is phosphorylated and the phosphorylation of the N protein has been implicated as having a role in viral RNA and protein interaction.

Packaging mechanisms of several coronaviruses, such as MHV, BoCV and more recently TGEV have been studied (44, 60, 124). MHV packages only viral genomic RNA, whereas IBV and BoCV have been shown to package not only genomic RNA, but also subgenomic RNAs (204). Using defective interfering (DI) RNA and deletion mutagenesis, Makino et al. have located packaging signal sequences in MHV and shown that M protein and packaging signal sequence interaction might mediate specific viral genomic RNA packaging into MHV virions (124, 129). The BoCV packaging signal sequence was identified based on a sequence homology search of BoCV genome with the MHV packaging signal sequence (44). In the presence of the packaging signal

sequence, non-viral RNA can be packaged into BoCV or MHV virions, respectively. However, it is interesting that one of the naturally occurring BoCV DIs, Drep can be packaged into BoCV virions without the known packaging signal sequence (44). Recently, the packaging signal sequence of TGEV has been identified by Escobars et al. (60). They also showed that highly purified TGEV only packaged genomic RNA like MHV and the packaging signal sequence is located within the 649nts at the 5’ UTR of TGEV genomic RNA (60). In the study, it was suggested that not only the packaging signal sequence itself, but also viral replication status, is important for efficient viral packaging in TGEV.

Semliki forest virus (SFV), a prototype of the alphavirus genus and a member of the *Togaviridae* family, has a single-strand, positive sense RNA genome (160). Several members of this group, in particular Sindbis virus (SIN), SFV, and Venezuelan equine encephalitis (VEE) virus, have provided valuable tools for understanding virus structure and replication. The two alphaviruses most extensively studied in laboratories, SIN and SFV, are generally considered avirulent for humans. The alphavirus genome is approximately 11.7 kb and is encapsidated within an icosahedral capsid protein (177). Cells infected with these viruses synthesize abundant amounts of viral genomic RNA and subgenomic RNA. The genomic and subgenomic RNAs are 5' capped and 3' polyadenylated (27). The 5’ two thirds of the genomic RNA encode the replicase polyproteins, which are cleaved to produce nsP1, nsP2, nsP3 and nsP4 products. The subgenomic RNA is identical in sequence to the 3' one-third of the genomic RNA and encodes the structural proteins. These include the capsid protein, which interacts with

the genomic RNA to form the viral nucleocapsid and two membrane glycoproteins (reviewed in (177)). Cytoplasmic replication of the genomic and subgenomic RNAs is mediated by the replicase gene using a full-length negative sense RNA as a template. The viral structural proteins are translated from the subgenomic mRNA as a polyprotein that is processed into the individual virion components by a viral protease.

Specific genomic RNA packaging of alphaviruses has been shown to depend on the packaging signal sequence that is present only on the genomic RNA. The signal sequences of SIN, SFV and Ross river virus (RRV) have been identified and used to make replicon vectors that can replicate and be packaged into virions produced by a helper construct. The helper construct encodes viral structural genes under the control of the subgenomic RNA promoter. Because the helper construct lacks the packaging signal sequence, it results in aberrant self-packaging, in spite of its high concentration in the cytoplasm during viral replication and transcription. The replicon, packaged into the newly made virions, can infect cells and replicate, but the progeny RNAs cannot be transmitted into new cells because they lack the viral structural proteins.

As an alternative to live attenuated vaccines, we were interested in developing a new type of vaccine by combining the advantages of two different viruses, IBV and SFV. In this study, as a prerequisite of this purpose, we decided to develop recombinant SFVs as a tool for identifying the packaging signal sequence of IBV. The SFV replicon can be replicated in the cytoplasm to produce high concentrations of this RNA. We hypothesized that if a recombinant SFV has the packaging signal sequence of IBV, the replicon can be packaged into an IBV virion. To our surprise, however, with or without any candidate

packaging signal sequence of IBV, rSFV can be packaged into an IBV virion suggesting IBV virion can be a useful candidate for pseudotyping of SFV vectors for specific targeting to respiratory system of poultry as a vaccine or for gene transfer.

MATERIALS AND METHODS

Viruses and Cells

A Vero cell culture adapted Beaudette strain of IBV was obtained from American Type Culture Collection (ATCC, Manassas, VA) and then plaque purified three times in the laboratory before use. The virus was propagated in the African green monkey kidney Vero cell line obtained from the ViroMed Laboratory (Minnetonka, MN) and maintained in Dubecco's modified Eagle medium (DMEM) containing 5% fetal bovine serum (FBS) supplemented with penicillin G (100 unit/ml) and streptomycin (100 ug/ml).

RNA Preparation

Viral RNA was prepared from the supernatant of IBV infected Vero cells. Briefly, Vero cells were infected with 0.1 multiplication of infection (m.o.i) and incubated in a CO_2 incubator at 37°C until the cells showed more than 80% cytopathogenic effect (CPE), such as syncytia formation. The cells showing extensive CPE were frozen and thawed three times and then cell debris was removed by centrifugation at 3,000 rpm using a tabletop centrifuge (CR 412; Jouan Inc. Winchester,

VA). The supernatants were then ultracentrifuged at 35,000 rpm for 2 hours at 4°C using an L7-55 ultracentrifuge (Beckman, Palo Alto, CA) with an SW55Ti swing bucket rotor to pellet the virus. The viral pellet was re-suspended in small volumes of TEN (10 mM Tris-Cl, pH 8.0, 1 mM ethylendiaminotetraacetate (EDTA), pH 8.0 and 0.1M NaCl) buffer.

TRIZOL reagent (Invitrogen, Carlsbad, CA) was used to extract the RNA from the re-suspended viral pellet following by the manufacturer's instruction. Briefly, 1 ml of TRIZOL reagent was added to 200 ul of viral pellet suspension in TEN buffer and then mixed thoroughly by inverting the microfuge tube several times. The mixture was incubated for 5 minutes at room temperature before adding 200 ul of chloroform and mixing thoroughly. The mixture was then incubated at room temperature for 3 minutes. To separate the aqueous and the organic phases, the mixture was centrifuged at 12,000 rpm for 15 minutes at 4°C using a microcentrifuge 5417 R (Eppendorf, Hamburg, Germany). The upper (aqueous) phase was then transferred to a new nuclease free microfuge tube and a 500 ul of isopropanol were added to precipitate the RNA. After a 10-minutes incubation at room temperature, the RNA was pelleted by centrifugation at 12,000 rpm for 15 minutes at 4°C. Before suspending the RNA pellet with nuclease free-water, the RNA pellet was washed with 70% ethanol, and then briefly air-dried. The RNA solution was quantified using a SmartSpec ^{TM} 3000 spectrophotometer (BIO-RAD, Hercules, CA) and stored at –70°C until further use as a template for RT-PCR or as a size marker for electrophoresis.

RT-PCR and PCR Amplification of Target Genes

The 3'UTR, 5'UTR, 1b region of DI 61(175) and bovine coronavirus packaging signal sequence homologous region of IBV (44) were cloned by RT-PCR. Sequences and locations of primers used in this study are listed in Table 4. The first cDNA reaction was done using the SUPERSCRIPT^{TM} First-Stranded Synthesis System for RT-PCR (Invitrogen, Carlsbad, CA) according to manufacture's directions. Briefly, 1-2 ug of RNA in 8 ul of nuclease free water with 1 ul of 10 mM deoxynucleotide-triphosphate (dNTP) and 10 pM of each reverse primer BE5R, IBVPR, and CPR were incubated in a 70°C water bath for 5 minutes. Reactions were chilled on ice for 5 minutes before adding 2 ul of 10X first strand buffer, 4 ul of 25 mM $MgCl_2$, 0.1 M dithiothreitol (DTT), 1 ul of RNase inhibitor, (50 units/ul, Invitrogen) and then incubated at 42°C for 50 minutes after adding 1 ul of Superscript reverse transcriptase (50 Units/ul). The reaction was terminated by incubating at 75°C for 15 minutes before degrading RNA template with 1 ul of *E. coli* RNase H (2 Units/ul), and incubating for 20 minute at 37°C.

Two ul of each completed reverse transcription reaction was used as a template for PCR reaction. A 50 ul reaction included 6 ul of 25 mM $MgCl_2$, 1 ul of 10 mM deoxynucleotide triphosphate (dNTP), 5 ul of PCR buffer A (Promega, Madison, WI) and 1 ul each of 10 pM of forward and reverse primer, and 0.5 ul of Taq polymerase (5 unit/ul, Promega) and distilled water was added to bring the total reaction volume to 50 ul. The BE5R and IBVLF oligos were used as forward and reverse primers, respectively for 5' UTR RT-PCR amplification. The IBVPR and IBVPF primer pair were used for amplification of the region homologous to the bovine coronavirus packaging signal

TABLE 4. Primer pairs used for RT-PCR or PCR amplification and sequencing of recombinant SFV replicons

Name	position	Sequence	polarity
IBVLF	1-26	5′ ACTTAAGATAGATATTAATATATATC 3′	+
BE5R	528-561	5′ GGGAGATACTCCCTGTTTTAG 3′	_
IBVPF	18821-18843	5′ AAATGGCCTAGTAGTTCTGTATG 3′	+
IBVPR	19115-19139	5′ ATACCTTTCTACAAAACTCTCCTC 3′	_
CPF	18200-18224	5′ CCTAAATTTGACCGCATTAGCTTCC 3′	+
CPR	18486-18510	5′ CAATATTGTCGATAGACTGGAGAGC 3′	_
EGFPF2		5′ GGATCCCAAGGGCGAGGAGCTGTTC 3′	+
EGFPR		5′ GGATCCTTACTTGTACAGCTCGTC C 3′	_
SFVR	7440-7466	5′ GGCGCCACCGGCGGCCGTAAAACGTC 3′	_
nsP4F	5761-5780	5′ CGGTGGTGGACAGGCTCACA 3′	+
nsP4R	6001-6200	5′ TCTGTCCAAGCAACTATCCG 3′	_

sequence. CPR and CPF primers were used to amplify the 1b region of CD-61. Reaction conditions included an initial denaturation at 94°C for 5 minutes followed by 30 cycles of denaturation at 94°C for 30 seconds, annealing at 55°C for 30 seconds and an elongation at 72°C for 30 minutes. The final step was an elongation at 72°C for 10 minutes. 10 pM of each forward and reverse primer, GFPF2, and EGFPR with 50 ng of pLEGFP-N1 vector as a template were used for EGFP PCR amplification. For the PCR reaction condition, the same condition described previously was used except for the primer sets. PCR amplification conditions included initial denaturation at 94°C for 5 minutes followed by 30 cycle of denaturation at 94°C for 30 seconds, annealing at 55°C for 30 seconds and elongation at 72°C for 40 seconds. This was followed by 7 minutes incubation at 72°C for the final elongation.

Cloning and Construction of Recombinant SFV Replicons

PCR products were run on 0.7% agarose gels in Tris-acetate-EDTA (TAE) buffer containing ethidium bromide (EtBr). DNA bands of appropriate size were excised from the gels on UV transilluminator and the PCR products from the gels were purified using a QUIAquick Gel Extraction Kit (QIAGEN Inc. Valencia, CA) following the manufacture's directions. The concentration of gel purified PCR products was measured with a SmartSpec 3000 spectrophotometer (BIO-RAD). Each PCR product was ligated into a cloning vector, pSTBlue (Novagen, Darmstadt, Germany) using T4 DNA ligase (Promega). Equal-molar ratios of insert and vector were incubated for 2 hours at 16°C and then transformed into chemically competent NovaBlue cell by the heat shock

method. Transformed bacteria were plated on Luria-Bertani (LB) medium agar plates containing 50 ug/ml ampicillin and grown overnight at 37°C. Each colony was grown overnight in LB media for mini preparation of plasmids. Plasmid prepared by the alkali lysis method and insert size and direction were confirmed by restriction enzyme digestion and nucleotide sequencing. pGEBN-1 described in chapter II was used to subclone the 3'UTR of IBV.

To subclone EGFP as a reporter gene into pSFV-1, pSFV-1 and pSTBEGFP plasmids were digested with BamHI followed by CIP treatment of pSFV-1 to prevent self-ligation. The small DNA fragment of the pSFTBEGFP BamHI digestion reaction was separated from the vector by running in a 0.7% agarose gel and the insert was purified with the gel extraction kit (QIAGEN) following manufacturer's directions. An equal-molar ratio of pSFV-1 and the EGFP insert were ligated overnight and transformed into Oneshot chemically competent cells (Invitrogen, Carlsbad, CA). The plasmids were prepared from the overnight mini culture of the colonies and plasmid having correct orientation of the EGFP gene downstream of SFV subgenomic promoter in the correct frame was confirmed by restriction enzyme digestion and nucleotide sequencing.

Candidate packaging signal sequences were subcloned downstream of EGFP in pSFGFP. pSFGFP was digested with SmaI restriction enzyme and then CIP treated to inhibit self-ligation. Amplicons containing 5' UTR, 3' UTR, ORF1b region and the BoCV packaging sequence homologous region were digested with EcoRI to excise the inserts from the vectors. Inserts were gel purified by agarose gel electrophoresis and to

make the ends blunt, the inserts were treated with T4 DNA polymerase (Promega). These prepared DNA inserts were phosphorylated using T4 DNA kinase (Promega) then ligated to pSFEGFP vector prepared by SmaI digestion and subsequent phosphatase treatment.

Nucleotide Sequencing

Each replicon DNA was prepared from transformed bacterial cultures grown overnight and DNA templates were prepared using Mini Prep kits (QIAGEN Inc., Valencia, CA). Sequencing was performed using the ABI prism BigDye Terminator Cycle Sequencing Ready Reaction Kit (Applied Biosystems, Foster City, CA). A standard sequencing reaction included 350-500 ng of plasmid DNAs mixed with 2 ul of Bigdye mixture (ABI) and 10 pM of primers. The remainder of the reaction mixture was adjusted to 6 ul with distilled water. Sequencing reactions were performed using a GeneAmp thermocycler (PerkinElmer) according to manufacturer's suggestion including a pre-denaturation at 96°C for 2 minutes and 30 cycles of 96°C for 30 seconds, 52°C for 15 seconds and 60°C for 4 minutes. Non-incorporated nucleotides were removed using micro Bio-spin chromatography columns (BIO-RAD, Hercules, CA) and completely dried using a vacuum drier. Completed sequencing reactions were sent to the Gene Technology Laboratory in the Department of Biology at Texas A&M University. Sequences were read using an ABI automatic sequencer 3100 (ABI, Foster City, California).

Analysis of Sequence

Sequence data were analyzed using SDS Biology Workbench (http://workbench.sdsc.edu) (San Diego Supercomputer Center, University of California, San Diego, CA). The LALIGN program was used for DNA and amino acid sequence comparison. The TACG program was used to search for restriction enzyme digestion profiles for the purpose of subcloning. The SIXFRAME program was used to translate the DNA sequence into the amino acid sequence. The MFOLD program (http://bioweb.pasteur.fr/seqanal/interfaces/mfold-simple.html) was used to compare RNA secondary structures.

***In vitro* transcription**

Capped runoff SP6 transcripts were synthesized *in vitro* from each recombinant SFV plasmids that were linearized by SpeI restriction digestion (Promega). Digested plasmids were phenol:chloroform extracted and then ethanol precipitated. Precipitated DNA was dissolved with diethypyrocarobonate (DEPC) treated water. 1.5 ug of template was used for each transcription reaction. *In vitro* transcription was performed using SP6 RNA polymerase (Invitrogen, Carlsbad, CA) following the transcription reaction directions described for the SFV-1 expression vector (Invitrogen). Briefly, 50 ul of transcription reaction consisting of 5X SP6 Buffer (0.2M Tris-HCl pH 7.9, 30 mM MgCl2, 10 mM spermidine- $(HCl)_3$), 20 ul of 2 NTP mix containing 2.5 mM ATP, 2.5 mM CTP, 2.5 mM UTP, 1.25 mM GTP, 5 ul of 10 mM capping analog, 10 mM DTT, 2 ul of recombinant ribonuclease inhibitor (40 units/ul) and 38 units of SP6 RNA

polymerase and the remaining reaction was filled with DEPC treated water. The transcription reaction was performed at 37°C for 2 hours and followed by DNase I digestion to remove template DNA. The transcripts were precipitated with isopropanol and washed with 70% ethanol. The transcripts were resuspended in DEPC treated water and then the concentration of the transcripts was measured using a SmartSpec ™ 3000 spectrophotometer (BIO-RAD, Hercules, CA) before storing at –70°C until used for transfection.

Transfection and Infection

DMRIE-C reagent (Invitrogen) was used for RNA transfection following the manufacturer's instructions. Five ug of *in vitro* transcribed RNA was used for transfection of cells in each 30 mm cell culture dish. Vero cells were seeded in six wells plates the day before transfection. The Vero cells were washed with phosphate buffered saline twice and 2 multiplicities of infection (m.o.i) of IBV Beaudette strain were added for 1 hour at 37°C. After adsorption, the cells were washed twice with PBS and then transfected with each replicon transcript. The infected cells were washed once with 2 ml of serum free media OPTI-MEM (Invitrogen) per well. Five ug of each transcript was suspended in 1 ml of OPTI-MEM containing 10 ul of DMRIE-C reagent. The reaction was thoroughly mixed by briefly vortexing and then overlaid on the Vero cells. After four hours incubation, medium was replaced with complete DMEM containing 10% FBS and further incubated for 16 more hours.

RNaseA and Antibody Treatment

Hyper-immune serum from chicks infected with IBV Beaudette strain was kindly provided by Dr. King (USDA, Southeast Poultry Research Laboratory, Athens, GA). The neutralizing titer of the antibody was determined. The antibody was two fold serially diluted with DMEM. One hundred plaque forming units (PFU) of IBV in 200 ul of DMEM was prepared by diluting viral stock with DMEM. Serial two-fold diluents of antibody and 100 PFU of IBV were incubated at 37°C for 30 minute and the mixture was overlaid on six well plates seeded with monolayers of Vero cells. After five days incubation, antibody titer was measured as the lowest dilution factor that completely neutralized plaque formation.

Passage 0 (P0) supernatants were treated with RNase A or neutralizing antibody before passage 1 (P1). A 500 ul aliquot of each passage 0 supernatant was incubated with a 2 fold dilution of antibody or 20 ul of RNase A (10 mg/ml), for 30 minutes at 37°C. A control was similarly incubated without serum or RNaseA. After incubation, the supernatants were inoculated onto fresh Vero cells seeded on 35 mm cell culture petri dish as passage 1.

Northern Blot Analysis

Preparation of a random primed isotope labeled probe.

Three different probes were used in this study to differentiate coronavirus subgenomic RNAs, SFV genomic RNA, GFP, genomic and subgenomic RNA of

recombinant SFV containing GFP. pGEBN-1 that is described in chapter II was used as a probe specific to the genomic and subgenomic RNAs of IBV. pGEGFP described in chapter III was used as a specific probe against GFP in recombinant SFV genomic RNA and subgenomic RNA. Part of nsP4 of pSFV was PCR amplified and cloned into pGEM vector and used as a specific probe against SFV genomic RNA. To prepare random primed probes, each amplicon was digested with PstI restriction enzyme and then phenol:chloroform extracted followed by ethanol precipitation to remove contaminating RNase. One ug of template was used for an *in vitro* transcription and labeling using T7 RNA polymerase (Promega). Briefly, 4 ul of 5X transcription buffer, 2 ul of 100 mM DTT, 1 ul of RNase inhibitor (Promega, 30 unit/ul), 4 ul of rNTP mix (2.5 mM rCTP, rATP, and rGTP, 1.2 ul of 200 uM rUTP, 5 ul of [α-^{32}P] rUTP) and 1.3 ul of T7 RNA polymerase (20 units/ul) were used in a 20 ul reaction. The reaction was incubated at 37°C for 1 hour and then ethanol precipitated. The probe was resuspended in deionized formamide and stored at –20°C. Radioisotope activity was measured with a liquid scintillation system (Beckman coulter Inc., Fullerton, CA) before using for hybridization reaction.

RNA transfer

To transfer RNAs to a nylon membrane for northern hybridization analysis, less than 5 ug of each total cellular RNAs was prepared from each sample and electrophoresed on a denaturing agarose gel containing formaldehyde following the standard method (153) with the following modifications; RNAs were denatured with

sample buffer with 1/10 v/v formaldehyde gel–running buffer (0.2M 3-(N-norpholino) propanesulfonic acid (MOPS) (pH 7.0), 80 mM sodium acetate and 10 mM EDTA (pH 8.0)), 1/5 v/v of formaldehyde, 1/2 v/v of deionized formamide, 2 ug of EtBr, and 1/10 v/v of formaldehyde gel-loading buffer (50% glycerol, 0.25% bromophenol blue, 0.25% xylene cyanol FF) per RNA sample containing a total 15 ul of reaction volume. RNAs and sample buffer were mixed and then denatured at 70°C for 5 minute and chilled on ice. Then, a 1% denaturing agarose gel was prepared with a 1/10 volume of 10 X formaldehyde gel running buffer and formaldehyde to give final concentration of 2.2 M formaldehyde. Each RNA sample was loaded on the agarose gel and run at 90 V in 1 X formaldehyde gel-running buffer. After one hour, the buffer from each reservoir was collected, mixed and returned to continue the electrophoresis. When the xylene cyanol dye front was at the bottom of the gel, electrophoresis was terminated. The gel was washed several times with distilled water and then soaked in 0.05N NaOH for 20 minutes and exposed to long wavelength UV light for 60 seconds. The gel was then washed with distilled water and soaked for 20 minutes in 10 X sodium chloride sodium citrate (SSC) buffer. RNA from the gel was transferred to a nylon membrane by capillary transfer in 10 X SSC overnight. RNA transfer was confirmed by EtBr staining of the nylon membrane and the molecular weight controls were marked with a pencil. The membrane was then fixed by UV cross-linking for 30 seconds with GS gene linker UV chamber (BIO-RAD).

Hybridization reactions

Duplicate or triplicate nylon membranes with the same samples were prepared and hybridized with different probes at the same time. The nylon membranes were hybridized with a different specific probe having specific activity of 2 x 10^7 cpm/ug that was α-^{32}P labeled. Hybridization reactions were performed using an autoblot hybridization oven (Bellco Glass Inc., Vineland, NJ). Hybridization conditions included incubation at 55°C for 12 hours in hybridization buffer containing 50% deionized formaldehyde, 2 X Denhardt's reagent, 5 X SSC and 0.1% SDS. After hybridization, excess probe was removed by washing with buffer containing 1 X SSC, 0.1% SDS, followed by three washes for 20 minutes each at 68°C in 0.2 X SSC and 0.1% SDS. After hybridization, the nylon paper was exposed to an image plate (IP) for 20 minutes to one hour depending on the signal intensity. The image was analyzed using a BAS-1800 II phosphoimage reader (Fusifilm Electronic Imaging Ltd. Tokyo, Japan) and analyzed using the Image gauge V3.12 and L processor V1.72 programs.

RESULTS

RT-PCR and Cloning

Based on a study which has shown that the IBV virion can package genomic RNA, as well as subgenomic RNA (38), I hypothesized that there must be more than one packaging signal sequence in IBV. To identify the packaging signal sequence, I selected several regions as putative packaging signal sequences of IBV based on several studies.

The 5’ and 3’ untranslated region of the IBV have been shown to be important for viral replication and transcription (48). Based on a study by Penzes et al, part of the ORF1b region in DI, CD-61 was selected as a candidate for a packaging signal sequence of IBV (140). CD-61 can be efficiently packaged into IBV virions. Another candidate signal sequence was selected after a homologous sequence search with bovine coronavirus signal sequences using the same approach as that used by Cologna et al. (44) to identify the packaging signal sequence of BoCV. The result was that only one candidate gene in IBV showed homology with BoCV and shared a similar location as the BoCV packaging signal. Packaging signal sequences of MHV, BoCV and putative candidate packaging signal sequence of IBV were compared in Figures 20 and 21. These four candidates genes were RT-PCR amplified using total cellular RNA prepared from IBV infected cells.

The MHV packaging signal sequence was identified by deletion mutation studies using DIs of MHV (124). We considered using a DI system to find the packaging signal sequence of IBV, but we rationalized that the interpretation of data in a DI system would be complex, especially if there was more than one packaging signal sequence for IBV. Therefore, we chose the more straightforward approach of constructing a system that can replicate by itself, while containing only one *cis* signal sequence of IBV per construct. We decided to use the SFV vector as the RNA expression system because it can replicate by itself in the absence of the IBV replicase. Furthermore, SFV only replicates in the cytoplasm so its recombinant RNA can be carried by the IBV virion in the presence of a packaging signal sequence.

```
 ALIGN calculates a global alignment of two sequences
BCV-pack                                                  290 nt vs.
MHV-packaging                                             291 nt
scoring matrix: DNA, gap penalties: -16/-4
73.3% identity;        Global alignment score: 722


           10        20        30        40        50
BCV  AATGGCGTAGTGGTGGACAAGGTTGGAGACACAGATTGTGTGTTTTATTTTGCTGTGCG-
     :::::::::::: ::::: :: ::::::::  : :::   :  ::::  ::::::::::::
MHV  AATGGCGTAGTTGTGGAGAAAGTTGGAGATTCTGATGTGGAATTTTGGTTTGCTGTGCGT
             10        20        30        40        50        60

    60        70        80        90       100       110
BCV  AAAGAGGGTCAGGATGTCATCTTCAGCCAATTCGACAGCCTGAGAGTCAGCTCTAACCAG
     ::::: ::: : ::::: ::::::::::     :  :::::   :   :::  : ::: :
MHV  AAAGACGGTGACGATGTTATCTTCAGCCGTACAGGGAGCCTTGAACCGAGCCATTACCGG
             70        80        90       100       110       120

   120       130       140       150       160       170
BCV  AGCCCACAAGGTAATCTGGGGAGTAATGAACCCGGTAATGTCGGTGGTAATGATGCTCTG
     ::::::::::::::::::::  :::::      ::: :: :: : :::::::: :::::
MHV  AGCCCACAAGGTAATCTGGGTGGTAATCGCGTGGGTGATCTCAGCGGTAATGAAGCTCTA
             130       140       150       160       170       180

   180       190       200       210        220       230
BCV  GCAACCTCCACTATCTTTACACAAAGCCGTGTTATTAGC-TCTTTTACATGTCGTACTGA
     ::      :::::::::::: :::::: :  :::::: : ::::: :::  :::  : ::
MHV  GCGCGTGGCACTATCTTTACTCAAAGCAGA-TTATTATCCTCTTTCACACCTCGATCAGA
             190       200       210        220       230

    240       250       260       270       280       290
BCV  TATGGAAAAAGATTTTATAGCTTTAGATCAAGATGTGTTTATTCAGAAGTAT
      ::::: :::::::::: : ::::::: : :::::::: :::   :: :::
MHV  GATGGAGAAAGATTTTATGGATTTAGATGATGATGTGTTCATTGCAAAATAT
   240       250       260       270       280       290
```

FIG. 20. Sequence alignment of MHV and BoCV packaging signal sequences.

```
ALIGN calculates a global alignment of two sequences
 version 2.0uPlease cite: Myers and Miller, CABIOS (1989) 4:11-17
BCV-pack                                                  290 nt vs.
ibv-pack                                                  319 nt
scoring matrix: DNA, gap penalties: -16/-4
53.9% identity;        Global alignment score: 74


               10           20        30        40        50
BCV     -AATGGCGTAGTGGT---GGACAAGGTTGGAGACACAGATTGTGTGTTTTATTTTGCTG-
         :::::: :::: ::   : :  : : : :: :    ::::    :: :: : ::::::
ibv     AAATGGCCTAGTAGTTCTGTATGATGATAGATATGGTGATTACCAGTCTTTTCTTGCTGC
               10        20        30        40        50        60

           60         70              80         90       100
BCV     TGCGAAAGAGGGTC-AGGATGT-CA-----TCTTCAGCCA-ATTCGACAGCCTGAGAGTC
        ::  :: :  : :: ::  : : ::     :  : ::: : :::   ::  :  :::
ibv     TGATAATGCTGTTCTAGTTTCTACACAGTGTTATAAGCGATATT---CATACGTAGAAAT
               70        80        90       100          110

        110        120          130           140        150
BCV     AGC-TCTAACCAGAGCC--CACAA-GGTA----ATCTGGGGA-GTAATGAACCCGG----
        : : :::::   :  :   :: :: ::::    ::     :: : :  ::::: :
ibv     ACCATCTAATTTGCTCGTTCAGAATGGTATGCCATTAAAAGATGGAGCGAACCTGTATGT
        120       130       140       150       160       170

           160       170       180             190       200
BCV     TAATGTCGGTGGTAATGATGCTCTGG-----CAACCTC-CACTATCTTTACACAAAGCCG
        : ::    ::: ::::: :::  : :     : ::::  ::: ::    :: ::  : ::
ibv     TTATAAGCGTGTTAATGGTGCGTTTGTTACACTACCTAACACAATAAACACCCAGGGTCG
        180       190       200       210       220       230

        210       220       230       240       250       260
BCV     T-GTTATTAGCTCTTTTACATGTCGTACTGATATGGAAAAAGATTTTATAGCTTTAGATC
          ::::: :   :::::  :  ::::: ::: :: ::    :::::: : ::: :
ibv     AAGTTATGAAA-CTTTTGAACCTCGTAGTGACATTGAGCGTGATTTTCTCGCTATGTCAG
        240        250       260       270       280       290

        270       280       290
BCV     AAGATGTGTTTATTCAGAAGTAT
        : ::    ::: :  : : ::::
ibv     AGGAGAGTTTTGTAGAAAGGTAT
         300       310
```

FIG 21. Sequence alignment of BoCV packaging signal sequence and the putative IBV homologue.

We decided to use enhanced green fluorescence protein (EGFP) as a reporter gene in order to verify transfectant replication by UV microscopy before northern analysis. The overall constructs of recombinant SFV replicons are illustrated in Figure 22. EGFP was PCR amplified using a primer pair containing a BamHI restriction enzyme recognition sequence at both the 3' and 5' ends, because the pSFV-1 expression vector has only one cloning site, a BamHI restriction enzyme recognition sequence that contains an internal start codon to express the recombinant protein. The genuine start codon of EGFP was removed and the 5' sequence of EGFP was mutated by PCR mutagenesis to use the SFV vector start codon. The EGFP PCR product was cloned into a TA-PCR cloning vector, pSTBlue (Novagen). The EGFP gene was cut from the cloning vector and then subcloned into SFV-1 digested with BamHI. The direction of EGFP ORF in SFV-1 was verified by PCR amplification using primer sets EGFPF and SFVR as forward and reverse primers, respectively. The recombinant SFV construct with EGFP in the proper orientation was named pSFGFP. Before subcloning the candidate packaging signal sequences into pSFGFP, expression of EGFP from the construct was confirmed by transfection of the construct into BHK-21 and Vero cells. The four RT-PCR amplified candidate IBV packaging signal sequences were cloned into pSTBLUE (Novagen) for further amplification and subcloning into pSFGFP. Except for a BamHI site that was used for the cloning of EGFP, pSFGFP has only one cloning site, SmaI. pSFGFP was digested with SmaI and treated with phosphatase to inhibit self-ligation of the vector. Each candidate sequence was digested from the cloning vector using EcoRI and each end was blunted using T4 DNA polymerase. Each candidate

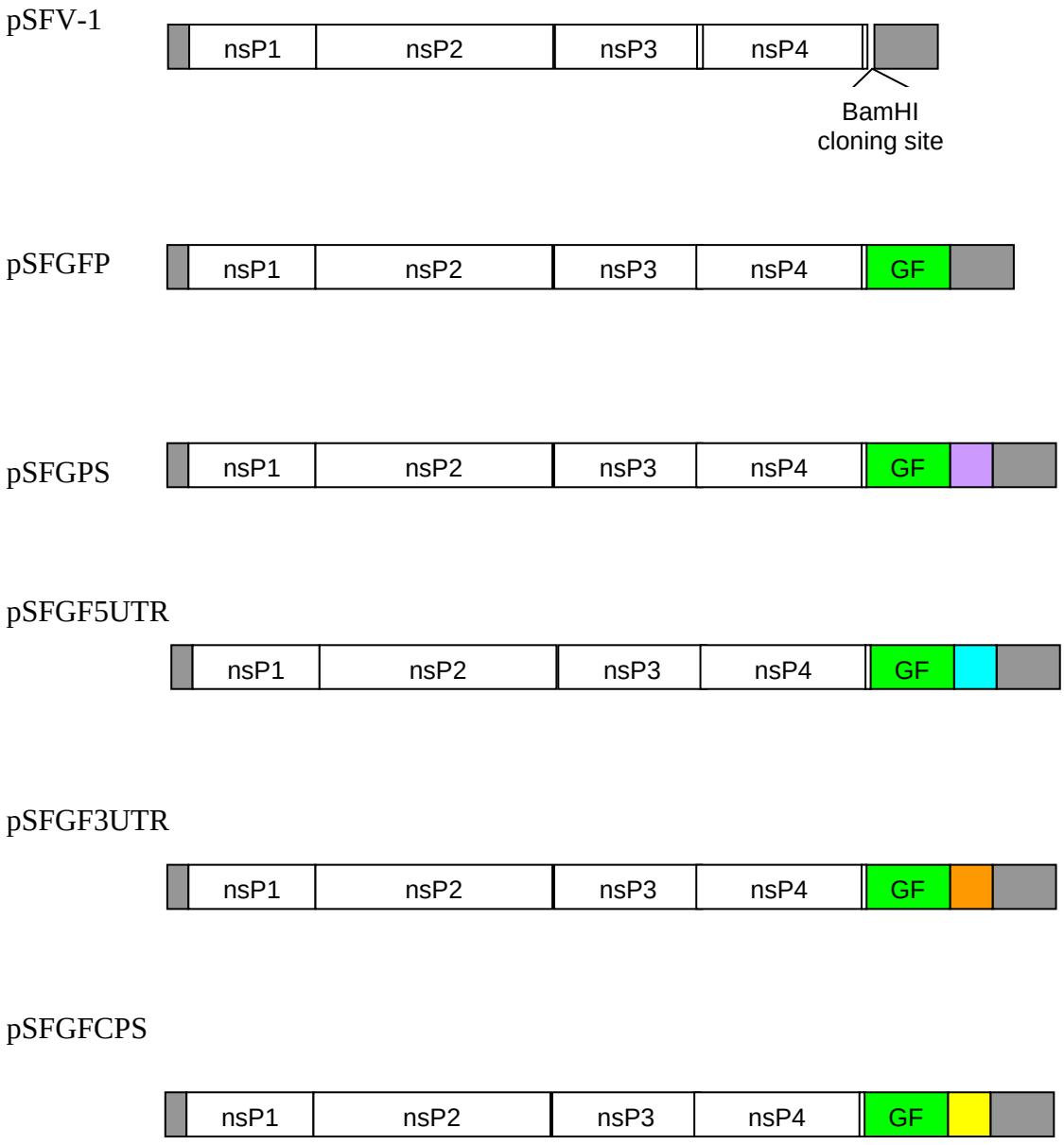

FIG. 22. Schematics of pSFV-1 eukaryotic expression vector and recombinant SFV replicons constructed using pSFV-1 vector. The reporter protein, EGFP was denoted as green boxes. The 3' and 5' untranslated region of SFV were denoted with gray boxes. Each candidate packaging sequence was marked with different colors. Small boxes in front of EGFP represent subgenomic promoter sequence of SFV.

packaging signal sequence was cloned downstream of EGFP. The direction of each candidate sequence in pSFGFP was analyzed by RT-PCR using the forward primer used to clone each gene and SFVR as a reverse primer. Sequencing reactions and analysis were performed to confirm the sequence and direction of each construct using SFVR. Each construct was named as illustrated in Figure 22. The construct with a homologous sequence of the BoCV packaging signal sequence was named pSFGPS and the construct having a sequence 1b region of DI was named pSFGFCPS. The other two constructs having 3' and 5' UTR sequences were referred to as pSFGF3'UTR and pSFGF5'UTR, respectively.

Three different probes were used for northern blot analysis. To identify the replication and transcription of IBV, a probe against the 3'UTR of IBV was used that is described in chapter II. To identify the replication and transcription of each SFV replicon, a probe against EGFP was used as described in chapter III. To differentiate the genomic RNA from subgenomic RNA of each recombinant SFV replicon, a probe against the nsP4 region of SFV was PCR amplified and cloned into a pGEM vector. Each probe was prepared by *in vitro* transcription and labeled by random priming with ^{32}P. Specific interaction of each probe with the target gene was examined by northern blot analysis using *in vitro* transcribed recombinant SFV replicons and total cellular RNA extracted from IBV infected Vero cells. The highly specific interaction of these probes with the target genes was confirmed. The probe against nsP4 showed small amount of non-specific interaction compared to the other two probes.

Recombinant Replicons can be Packaged into IBV Virions

Each replicon was *in vitro* transcribed using SP6 RNA polymerase following the manufacture's instructions, precipitated with isopropyl alcohol and resuspended in DEPC treated water. Before transfection, the concentration of each replicon was quantified with spectrophotometer at OD_{260} and denaturing gel electrophoresis was used to confirm the size of each replicon. The overall experimental procedure is illustrated in Figure 23. Vero cells were infected with IBV Beaudette helper virus at 2 PFU per cell in order to provide virion structural proteins. One hour after infection, each replicon was transfected with DMRIE-C reagent (Invitrogen). Four hours after transfection, the media was replaced with complete DMEM media containing 10% FBS. Vero cells showed extensive syncytia formation 16 hours after infection. The supernatants were harvested and frozen before passaging to new Vero cells and the RNA from the cells was harvested for northern blot analysis using TRIZOL reagent. Passage 0 cellular RNAs were used to confirm the replication and transcription of replicons by northern blot analysis. To verify whether the replicons could be packaged into IBV virions, we passaged the supernatant into fresh susceptible cells instead of identifying the virion RNA from the supernatants after transfection. If the replicon could be packaged into virions, expression of EGFP could be detected using UV microscopy at Passage 1. IBV helper virus that supplied the structural proteins of IBV was inoculated into Vero cells before the transfection of the replicons. The total cellular RNA profile was analyzed by northern blot assays from passage 0 and PASSAGE 1. In multiple experiments, we found that every replicon could be passaged from passage 0 into passage 1

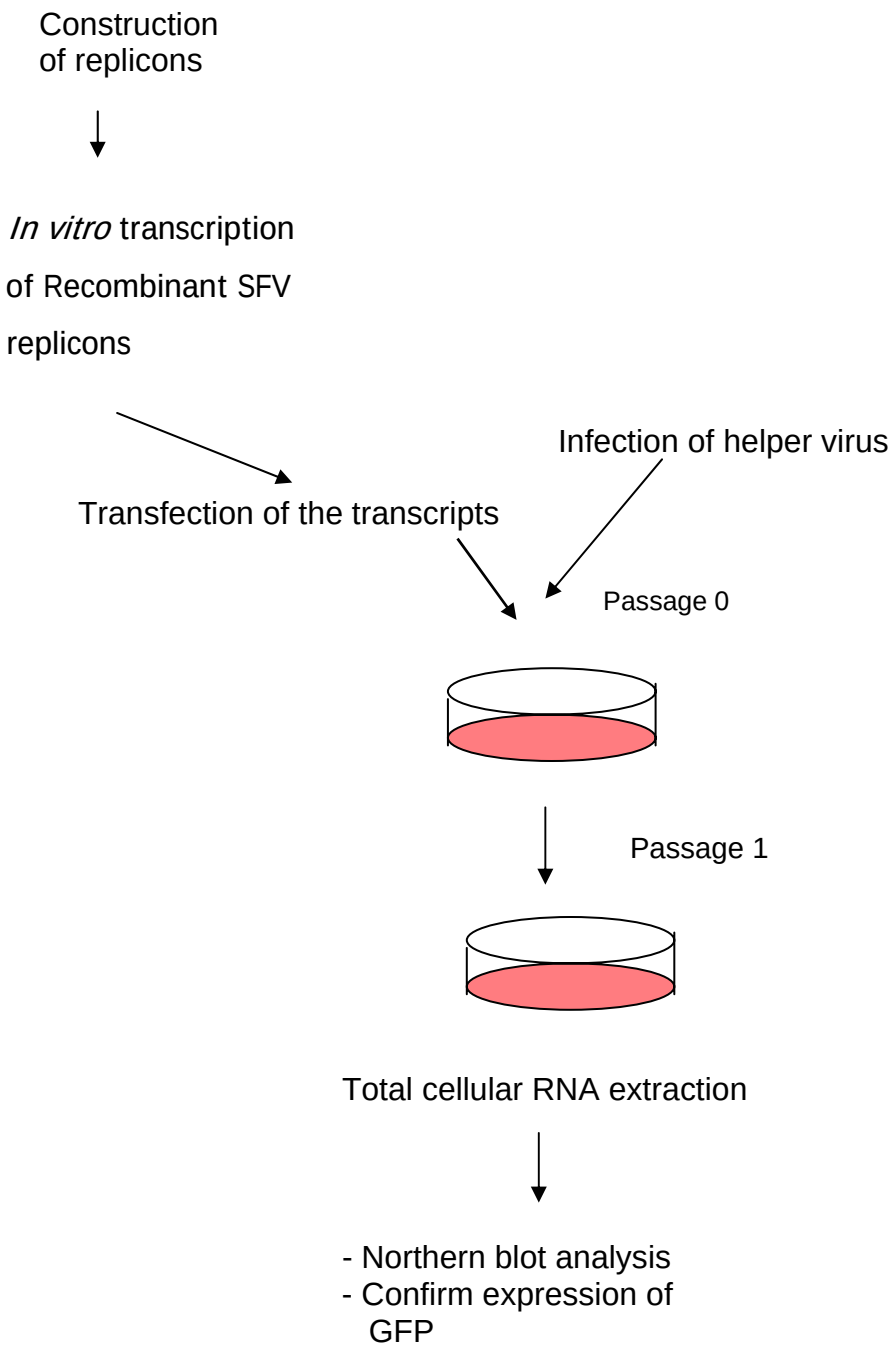

FIG. 23. Schematic of the overall experimental design.

Figure 24. shows the northern blot analysis of the total cellular RNAs of passage 1 transfected with pSFGFP and pSFGPS. A probe against EGFP can detect the genomic and subgenomic RNAs of replicons (Figure 24). Lanes 2 and 4 were used as controls that didn't have packaging signal sequences in the construct. pSFGPS can be passaged into and replicates in passage 1 cells. These results show that not only the IBV virion can package recombinant SFV replicon without any *cis* signal sequence of IBV, but also the replicons can successfully infect and replicate in the infected cells.

Packaging of the Recombinant SFV Replicons into IBV Virion is Helper Virus Dependent

To determine whether packaging is truly helper virus dependant, we repeated the experiment with and without helper virus. As shown in Figure 25 in pictures B and D, only with helper virus infection the recombinant SFV replicon was transferred into new Vero cells and expressed EGFP in passage 1. To assure that this observation was not due to contamination of *in vitro* transcripts from passage 0, we treated passage 0 supernatant with RNaseA to remove possible residual RNA or RNA coating the outside of helper virions. As shown in Figure 24, there was no difference between RNase treatment and a control without RNase treatment. This suggests that the RNA is packaged inside of the

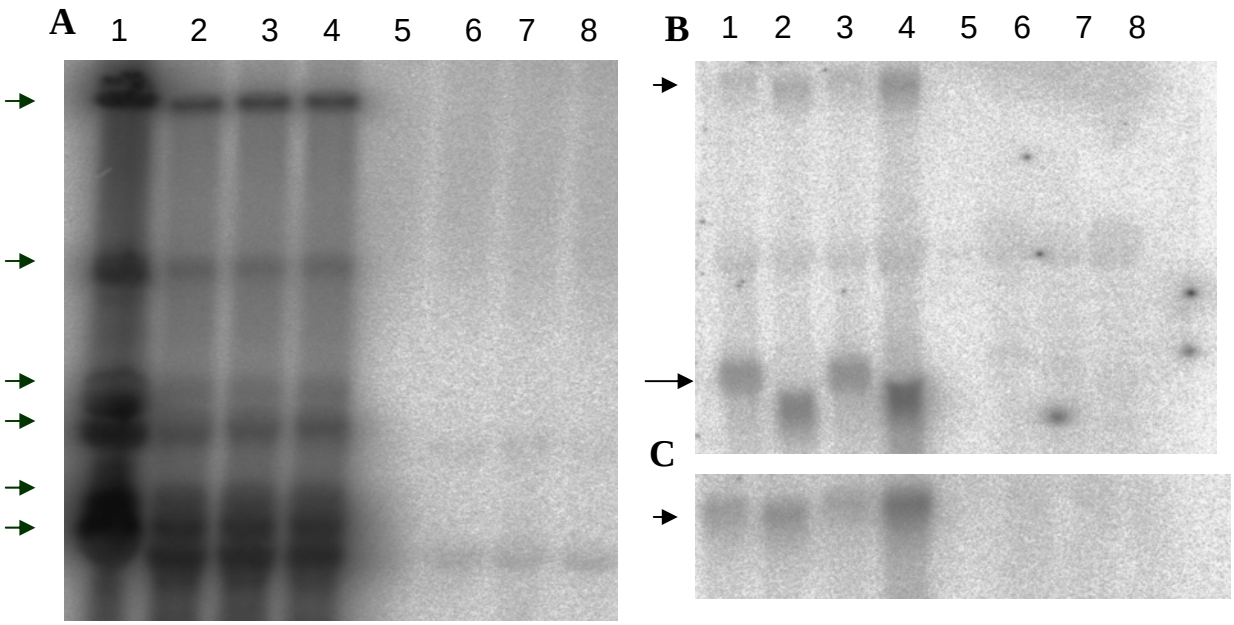

FIG. 24. Recombinant SFV replicons can be packaged into IBV virions with or without IBV *cis* sequences. Northern blot analysis of total cellular RNA of passage 1 Vero cells infected with helper virus and then transfected with pSFGFP and pSFPS. A. Northern blot analysis using a probe specific to the IBV 3' UTR to show each subgenomic RNA of IBV. Arrows indicate each subgenomic RNA of IBV. B. Northern blot analysis using a probe specific to the green fluorescent protein gene. The arrow heads indicates the genomic size of recombinant SFV replicons and arrow indicate subgenomic RNAs of replicons. C. Northern blot analysis using a probe against nsP4 gene of SFV. Odd numbers indicate the replicons containing putative packaging signal sequences and even numbers indicate the replicons without any IBV sequences. Lane 1 to 2, control, lane 3-4, treated with RNaseA, lane 5-6, treated with hyper immune serum against the IBV Beaudette strain from chickens, and lane 7-8,

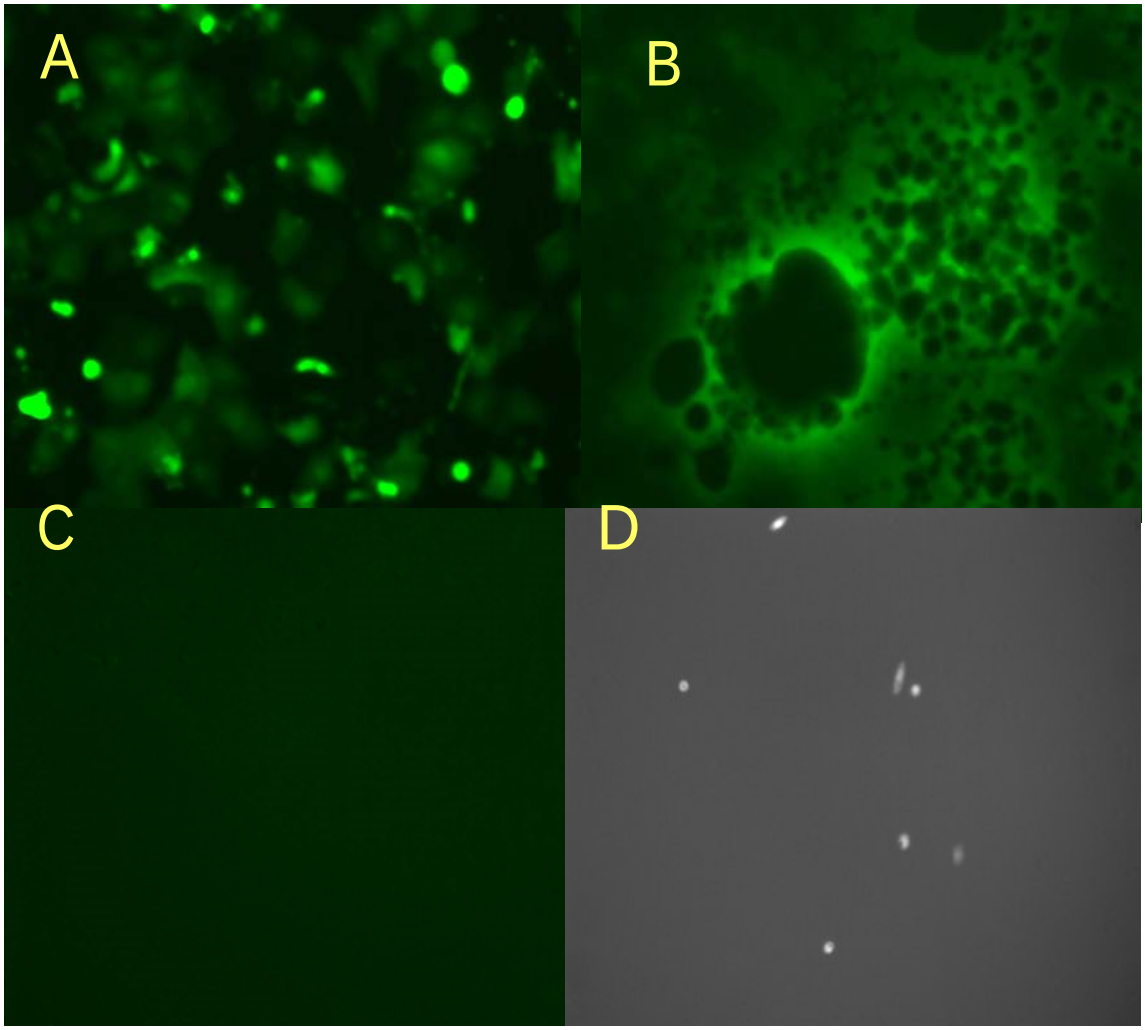

FIG. 25. Without helper virus, recombinant SFV replicons cannot be passaged from passage 0 to passage 1. A and B are P0 and C and D are P1. A and C are the cells transfected with only pSFGFP constructs. B and D are the cells transfected with pSFGFP construct and infected with IBV Beaudette virus one hour post transfection.

virion or that RNA coating the outside of the virion can be protected from RNaseA digestion by virion protein. To verify whether the replicons are inside of the virion, we decided to remove the virion from the supernatant to see whether the replicon can be passaged into passage 1 from passage 0 without virion. To remove the virion from the supernatant, we utilized a neutralizing antibody against the helper virus to inhibit the infection of the helper virus and inhibit the carry over of recombinant SFV interacting with helper virion. To determine the amount of antibody that can completely neutralize the virus in the supernatant, a neutralization assay was performed. Only a 2-fold dilution of the antibody could completely neutralize the helper virus, therefore, this dilution was used to neutralize the passage 0 supernatant. After antibody treatment, no replicon was detected in passage 1 by Northern blot analysis nor was any helper virus replication as observed in Figure 24.

Surprisingly, replication of every replicon was detected even though the controls only have EGFP but no IBV sequences and no enhancement of packaging was observed in other recombinant SFVs containing packaging candidate sequences. It is concluded that packaging is more dependent on the concentration of transfectant than the presence of IBV sequences. With RNase treatment, the pSFGFP construct could still be passaged form passage 0 to passage 1. Based on this finding, we conclude that recombinant SFV replicons can be packaged into IBV virion even though we don’t know the mechanism of this packaging.

DISCUSSION

Viral RNA packaging mechanisms are comparatively well studied in plant viruses and retroviruses. It has been shown that the primary interaction of protein and RNA is important for viral RNA encapsidation and packaging into virions. In single stranded RNA viruses with icosahedral virions, it has been proposed that binding of structural proteins to a specific RNA structure forms an assembly initiation complex, which nucleates the subsequent addition of capsid protein subunits to complete a mature virion (80). For Tobacco mosaic virus (TMV), viral RNA interacts with the capsid protein and this interaction results in a polymer of helical ribonucelocapid complexes depending on the pH or other environmental factors and that the encapsidation process has been shown *in vitro* (29). For retroviruses, one protein, gag, is sufficient for virus particle assembly and is capable of specifically packaging the genomic RNA into particles (127). Without the packaging signal sequence that is referred as ψ, viral genomic packaging is significantly decreased. However, virions still contain non-viral RNA inside. Murjaux et al. (127) have shown that in Moloney murine leukemia virus (MMLV), viral RNA confers the stability of the virion. This study also reported an interesting observation. When the gag protein is expressed with SFV, the virus like particles package the SFV replicon inside of the virion. These study showed the possibility that RNA plays role as a structural component of virus and not only as a packaging signal sequence but also other unknown packaging. However, other unknown packaging mechanisms are important for viral RNA packaging.

Coronaviruses are largest known RNA virus containing from 27.6 to 31 kb of genomic RNA. It has been reported that TGEV have icosahedral cores inside of the viral envelope but this kind of internal core structure has not been shown in IBV (143). Because MHV produces subgenomic RNAs inside of infected cells and because of its specificity of genomic RNA packaging, it has been speculated that the packaging signal sequence of MHV might be located only in the genomic RNA region and not in subgenomic RNA.

However, it has been reported that IBV, BoCV and TGEV package some subgenomic RNA into their virion, in addition to genomic RNA (38, 204). The MHV packaging signal sequence was identified by studying DI by deletion mutation (124). It has been shown that the presence of the packaging signal sequence can confer the packaging of heterologous sequences into MHV virions (63).

The bovine coronavirus packaging signal sequence was identified by using sequence homologue searches (44). Cologna et al. found one region showing high sequence homology (~70%) with the MHV packaging signal sequence and went on to show that the presence of the packaging signal sequence conferred the specific packaging of foreign genes into BoCV virions (44, 63). One interesting point is that every DI that has the MHV packaging signal sequence can be packaged into MHV virions, but one of BoCV DI, Drep, that does not have the known BoCV packaging signal sequence, can still be packaged into BoCV virions (44).

We are interested in developing an efficient vaccine against IBV. One of the problems with IBV live vaccine development is its high rate of recombination and

frequent mutations caused by the lack of proofreading of the RdRp. Attenuated live vaccines, therefore, sometimes evolve into a new recombinant variant increasing the viral gene pool in field strains. To reduce the possible homologous recombination between vaccine strains and field strains, we proposed to express IBV proteins using other viral vectors in order to induce the cellular and humoral immunity against IBV. One of the candidates was the SFV vector. SFV eukaryotic expression vector has been known to be an efficient eukaryotic expression vector because of its promiscuous cell tropism and high expression of recombinant proteins. To engineer the SFV for an IBV vaccine, we wanted to use the IBV virion as a transfer vehicle for specifically targeting to the organs affected by IBV. To package the recombinant SFV into an IBV virion, identification of the packaging mechanism or packaging signal sequence is a prerequisite. Location of the packaging signal sequence of IBV was a focus of this work. Because previous reports indicated that the IBV virion packages not only genomic RNA but also packages varying amounts of subgenomic RNA depending on the virus strain, we proposed that IBV may have a different packaging mechanism from MHV. IBV might have more than one packaging signal sequence to allow packaging of both subgenomic and genomic RNA. We identified four different candidate packaging signal sequences. These sequences are located in the 3’ and 5’ untranslated regions, the ORF1b region in one DI of IBV that is efficient packaged into the virion and the one located by a sequence homology search with BoCV packaging sequence.

As explained previously, the packaging signal sequence of IBV could not be identified using a recombinant SFV replicon. From our study, however, an interesting

finding is that rSFV replicons can be packaged into IBV virions in a concentration dependent manner. The exact mechanism of rSFV replicon packaging into the IBV virion is unknown. There is no significant sequence homology between the IBV and SFV genomes, but the putative packaging signal sequence may share a secondary structure. It is a possibility that, like retroviruses, coronaviruses need RNA to stabilize the RNP structure in order to facilitate the viral assembly process. This possibility is supported by the observation that N proteins interact with viral RNA producing RNP and that the protein has a high affinity to RNA. In MHV, Makino et al. (128) proposed that contrary to icosahedral virus packaging mechanisms, which utilize capsid protein interaction with viral RNA, integral membrane protein and packaging signal sequence interaction confer the specificity of genomic RNA packaging in MHV. M proteins have also been shown to interact with viral RNA.

It is possible that one of the candidates we have identified is the packaging signal sequence even though significant differences in packaging efficiency of each recombinant replicon was not seen. In retroviruses, it has been shown that not only the packaging signal sequence itself, but also neighboring sequences significantly increase the packaging efficiency. It is also possible that the putative packaging signal sequence in SFV may have changed its secondary structure, such that the SFV RNA buries the packaging sequence. Because every candidate sequence was located down stream of EGFP, the location of the packaging signal may be important for efficient packaging and does not solely rely on the secondary structure of the packaging signal sequence. It is

also possible that IBV may need the cooperation of more than one packaging signal sequences.

Alternatively, in addition to using packaging signal sequence for packaging, other packaging mechanisms have been reported. It is noteworthy that Cavangh's group tried to identify the *cis* signal sequence necessary for viral RNA packaging using deletion mutations with IBV (48). Although this approach has not identified definitive sequences, it has been successful in understanding the cis signal sequences necessary for viral replication and transcription.

Because of the availability of infectious cDNA clones of coronaviruses, it will be interesting to see whether the recombinant infectious cDNA having deletions in known packaging signal sequences of coronaviruses such as MHV, BoCV and TGEV can be packaged into virions. The infectious cDNA clone could further elucidate the packaging mechanisms of IBV.

CHAPTER V

CONCLUSION

Recently, there has been an escalation of interest in coronaviruses because of recent outbreak of severe acute respiratory syndrome (SARS) caused by a coronavirus now referred to as SCoV. However, coronavirus infection is a well known problem causing severe illness in infected animals from laboratory animals to agricultural animals including swine, cattle and poultry subsequently causing severe economic losses in agricultural industry. Avian infectious bronchitis is one of the oldest known diseases caused by the coronavirus, infectious bronchitis virus.

A major focus of my efforts has been to develop an effective vaccine against IBV. Knowing the mechanism of viral pathogenesis is the prerequisite of developing effective methods to control viral infection. Infectious cDNA clones are the most useful tools to study the viral replication and pathogenesis. Several groups have been successful in constructing infectious cDNA clones of coronaviruses in the past three years. Three different approaches have been used for construction of infectious cDNA clones of coronaviruses. To overcome the cloning size limitation of plasmid vector, two vector systems were used which included bacterial artificial chromosome (BAC) for the construction of infectious cDNA of transmissible gastroenteritis virus (TGEV) and vaccinia virus for the infectious cDNA clones of infectious bronchitis virus (IBV) and human coronavirus (HCoV) (2, 31, 185). The third approach is an *in vitro* assembly

strategy. Instead of cloning the entire viral genome into a cloning vector, *in vitro* assembled DNA templates are used to transcribe full-length RNA transcripts using T7 RNA polymerase (201, 202). By using this approach, infectious cDNA clones of MHV and TGEV have been constructed.

Although, IBV infectious cDNA clones have been constructed using vaccinia virus as a cloning vector (31), the vaccinia system is time consuming because of its selection process for the recombinant vaccinia virus containing infectious cDNA clones of coronaviruses, and it is cumbersome to manipulate the recombinant vaccinia vector for producing mutations in coronavirus genes inside of vaccinia virus. Casai et al. (30) mentioned that they were not able to rescue infectious cDNA clones of IBV using the *in vitro* assembly technique. However, in our study we showed that construction of an infectious cDNA clone of IBV using an *in vitro* assembly strategy is possible.

Several subsequent publications suggest that not only the infectious cDNA of coronaviruses can be used to study the molecular biology of the virus itself, but also can be used as a gene transfer vector or expression vector. One recent report also exploited the coronavirus to demonstrate that coronaviruses can be valuable candidates for a multigene transfer or making expression vectors because of their ability to produce multiple subgenomic RNA. Using more than two different promoters, proteins can be co-expressed without the interruption from other transcription unit that is inherent in some other expression vectors (187).

To show the potential for using infectious cDNA clones of IBV as a gene transfer vector, I constructed a recombinant cDNA clone of IBV with the enhanced green

fluorescent protein (EGFP) gene. Compared to other coronaviruses, the IBV genome is compact and several ORFs overlap. However, IBV has several small ORFs known as group specific proteins whose functions are not well understood. Based on work with MHV, it is possible that these gene products are not necessary for viral survival *in vitro*. In this study, we replaced ORF5a with EGFP and the recombinant virus was viable and expressed EGFP in the virus infected cells. This showed the possibility that other group specific proteins may not be necessary for the viral survival at least *in vitro*.

One of the problems with IBV live vaccine development is its high rate of recombination and frequent mutations, likely caused by the lack of the proofreading ability of the RdRp. Attenuated live vaccines sometimes evolve into a new recombinant variants, increasing the viral gene pool in field situations. To reduce the possible homologous recombination between vaccine strains and field strains, we proposed using other viral vectors to express the IBV S protein that can induce both cellular and humoral immunity against IBV. One of the candidates was SFV vector. SFV eukaryotic expression vector is an efficient eukaryotic expression vector because of its promiscuous cell tropism and high expression of recombinant proteins. To engineer SFV for an IBV vaccine, we wanted to use the IBV virion as a transfer vehicle that can be specifically targeted to the organs affected by IBV. To package the recombinant SFV into an IBV virion, identification of the packaging mechanism or packaging signal sequence is a prerequisite. Location of the packaging signal sequence of IBV was a focus of the work. Because previous reports indicated that the IBV virion packages not only genomic RNA but also packages varying amounts of subgenomic RNA depending on the virus strain,

we proposed that IBV may have a different packaging mechanism from MHV. IBV might have more than one packaging signal sequence that could be located in both subgenomic and genomic RNA. We identified four different candidate packaging signal sequences. These sequences are located in the 3' and 5' untranslated regions, the ORF1b region in one DI of IBV that is efficiently packaged into the virion and the one located by a sequence homology search with the BoCV packaging sequence.

As explained previously, the packaging signal sequence of IBV could not be identified using a recombinant SFV replicon, however, an interesting finding of our studies is that rSFV replicons can be packaged into IBV virions in a concentration dependent manner. The exact mechanism of rSFV replicon packaging into the IBV virion is unknown. There is no significant sequence homology between the IBV and SFV genomes but the putative packaging signal sequence may share a secondary structure. It is a possibility that, like retroviruses, coronaviruses need RNA to stabilize the RNP structure facilitating the viral assembly process. This possibility is supported by the observation that N proteins interact with viral RNA producing RNP and that the protein has a high affinity for RNA. In MHV, Makino et al. proposed that contrary to icosahedral virus packaging mechanisms, which utilize capsid protein interaction with viral RNA, integral membrane protein and the packaging signal sequence interaction confer the specificity of genomic RNA packaging in MHV. M proteins have also been shown to interact with viral RNA.

Because we now have infectious cDNA clones of coronaviruses, it will be interesting to see whether the recombinant infectious cDNA having deletions in known

packaging signal sequences of coronaviruses such as MHV, BoCV and TGEV can be packaged into virions. In addition, the infectious cDNA clone constructed in our laboratory could be a better tool for the study of the packaging mechanisms of IBV.

In summary, an infectious cDNA clone originating from the Vero cell adapted Beaudette strain of IBV was constructed using the *in vitro* assembly technique. This cDNA clone was used to construct a recombinant infectious cDNA clone of IBV expressing EGFP. ORF5a was replaced with EGFP and this also showed that ORF5a is not necessary for the viral survival. The recombinant SFV vector system was used to identify the packaging signal sequence of IBV using four candidate IBV *cis* acting signal sequences. A specific packaging signal sequence was not found in any of the candidate signal sequences, however, it has been shown that SFV can be packaged into IBV virion without any IBV *cis* acting signal sequence showing the possibility of using SFV for the construction of chimeric SFV-IBV vector for vaccine development in the absence of IBV specific packaging signal sequences.

REFERENCES

1. **Albassam, M. A., R. W. Winterfield, and H. L. Thacker.** 1986. Comparison of the nephropathogenicity of four strains of infectious bronchitis virus. Avian Dis. **30:**468-476.
2. **Almazan, F., J. M. Gonzalez, Z. Penzes, A. Izeta, E. Calvo, J. Plana-Duran, and L. Enjuanes.** 2000. Engineering the largest RNA virus genome as an infectious bacterial artificial chromosome. Proc. Natl. Acad. Sci. USA **97:**5516-5521.
3. **Alonso, S., I. Sola, J. P. Teifke, I. Reimann, A. Izeta, M. Balasch, J. Plana-Duran, R. J. Moormann, and L. Enjuanes.** 2002. *In vitro* and *in vivo* expression of foreign genes by transmissible gastroenteritis coronavirus-derived minigenomes. J. Gen. Virol. **83:**567-579.
4. **Alonso-Caplen, F. V., Y. Matsuoka, G. E. Wilcox, and R. W. Compans.** 1984. Replication and morphogenesis of avian coronavirus in Vero cells and their inhibition by monensin. Virus Res. **1:**153-167.
5. **Armstrong, J., H. Niemann, S. Smeekens, P. Rottier, and G. Warren.** 1984. Sequence and topology of a model intracellular membrane protein, E1 glycoprotein, from a coronavirus. Nature **308:**751-752.
6. **Avellaneda, G. E., P. Villegas, M. W. Jackwood, and D. J. King.** 1994. *In vivo* evaluation of the pathogenicity of field isolates of infectious bronchitis virus. Avian Dis. **38:**589-597.
7. **Baker, S. C., and M. M. Lai.** 1990. An *in vitro* system for the leader-primed transcription of coronavirus mRNAs. EMBO J. **9:**4173-4179.
8. **Banner, L. R., J. G. Keck, and M. M. Lai.** 1990. A clustering of RNA recombination sites adjacent to a hypervariable region of the peplomer gene of murine coronavirus. Virology **175:**548-555.

9. **Baric, R. S., K. Fu, M. C. Schaad, and S. A. Stohlman.** 1990. Establishing a genetic recombination map for murine coronavirus strain A59 complementation groups. Virology **177:**646-656.

10. **Baric, R. S., G. W. Nelson, J. O. Fleming, R. J. Deans, J. G. Keck, N. Casteel, and S. A. Stohlman.** 1988. Interactions between coronavirus nucleocapsid protein and viral RNAs: implications for viral transcription. J. Virol. **62:**4280-4287.

11. **Baric, R. S., S. A. Stohlman, M. K. Razavi, and M. M. Lai.** 1985. Characterization of leader-related small RNAs in coronavirus-infected cells: further evidence for leader-primed mechanism of transcription. Virus Res. **3:**19-33.

12. **Baric, R. S., and B. Yount.** 2000. Subgenomic negative-strand RNA function during mouse hepatitis virus infection. J. Virol. **74:**4039-4046.

13. **Baudoux, P., C. Carrat, L. Besnardeau, B. Charley, and H. Laude.** 1998. Coronavirus pseudoparticles formed with recombinant M and E proteins induce alpha interferon synthesis by leukocytes. J. Virol. **72:**8636-8643.

14. **Beaudette F.R., H. C. B.** 1937. Cultivation of the virus of infectious bronchitis. J Am. Vet. Med. Assoc. **90:**51-60.

15. **Becker, W. B., K. McIntosh, J. H. Dees, and R. M. Chanock.** 1967. Morphogenesis of avian infectious bronchitis virus and a related human virus (strain 229E). J. Virol. **1:**1019-1027.

16. **Binns, M. M., M. E. Boursnell, D. Cavanagh, D. J. Pappin, and T. D. Brown.** 1985. Cloning and sequencing of the gene encoding the spike protein of the coronavirus IBV. J. Gen. Virol. **66 :**719-726.

17. **Bos, E. C., W. Luytjes, H. V. van der Meulen, H. K. Koerten, and W. J. Spaan.** 1996. The production of recombinant infectious DI-particles of a murine coronavirus in the absence of helper virus. Virology **218:**52-60.

18. **Bosch, B. J., R. Van Der Zee, C. A. De Haan, and P. J. Rottier.** 2003. The coronavirus spike protein is a class I virus fusion protein: structural and functional characterization of the fusion core complex. J. Virol. **77:**8801-8811.

19. **Bost, A. G., R. H. Carnahan, X. T. Lu, and M. R. Denison.** 2000. Four proteins processed from the replicase gene polyprotein of mouse hepatitis virus colocalize in the cell periphery and adjacent to sites of virion assembly. J. Virol. **74:**3379-3387.

20. **Bost, A. G., E. Prentice, and M. R. Denison.** 2001. Mouse hepatitis virus replicase protein complexes are translocated to sites of M protein accumulation in the ERGIC at late times of infection. Virology **285:**21-29.

21. **Boursnell, M. E., T. D. Brown, and M. M. Binns.** 1984. Sequence of the membrane protein gene from avian coronavirus IBV. Virus Res. **1:**303-313.

22. **Boursnell, M. E., T. D. Brown, I. J. Foulds, P. F. Green, F. M. Tomley, and M. M. Binns.** 1987. Completion of the sequence of the genome of the coronavirus avian infectious bronchitis virus. J. Gen. Virol. **68 :**57-77.

23. **Boyer, J. C., and A. L. Haenni.** 1994. Infectious transcripts and cDNA clones of RNA viruses. Virology **198:**415-426.

24. **Brayton, P. R., M. M. Lai, C. D. Patton, and S. A. Stohlman.** 1982. Characterization of two RNA polymerase activities induced by mouse hepatitis virus. J. Virol. **42:**847-853.

25. **Brierley, I., M. E. Boursnell, M. M. Binns, B. Bilimoria, V. C. Blok, T. D. Brown, and S. C. Inglis.** 1987. An efficient ribosomal frame-shifting signal in the polymerase-encoding region of the coronavirus IBV. EMBO J. **6:**3779-3385.

26. **Brierley, I., P. Digard, and S. C. Inglis.** 1989. Characterization of an efficient coronavirus ribosomal frameshifting signal: requirement for an RNA pseudoknot. Cell **57:**537-547.

27. **Brzeski, H., and S. I. Kennedy.** 1978. Synthesis of alphavirus-specified RNA. J. Virol. **25:**630-640.

28. **Budzilowicz, C. J., S. P. Wilczynski, and S. R. Weiss.** 1985. Three intergenic regions of coronavirus mouse hepatitis virus strain A59 genome RNA contain a common nucleotide sequence that is homologous to the 3' end of the viral mRNA leader sequence. J. Virol. **53:**834-840.

29. **Butler, P. J., and A. Klug.** 1971. Assembly of the particle of tobacco mosaic virus from RNA and disks of protein. Nat. New. Biol. **229:**47-50.

30. **Casais, R., B. Dove, D. Cavanagh, and P. Britton.** 2003. Recombinant avian infectious bronchitis virus expressing a heterologous spike gene demonstrates that the spike protein is a determinant of cell tropism. J. Virol. **77:**9084-9089.

31. **Casais, R., V. Thiel, S. G. Siddell, D. Cavanagh, and P. Britton.** 2001. Reverse genetics system for the avian coronavirus infectious bronchitis virus. J. Virol. **75:**12359-12369.

32. **Cavanagh, D.** 1983. Coronavirus IBV glycopolypeptides: size of their polypeptide moieties and nature of their oligosaccharides. J. Gen. Virol. **64:**1187-1191.

33. **Cavanagh, D.** 1983. Coronavirus IBV: structural characterization of the spike protein. J. Gen. Virol. **64 :**2577-2583.

34. **Cavanagh, D.** 1997. Nidoviales: a new order comprising Coronaviridae and Arteriviridae. Arch. Virol. **142:**629-633.

35. **Cavanagh, D., D. A. Brian, L. Enjuanes, K. V. Holmes, M. M. Lai, H. Laude, S. G. Siddell, W. Spaan, F. Taguchi, and P. J. Talbot.** 1990. Recommendations of the Coronavirus Study Group for the nomenclature of the structural proteins, mRNAs, and genes of coronaviruses. Virology **176:**306-307.

36. **Cavanagh, D., P. J. Davis, J. H. Darbyshire, and R. W. Peters.** 1986. Coronavirus IBV: virus retaining spike glycopolypeptide S2 but not S1 is unable to induce virus-neutralizing or haemagglutination-inhibiting antibody, or induce chicken tracheal protection. J. Gen. Virol. **67 :**1435-1442.

37. **Cavanagh, D., P. J. Davis, D. J. Pappin, M. M. Binns, M. E. Boursnell, and T. D. Brown.** 1986. Coronavirus IBV: partial amino terminal sequencing of spike polypeptide S2 identifies the sequence Arg-Arg-Phe-Arg-Arg at the cleavage site of the spike precursor propolypeptide of IBV strains Beaudette and M41. Virus Res. **4:**133-143.

38. **Cavanagh, D., K. Shaw, and X. Zhao.** 1993. Analysis of messenger RNA within virions of IBV. Adv. Exp. Med. Biol. **342:**123-128.

39. **Cavanagh, D. N., S.** 1997. *Diseases of Poultry*. Iowa State University Press, Ames, IA.

40. **Chang, S. H., J. L. Bae, T. J. Kang, J. Kim, G. H. Chung, C. W. Lim, H. Laude, M. S. Yang, and Y. S. Jang.** 2002. Identification of the epitope region capable of inducing neutralizing antibodies against the porcine epidemic diarrhea virus. Mol. Cells **14:**295-299.

41. **Chew, P. H., P. S. Wakenell, and T. B. Farver.** 1997. Pathogenicity of attenuated infectious bronchitis viruses for oviducts of chickens exposed *in ovo*. Avian Dis. **41:**598-603.

42. **Collins, A. R., R. L. Knobler, H. Powell, and M. J. Buchmeier.** 1982. Monoclonal antibodies to murine hepatitis virus-4 (strain JHM) define the viral glycoprotein responsible for attachment and cell-cell fusion. Virology **119:**358-371.

43. **Collisson, E. W., A. K. Williams, S. I. Chung, and M. Zhou.** 1995. Interactions between the IBV nucleocapsid protein and RNA sequences specific for the 3' end of the genome. Adv. Exp. Med. Biol. **380:**523-528.

44. **Cologna, R., and B. G. Hogue.** 2000. Identification of a bovine coronavirus packaging signal. J. Virol. **74:**580-583.

45. **Compton, S. R., D. B. Rogers, K. V. Holmes, D. Fertsch, J. Remenick, and J. J. McGowan.** 1987. *In vitro* replication of mouse hepatitis virus strain A59. J. Virol. **61:**1814-1820.

46. **Compton, S. R., C. B. Stephensen, S. W. Snyder, D. G. Weismiller, and K. V. Holmes.** 1992. Coronavirus species specificity: murine coronavirus binds to a mouse-specific epitope on its carcinoembryonic antigen-related receptor glycoprotein. J. Virol. **66:**7420-7428.

47. **Corse, E., and C. E. Machamer.** 2000. Infectious bronchitis virus E protein is targeted to the Golgi complex and directs release of virus-like particles. J. Virol. **74:**4319-4326.

48. **Dalton, K., R. Casais, K. Shaw, K. Stirrups, S. Evans, P. Britton, T. D. Brown, and D. Cavanagh.** 2001. *cis*-acting sequences required for coronavirus infectious bronchitis virus defective-RNA replication and packaging. J. Virol. **75:**125-133.

49. **Davies, H. A., R. R. Dourmashkin, and M. R. Macnaughton.** 1981. Ribonucleoprotein of avian infectious bronchitis virus. J. Gen. Virol. **53:**67-74.

50. **de Haan, C. A., L. Kuo, P. S. Masters, H. Vennema, and P. J. Rottier.** 1998. Coronavirus particle assembly: primary structure requirements of the membrane protein. J. Virol. **72:**6838-6850.

51. **de Haan, C. A., P. S. Masters, X. Shen, S. Weiss, and P. J. Rottier.** 2002. The group-specific murine coronavirus genes are not essential, but their deletion, by reverse genetics, is attenuating in the natural host. Virology **296:**177-189.

52. **de Haan, C. A., M. Smeets, F. Vernooij, H. Vennema, and P. J. Rottier.** 1999. Mapping of the coronavirus membrane protein domains involved in interaction with the spike protein. J. Virol. **73:**7441-7452.

53. **de Haan, C. A., H. Vennema, and P. J. Rottier.** 2000. Assembly of the coronavirus envelope: homotypic interactions between the M proteins. J. Virol. **74:**4967-4978.

54. **Delmas, B., J. Gelfi, R. L'Haridon, L. K. Vogel, H. Sjostrom, O. Noren, and H. Laude.** 1992. Aminopeptidase N is a major receptor for the entero-pathogenic coronavirus TGEV. Nature **357:**417-420.

55. **Delmas, B., and H. Laude.** 1990. Assembly of coronavirus spike protein into trimers and its role in epitope expression. J. Virol. **64:**5367-5375.

56. **Denison, M. R., W. J. Spaan, Y. van der Meer, C. A. Gibson, A. C. Sims, E. Prentice, and X. T. Lu.** 1999. The putative helicase of the coronavirus mouse hepatitis virus is processed from the replicase gene polyprotein and localizes in complexes that are active in viral RNA synthesis. J. Virol. **73:**6862-6871.

57. **Dougherty, W. G., and B. L. Semler.** 1993. Expression of virus-encoded proteinases: functional and structural similarities with cellular enzymes. Microbiol. Rev. **57:**781-822.

58. **Dveksler, G. S., C. W. Dieffenbach, C. B. Cardellichio, K. McCuaig, M. N. Pensiero, G. S. Jiang, N. Beauchemin, and K. V. Holmes.** 1993. Several members of the mouse carcinoembryonic antigen-related glycoprotein family are functional receptors for the coronavirus mouse hepatitis virus-A59. J. Virol. **67:**1-8.

59. **Dveksler, G. S., M. N. Pensiero, C. B. Cardellichio, R. K. Williams, G. S. Jiang, K. V. Holmes, and C. W. Dieffenbach.** 1991. Cloning of the mouse hepatitis virus (MHV) receptor: expression in human and hamster cell lines confers susceptibility to MHV. J. Virol. **65:**6881-6891.

60. **Escors, D., A. Izeta, C. Capiscol, and L. Enjuanes.** 2003. Transmissible gastroenteritis coronavirus packaging signal is located at the 5' end of the virus genome. J. Virol. **77:**7890-7902.

61. **Evans, M. R., and R. W. Simpson.** 1980. The coronavirus avian infectious bronchitis virus requires the cell nucleus and host transcriptional factors. Virology **105:**582-591.

62. **Flanagan, E. B., J. M. Zamparo, L. A. Ball, L. L. Rodriguez, and G. W. Wertz.** 2001. Rearrangement of the genes of vesicular stomatitis virus eliminates clinical disease in the natural host: new strategy for vaccine development. J. Virol. **75:**6107-6114.

63. **Fosmire, J. A., K. Hwang, and S. Makino.** 1992. Identification and characterization of a coronavirus packaging signal. J. Virol. **66:**3522-3530.

64. **Gallagher, T. M., C. Escarmis, and M. J. Buchmeier.** 1991. Alteration of the pH dependence of coronavirus-induced cell fusion: effect of mutations in the spike glycoprotein. J. Virol. **65:**1916-1928.

65. **Gelb, J., Jr., J. B. Wolff, and C. A. Moran.** 1991. Variant serotypes of infectious bronchitis virus isolated from commercial layer and broiler chickens. Avian Dis. **35:**82-87.

66. **Godeke, G. J., C. A. de Haan, J. W. Rossen, H. Vennema, and P. J. Rottier.** 2000. Assembly of spikes into coronavirus particles is mediated by the carboxy-terminal domain of the spike protein. J. Virol. **74:**1566-1571.

67. **Gonzalez, J. M., Z. Penzes, F. Almazan, E. Calvo, and L. Enjuanes.** 2002. Stabilization of a full-length infectious cDNA clone of transmissible gastroenteritis coronavirus by insertion of an intron. J. Virol. **76:**4655-4661.

68. **Gorbalenya, A. E., E. V. Koonin, A. P. Donchenko, and V. M. Blinov.** 1989. Coronavirus genome: prediction of putative functional domains in the non-structural polyprotein by comparative amino acid sequence analysis. Nucleic Acids Res. **17:**4847-4861.

69. **Grotzinger, C., G. Heusipp, J. Ziebuhr, U. Harms, J. Suss, and S. G. Siddell.** 1996. Characterization of a 105-kDa polypeptide encoded in gene 1 of the human coronavirus HCV 229E. Virology **222:**227-235.

70. **Guan, Y., B. J. Zheng, Y. Q. He, X. L. Liu, Z. X. Zhuang, C. L. Cheung, S. W. Luo, P. H. Li, L. J. Zhang, Y. J. Guan, K. M. Butt, K. L. Wong, K. W. Chan, W. Lim, K. F. Shortridge, K. Y. Yuen, J. S. Peiris, and L. L. Poon.** 2003. Isolation and characterization of viruses related to the SARS coronavirus from animals in southern china. Science. **302:**276-278

71. **Haijema, B. J., H. Volders, and P. J. Rottier.** 2003. Switching species tropism: an effective way to manipulate the feline coronavirus genome. J. Virol. **77:**4528-4538.

72. **Hatta, M., G. Neumann, and Y. Kawaoka.** 2001. Reverse genetics approach towards understanding pathogenesis of H5N1 Hong Kong influenza A virus infection. Philos. Trans R. Soc. Lond. B Biol. Sci. **356:**1841-1843.

73. **Hegyi, A., and J. Ziebuhr.** 2002. Conservation of substrate specificities among coronavirus main proteases. J. Gen. Virol. **83:**595-599.

74. **Heusipp, G., C. Grotzinger, J. Herold, S. G. Siddell, and J. Ziebuhr.** 1997. Identification and subcellular localization of a 41 kDa, polyprotein 1ab processing product in human coronavirus 229E-infected cells. J. Gen. Virol. **78 :**2789-2794.

75. **Hoffmann, E., K. Mahmood, C. F. Yang, R. G. Webster, H. B. Greenberg, and G. Kemble.** 2002. Rescue of influenza B virus from eight plasmids. Proc. Natl. Acad. Sci. USA **99:**11411-11416.

76. **Hofstad, M. S., and H. W. Yoder, Jr.** 1966. Avian infectious bronchitis--virus distribution in tissues of chicks. Avian Dis. **10:**230-239.

77. **Holmes, K. V., J. F. Boyle, D. G. Weismiller, S. R. Compton, R. K. Williams, C. B. Stephensen, and M. F. Frana.** 1987. Identification of a receptor for mouse hepatitis virus. Adv. Exp. Med. Biol. **218:**197-202.

78. **Horzinek, M. C., H. Lutz, and N. C. Pedersen.** 1982. Antigenic relationships among homologous structural polypeptides of porcine, feline, and canine coronaviruses. Infect. Immun. **37:**1148-1155.

79. **Jacobs, L., W. J. Spaan, M. C. Horzinek, and B. A. van der Zeijst.** 1981. Synthesis of subgenomic mRNA's of mouse hepatitis virus is initiated independently: evidence from UV transcription mapping. J. Virol. **39:**401-406.

80. **James M. Fox, J. E. J. a. M. J. Y.** 1994. RNA/protein interactions in icosahedral virus assembly. Sem. Virol. **5:**51-60.

81. **Jimenez, G., I. Correa, M. P. Melgosa, M. J. Bullido, and L. Enjuanes.** 1986. Critical epitopes in transmissible gastroenteritis virus neutralization. J. Virol. **60:**131-139.

82. **Keck, J. G., G. K. Matsushima, S. Makino, J. O. Fleming, D. M. Vannier, S. A. Stohlman, and M. M. Lai.** 1988. *In vivo* RNA-RNA recombination of coronavirus in mouse brain. J. Virol. **62:**1810-1813.

83. **Krijnse-Locker, J., M. Ericsson, P. J. Rottier, and G. Griffiths.** 1994. Characterization of the budding compartment of mouse hepatitis virus: evidence that transport from the RER to the Golgi complex requires only one vesicular transport step. J. Cell Biol. **124:**55-70.

84. **Kubo, H., S. Takase-Yoden, and F. Taguchi.** 1993. Neutralization and fusion inhibition activities of monoclonal antibodies specific for the S1 subunit of the spike protein of neurovirulent murine coronavirus JHMV c1-2 variant. J. Gen. Virol. **74 :**1421-1425.

85. **Kuo, L., and P. S. Masters.** 2003. The small envelope protein e is not essential for murine coronavirus replication. J. Virol. **77:**4597-4608.

86. **Kusters, J. G., E. J. Jager, H. G. Niesters, and B. A. van der Zeijst.** 1990. Sequence evidence for RNA recombination in field isolates of avian coronavirus infectious bronchitis virus. Vaccine **8:**605-608.

87. **Ladman, B. S., C. R. Pope, A. F. Ziegler, T. Swieczkowski, C. J. Callahan, S. Davison, and J. Gelb, Jr.** 2002. Protection of chickens after live and inactivated virus vaccination against challenge with nephropathogenic infectious bronchitis virus PA/Wolgemuth/98. Avian Dis. **46:**938-944.

88. **Lai, M. M.** 1990. Coronavirus: organization, replication and expression of genome. Annu. Rev. Microbiol. **44:**303-333.

89. **Lai, M. M., R. S. Baric, P. R. Brayton, and S. A. Stohlman.** 1984. Characterization of leader RNA sequences on the virion and mRNAs of mouse hepatitis virus, a cytoplasmic RNA virus. Proc. Natl. Acad. Sci. USA **81:**3626-30.

90. **Lai, M. M., and D. Cavanagh.** 1997. The molecular biology of coronaviruses. Adv. Virus Res. **48:**1-100.

91. **Lai, M. M., C. D. Patton, R. S. Baric, and S. A. Stohlman.** 1983. Presence of leader sequences in the mRNA of mouse hepatitis virus. J. Virol. **46:**1027-1033.

92. **Lai, M. M., C. D. Patton, and S. A. Stohlman.** 1982. Further characterization of mRNA's of mouse hepatitis virus: presence of common 5'-end nucleotides. J. Virol. **41:**557-565.

93. **Lai, M. M., C. D. Patton, and S. A. Stohlman.** 1982. Replication of mouse hepatitis virus: negative-stranded RNA and replicative form RNA are of genome length. J. Virol. **44:**487-492.

94. **Lanser, J. A., and C. R. Howard.** 1980. The polypeptides of infectious bronchitis virus (IBV-41 strain). J. Gen. Virol. **46:**349-361.

95. **Le, S. Y., N. Sonenberg, and J. V. Maizel, Jr.** 1994. Distinct structural elements and internal entry of ribosomes in mRNA3 encoded by infectious bronchitis virus. Virology **198:**405-411.

96. **Liao, C. L., and M. M. Lai.** 1992. RNA recombination in a coronavirus: recombination between viral genomic RNA and transfected RNA fragments. J. Virol. **66:**6117-6124.

97. **Lim, K. P., and D. X. Liu.** 1998. Characterization of the two overlapping papain-like proteinase domains encoded in gene 1 of the coronavirus infectious bronchitis virus and determination of the C-terminal cleavage site of an 87-kDa protein. Virology **245:**303-312.

98. **Lim, K. P., and D. X. Liu.** 2001. The missing link in coronavirus assembly. Retention of the avian coronavirus infectious bronchitis virus envelope protein in the pre-Golgi compartments and physical interaction between the envelope and membrane proteins. J. Biol. Chem. **276:**17515-17523.

99. **Lim, K. P., L. F. Ng, and D. X. Liu.** 2000. Identification of a novel cleavage activity of the first papain-like proteinase domain encoded by open reading frame 1a of the coronavirus Avian infectious bronchitis virus and characterization of the cleavage products. J. Virol. **74:**1674-1685.

100. **Liu, D. X., I. Brierley, and T. D. Brown.** 1995. Identification of a trypsin-like serine proteinase domain encoded by ORF 1a of the coronavirus IBV. Adv. Exp. Med. Biol. **380:**405-411.

101. **Liu, D. X., I. Brierley, K. W. Tibbles, and T. D. Brown.** 1994. A 100-kilodalton polypeptide encoded by open reading frame (ORF) 1b of the coronavirus infectious bronchitis virus is processed by ORF 1a products. J. Virol. **68:**5772-5780.

102. **Liu, D. X., and T. D. Brown.** 1995. Characterization and mutational analysis of an ORF 1a-encoding proteinase domain responsible for proteolytic processing of the infectious bronchitis virus 1a/1b polyprotein. Virology **209:**420-427.

103. **Liu, D. X., D. Cavanagh, P. Green, and S. C. Inglis.** 1991. A polycistronic mRNA specified by the coronavirus infectious bronchitis virus. Virology **184:**531-544.

104. **Liu, D. X., and S. C. Inglis.** 1991. Association of the infectious bronchitis virus 3c protein with the virion envelope. Virology **185:**911-917.

105. **Liu, D. X., and S. C. Inglis.** 1992. Identification of two new polypeptides encoded by mRNA5 of the coronavirus infectious bronchitis virus. Virology **186:**342-347.

106. **Liu, D. X., and S. C. Inglis.** 1992. Internal entry of ribosomes on a tricistronic mRNA encoded by infectious bronchitis virus. J. Virol. **66:**6143-6154.

107. **Liu, D. X., S. Shen, H. Y. Xu, and S. F. Wang.** 1998. Proteolytic mapping of the coronavirus infectious bronchitis virus 1b polyprotein: evidence for the presence of four cleavage sites of the 3C-like proteinase and identification of two novel cleavage products. Virology **246:**288-297.

108. **Locker, J. K., G. Griffiths, M. C. Horzinek, and P. J. Rottier.** 1992. O-glycosylation of the coronavirus M protein. Differential localization of sialyltransferases in N- and O-linked glycosylation. J. Biol. Chem. **267:**14094-14101.

109. **Locker, J. K., J. Klumperman, V. Oorschot, M. C. Horzinek, H. J. Geuze, and P. J. Rottier.** 1994. The cytoplasmic tail of mouse hepatitis virus M protein is essential but not sufficient for its retention in the Golgi complex. J. Biol. Chem. **269:**28263-28269.

110. **Locker, J. K., D. J. Opstelten, M. Ericsson, M. C. Horzinek, and P. J. Rottier.** 1995. Oligomerization of a trans-Golgi/trans-Golgi network retained protein occurs in the Golgi complex and may be part of its retention. J. Biol. Chem. **270:**8815-8821.

111. **Locker, J. K., J. K. Rose, M. C. Horzinek, and P. J. Rottier.** 1992. Membrane assembly of the triple-spanning coronavirus M protein. Individual transmembrane domains show preferred orientation. J. Biol. Chem. **267:**21911-21918.

112. **Lomniczi, B.** 1977. Biological properties of avian coronavirus RNA. J. Gen. Virol. **36:**531-533.

113. **Lomniczi, B., and I. Kennedy.** 1977. Genome of infectious bronchitis virus. J. Virol. **24:**99-107.

114. **Lu, X. T., A. C. Sims, and M. R. Denison.** 1998. Mouse hepatitis virus 3C-like protease cleaves a 22-kilodalton protein from the open reading frame 1a polyprotein in virus-infected cells and in vitro. J. Virol. **72:**2265-2271.

115. **Lu, Y., X. Lu, and M. R. Denison.** 1995. Identification and characterization of a serine-like proteinase of the murine coronavirus MHV-A59. J. Virol. **69:**3554-3559.

116. **Luytjes, W., P. J. Bredenbeek, A. F. Noten, M. C. Horzinek, and W. J. Spaan.** 1988. Sequence of mouse hepatitis virus A59 mRNA 2: indications for RNA recombination between coronaviruses and influenza C virus. Virology **166:**415-422.

117. **Luytjes, W., L. S. Sturman, P. J. Bredenbeek, J. Charite, B. A. van der Zeijst, M. C. Horzinek, and W. J. Spaan.** 1987. Primary structure of the glycoprotein E2 of coronavirus MHV-A59 and identification of the trypsin cleavage site. Virology **161:**479-487.

118. **Machamer, C. E., S. A. Mentone, J. K. Rose, and M. G. Farquhar.** 1990. The E1 glycoprotein of an avian coronavirus is targeted to the cis Golgi complex. Proc. Natl. Acad. Sci. USA **87:**6944-6948.

119. **Macnaughton, M. R., and H. A. Davies.** 1980. Two particle types of avian infectious bronchitis virus. J. Gen. Virol. **47:**365-372.

120. **Maeda, J., A. Maeda, and S. Makino.** 1999. Release of coronavirus E protein in membrane vesicles from virus-infected cells and E protein-expressing cells. Virology **263:**265-272.

121. **Maeda, J., J. F. Repass, A. Maeda, and S. Makino.** 2001. Membrane topology of coronavirus E protein. Virology **281:**163-169.

122. **Mahy, B. W., S. Siddell, H. Wege, and V. ter Meulen.** 1983. RNA-dependent RNA polymerase activity in murine coronavirus-infected cells. J. Gen. Virol. **64 :**103-111.

123. **Makino, S., J. G. Keck, S. A. Stohlman, and M. M. Lai.** 1986. High-frequency RNA recombination of murine coronaviruses. J. Virol. **57:**729-737.

124. **Makino, S., K. Yokomori, and M. M. Lai.** 1990. Analysis of efficiently packaged defective interfering RNAs of murine coronavirus: localization of a possible RNA-packaging signal. J. Virol. **64:**6045-6053.

125. **Masters, P. S.** 1992. Localization of an RNA-binding domain in the nucleocapsid protein of the coronavirus mouse hepatitis virus. Arch. Virol. **125:**141-160.

126. **Mcintosh, K.** 1974. Coronaviruses: a comparative review. current topics in microbiology and immunology **63:**85-129.

127. **Muriaux, D., J. Mirro, D. Harvin, and A. Rein.** 2001. RNA is a structural element in retrovirus particles. Proc. Natl. Acad. Sci. USA **98:**5246-5251.

128. **Narayanan, K., C. J. Chen, J. Maeda, and S. Makino.** 2003. Nucleocapsid-independent specific viral RNA packaging via viral envelope protein and viral RNA signal. J. Virol. **77:**2922-2927.

129. **Narayanan, K., and S. Makino.** 2001. Cooperation of an RNA packaging signal and a viral envelope protein in coronavirus RNA packaging. J. Virol. **75:**9059-9067.

130. **Nelson, G. W., and S. A. Stohlman.** 1993. Localization of the RNA-binding domain of mouse hepatitis virus nucleocapsid protein. J. Gen. Virol. **74 :**1975-1979.

131. **Neumann, G., and Y. Kawaoka.** 2002. Generation of influenza A virus from cloned cDNAs--historical perspective and outlook for the new millennium. Rev. Med. Virol. **12:**13-30.

132. **Neumann, G., and Y. Kawaoka.** 2002. Synthesis of influenza virus: new impetus from an old enzyme, RNA polymerase I. Virus Res. **82:**153-158.

133. **Ng, L. F., and D. X. Liu.** 2002. Membrane association and dimerization of a cysteine-rich, 16-kilodalton polypeptide released from the C-terminal region of the coronavirus infectious bronchitis virus 1a polyprotein. J. Virol. **76:**6257-6267.

134. **Niemann, H., B. Boschek, D. Evans, M. Rosing, T. Tamura, and H. D. Klenk.** 1982. Post-translational glycosylation of coronavirus glycoprotein E1: inhibition by monensin. EMBO J. **1:**1499-1504.

135. **Niemann, H., and H. D. Klenk.** 1981. Coronavirus glycoprotein E1, a new type of viral glycoprotein. J. Mol. Biol. **153:**993-1010.

136. **Oleszak, E. L., S. Perlman, and J. L. Leibowitz.** 1992. MHV S peplomer protein expressed by a recombinant vaccinia virus vector exhibits IgG Fc-receptor activity. Virology **186:**122-132.

137. **Opstelten, D. J., M. J. Raamsman, K. Wolfs, M. C. Horzinek, and P. J. Rottier.** 1995. Envelope glycoprotein interactions in coronavirus assembly. J. Cell. Biol. **131:**339-349.

138. **Patterson, S., and R. W. Bingham.** 1976. Electron microscope observations on the entry of avian infectious bronchitis virus into susceptible cells. Arch. Virol. **52:**191-200.

139. **Pekosz, A., B. He, and R. A. Lamb.** 1999. Reverse genetics of negative-strand RNA viruses: closing the circle. Proc. Natl. Acad. Sci. USA **96:**8804-8806.

140. **Penzes, Z., K. Tibbles, K. Shaw, P. Britton, T. D. Brown, and D. Cavanagh.** 1994. Characterization of a replicating and packaged defective RNA of avian coronavirus infectious bronchitis virus. Virology **203:**286-293.

141. **Rice, C. M., R. Levis, J. H. Strauss, and H. V. Huang.** 1987. Production of infectious RNA transcripts from Sindbis virus cDNA clones: mapping of lethal mutations, rescue of a temperature-sensitive marker, and in vitro mutagenesis to generate defined mutants. J. Virol. **61:**3809-3819.

142. **Risco, C., I. M. Anton, L. Enjuanes, and J. L. Carrascosa.** 1996. The transmissible gastroenteritis coronavirus contains a spherical core shell consisting of M and N proteins. J. Virol. **70:**4773-4777.

143. **Risco, C., M. Muntion, L. Enjuanes, and J. L. Carrascosa.** 1998. Two types of virus-related particles are found during transmissible gastroenteritis virus morphogenesis. J. Virol. **72:**4022-4031.

144. **Robbins, S. G., M. F. Frana, J. J. McGowan, J. F. Boyle, and K. V. Holmes.** 1986. RNA-binding proteins of coronavirus MHV: detection of monomeric and

multimeric N protein with an RNA overlay-protein blot assay. Virology **150:**402-410.

145. **Rossen, J. W., C. P. Bekker, G. J. Strous, M. C. Horzinek, G. S. Dveksler, K. V. Holmes, and P. J. Rottier.** 1996. A murine and a porcine coronavirus are released from opposite surfaces of the same epithelial cells. Virology **224:**345-351.

146. **Rossen, J. W., C. P. Bekker, W. F. Voorhout, G. J. Strous, A. van der Ende, and P. J. Rottier.** 1994. Entry and release of transmissible gastroenteritis coronavirus are restricted to apical surfaces of polarized epithelial cells. J. Virol. **68:**7966-7973.

147. **Rossen, J. W., G. J. Strous, M. C. Horzinek, and P. J. Rottier.** 1997. Mouse hepatitis virus strain A59 is released from opposite sides of different epithelial cell types. J. Gen. Virol. **78 :**61-69.

148. **Rottier, P., J. Armstrong, and D. I. Meyer.** 1985. Signal recognition particle-dependent insertion of coronavirus E1, an intracellular membrane glycoprotein. J. Biol. Chem. **260:**4648-4652.

149. **Rottier, P. J., and J. K. Rose.** 1987. Coronavirus E1 glycoprotein expressed from cloned cDNA localizes in the Golgi region. J. Virol. **61:**2042-2045.

150. **Rottier, P. J., W. J. Spaan, M. C. Horzinek, and B. A. van der Zeijst.** 1981. Translation of three mouse hepatitis virus strain A59 subgenomic RNAs in Xenopus laevis oocytes. J. Virol. **38:**20-26.

151. **Rottier, P. J., G. W. Welling, S. Welling-Wester, H. G. Niesters, J. A. Lenstra, and B. A. Van der Zeijst.** 1986. Predicted membrane topology of the coronavirus protein E1. Biochemistry **25:**1335-1339.

152. **Rottier, P. J. M.** 1995. *The coronavirus*. Plenum Press, New York.

153. **Sambrook, J., E.F. Fritsch, and T. Maniatis.** 1989. *Molecular Cloning: a Laboratory Manual*, 2nd ed. Cold Spring Harbor Laboratory Press, Plainview, NY.

154. **Sawicki, S. G., and D. L. Sawicki.** 1986. Coronavirus minus-strand RNA synthesis and effect of cycloheximide on coronavirus RNA synthesis. J. Virol. **57:**328-334.

155. **Sawicki, S. G., and D. L. Sawicki.** 1990. Coronavirus transcription: subgenomic mouse hepatitis virus replicative intermediates function in RNA synthesis. J. Virol. **64:**1050-1056.

156. **Sawicki, S. G., and D. L. Sawicki.** 1998. A new model for coronavirus transcription. Adv. Exp. Med. Biol. **440:**215-219.

157. **Schaad, M. C., and R. S. Baric.** 1994. Genetics of mouse hepatitis virus transcription: evidence that subgenomic negative strands are functional templates. J. Virol. **68:**8169-8179.

158. **Schalk, A. F., and M.C. Hawn.** 1931. An apparently new respiratory disease of baby chicks. J. Am. Vet. Med. Assoc. **78:**413-422.

159. **Schiller, J. J., A. Kanjanahaluethai, and S. C. Baker.** 1998. Processing of the coronavirus MHV-JHM polymerase polyprotein: identification of precursors and proteolytic products spanning 400 kilodaltons of ORF1a. Virology **242:**288-302.

160. **Schlesinger, S. S. a. M. J.** 2001. Togaviridae: The viruses and their replication, p. 895-916. *In* A. P. M. H. Bernard N. Field (ed.), Fields-Virology, vol. 1. Lippincott Williams and Wilkins Publisher, Philadelphia.

161. **Schochetman, G., R. H. Stevens, and R. W. Simpson.** 1977. Presence of infectious polyadenylated RNA in coronavirus avian bronchitis virus. Virology **77:**772-782.

162. **Sethna, P. B., M. A. Hofmann, and D. A. Brian.** 1991. Minus-strand copies of replicating coronavirus mRNAs contain antileaders. J. Viro.l **65:**320-325.

163. **Shen, S., Z. L. Wen, and D. X. Liu.** 2003. Emergence of a coronavirus infectious bronchitis virus mutant with a truncated 3b gene: functional characterization of the 3b protein in pathogenesis and replication. Virology **311:**16-27.

164. **Shi, S. T., J. J. Schiller, A. Kanjanahaluethai, S. C. Baker, J. W. Oh, and M. M. Lai.** 1999. Colocalization and membrane association of murine hepatitis virus gene 1 products and De novo-synthesized viral RNA in infected cells. J. Virol. **73:**5957-5969.

165. **Siddell, S., H. Wege, and V. Ter Meulen.** 1983. The biology of coronaviruses. J. Gen. Virol. **64 :**761-776.

166. **Sims, A. C., J. Ostermann, and M. R. Denison.** 2000. Mouse hepatitis virus replicase proteins associate with two distinct populations of intracellular membranes. J. Virol. **74:**5647-5654.

167. **Snijder, E. J., P. J. Bredenbeek, J. C. Dobbe, V. Thiel, J. Ziebuhr, L. L. Poon, Y. Guan, M. Rozanov, W. J. Spaan, and A. E. Gorbalenya.** 2003. Unique and conserved features of genome and proteome of SARS-coronavirus, an early split-off from the coronavirus group 2 lineage. J. Mol. Biol. **331:**991-1004.

168. **Snijder, E. J., and M. C. Horzinek.** 1993. Toroviruses: replication, evolution and comparison with other members of the coronavirus-like superfamily. J. Gen. Virol. **74 (Pt 11):**2305-2316.

169. **Sola, I., S. Alonso, S. Zuniga, M. Balasch, J. Plana-Duran, and L. Enjuanes.** 2003. Engineering the transmissible gastroenteritis virus genome as an expression vector inducing lactogenic immunity. J. Virol. **77:**4357-4369.

170. **Spaan, W., D. Cavanagh, and M. C. Horzinek.** 1988. Coronaviruses: structure and genome expression. J. Gen. Virol. **69 (Pt 12):**2939-2952.

171. **Spaan, W. J., P. J. Rottier, M. C. Horzinek, and B. A. van der Zeijst.** 1982. Sequence relationships between the genome and the intracellular RNA species 1, 3, 6, and 7 of mouse hepatitis virus strain A59. J. Virol. **42:**432-439.

172. **Stern, D. F., and S. I. Kennedy.** 1980. Coronavirus multiplication strategy. I. Identification and characterization of virus-specified RNA. J. Virol. **34:**665-674.

173. **Stern, D. F., and S. I. Kennedy.** 1980. Coronavirus multiplication strategy. II. Mapping the avian infectious bronchitis virus intracellular RNA species to the genome. J. Virol. **36:**440-449.

174. **Stern, D. F., and B. M. Sefton.** 1982. Synthesis of coronavirus mRNAs: kinetics of inactivation of infectious bronchitis virus RNA synthesis by UV light. J. Virol. **42:**755-759.

175. **Stirrups, K., K. Shaw, S. Evans, K. Dalton, R. Casais, D. Cavanagh, and P. Britton.** 2000. Expression of reporter genes from the defective RNA CD-61 of the coronavirus infectious bronchitis virus. J. Gen. Virol. **81:**1687-1698.

176. **Stohlman, S. A., R. S. Baric, G. N. Nelson, L. H. Soe, L. M. Welter, and R. J. Deans.** 1988. Specific interaction between coronavirus leader RNA and nucleocapsid protein. J. Virol. **62:**4288-4295.

177. **Strauss, J. H., and E. G. Strauss.** 1994. The alphaviruses: gene expression, replication, and evolution. Microbiol. Rev. **58:**491-562.

178. **Sturman, L. S., and K. V. Holmes.** 1977. Characterization of coronavirus II. Glycoproteins of the viral envelope: tryptic peptide analysis. Virology **77:**650-60.

179. **Sturman, L. S., K. V. Holmes, and J. Behnke.** 1980. Isolation of coronavirus envelope glycoproteins and interaction with the viral nucleocapsid. J. Virol. **33:**449-462.

180. **Sturman, L. S., C. S. Ricard, and K. V. Holmes.** 1990. Conformational change of the coronavirus peplomer glycoprotein at pH 8.0 and 37 degrees C correlates with virus aggregation and virus-induced cell fusion. J. Virol. **64:**3042-3050.

181. **Sturman, L. S., C. S. Ricard, and K. V. Holmes.** 1985. Proteolytic cleavage of the E2 glycoprotein of murine coronavirus: activation of cell-fusing activity of virions by trypsin and separation of two different 90K cleavage fragments. J. Virol. **56:**904-911.

182. **Swift, A. M., and C. E. Machamer.** 1991. A Golgi retention signal in a membrane-spanning domain of coronavirus E1 protein. J. Cell. Biol. **115:**19-30.

183. **Taguchi, F., H. Kubo, H. Suzuki, and Y. K. Yamada.** 1995. Localization of neutralizing epitopes and receptor-binding site in murine coronavirus spike protein. Adv. Exp. Med. Biol. **380:**359-365.

184. **Tahara, S. M., T. A. Dietlin, C. C. Bergmann, G. W. Nelson, S. Kyuwa, R. P. Anthony, and S. A. Stohlman.** 1994. Coronavirus translational regulation: leader affects mRNA efficiency. Virology **202:**621-630.

185. **Thiel, V., J. Herold, B. Schelle, and S. G. Siddell.** 2001. Infectious RNA transcribed in vitro from a cDNA copy of the human coronavirus genome cloned in vaccinia virus. J. Gen. Virol. **82:**1273-1281.

186. **Thiel, V., K. A. Ivanov, A. Putics, T. Hertzig, B. Schelle, S. Bayer, B. Weissbrich, E. J. Snijder, H. Rabenau, H. W. Doerr, A. E. Gorbalenya, and J. Ziebuhr.** 2003. Mechanisms and enzymes involved in SARS coronavirus genome expression. J. Gen. Virol. **84:**2305-2315.

187. **Thiel, V., N. Karl, B. Schelle, P. Disterer, I. Klagge, and S. G. Siddell.** 2003. Multigene RNA vector based on coronavirus transcription. J. Virol. **77:**9790-9798.

188. **Thiel, V., and S. G. Siddell.** 1994. Internal ribosome entry in the coding region of murine hepatitis virus mRNA 5. J. Gen.Virol. **75 :**3041-3046.

189. **Tooze, J., S. Tooze, and G. Warren.** 1984. Replication of coronavirus MHV-A59 in sac- cells: determination of the first site of budding of progeny virions. Eur. J. Cell Biol. **33:**281-293.

190. **Tooze, J., S. A. Tooze, and S. D. Fuller.** 1987. Sorting of progeny coronavirus from condensed secretory proteins at the exit from the trans-Golgi network of AtT20 cells. J. Cell Biol. **105:**1215-1226.

191. **Tooze, S. A., J. Tooze, and G. Warren.** 1988. Site of addition of N-acetyl-galactosamine to the E1 glycoprotein of mouse hepatitis virus-A59. J. Cell Biol. **106:**1475-1487.

192. **van der Meer, Y., E. J. Snijder, J. C. Dobbe, S. Schleich, M. R. Denison, W. J. Spaan, and J. K. Locker.** 1999. Localization of mouse hepatitis virus nonstructural proteins and RNA synthesis indicates a role for late endosomes in viral replication. J. Virol. **73:**7641-7657.

193. **Vennema, H., G. J. Godeke, J. W. Rossen, W. F. Voorhout, M. C. Horzinek, D. J. Opstelten, and P. J. Rottier.** 1996. Nucleocapsid-independent assembly of coronavirus-like particles by co-expression of viral envelope protein genes. EMBO J. **15:**2020-2028.

194. **Wang, G., C. Deering, M. Macke, J. Shao, R. Burns, D. M. Blau, K. V. Holmes, B. L. Davidson, S. Perlman, and P. B. McCray, Jr.** 2000. Human coronavirus 229E infects polarized airway epithelia from the apical surface. J. Virol. **74:**9234-9239.

195. **Wang, L., Y. Xu, and E. W. Collisson.** 1997. Experimental confirmation of recombination upstream of the S1 hypervariable region of infectious bronchitis virus. Virus Res. **49:**139-145.

196. **Wege, H., A. Muller, and V. ter Meulen.** 1978. Genomic RNA of the murine coronavirus JHM. J. Gen. Virol. **41:**217-227.

197. **Wege, H., S. Siddell, and V. ter Meulen.** 1982. The biology and pathogenesis of coronaviruses. Curr. Top. Microbiol. Immunol. **99:**165-200.

198. **Wilbur, S. M., G. W. Nelson, M. M. Lai, M. McMillan, and S. A. Stohlman.** 1986. Phosphorylation of the mouse hepatitis virus nucleocapsid protein. Biochem. Biophys. Res. Commun. **141:**7-12.

199. **Williams, A. K., L. Wang, L. W. Sneed, and E. W. Collisson.** 1992. Comparative analyses of the nucleocapsid genes of several strains of infectious bronchitis virus and other coronaviruses. Virus Res. **25:**213-222.

200. **Williams, R. K., G. S. Jiang, and K. V. Holmes.** 1991. Receptor for mouse hepatitis virus is a member of the carcinoembryonic antigen family of glycoproteins. Proc. Natl. Acad. Sci. USA **88:**5533-5536.

201. **Yount, B., K. M. Curtis, and R. S. Baric.** 2000. Strategy for systematic assembly of large RNA and DNA genomes: transmissible gastroenteritis virus model. J. Virol. **74:**10600-10611.

202. **Yount, B., M. R. Denison, S. R. Weiss, and R. S. Baric.** 2002. Systematic assembly of a full-length infectious cDNA of mouse hepatitis virus strain A59. J. Virol. **76:**11065-10678.

203. **Yu, X., W. Bi, S. R. Weiss, and J. L. Leibowitz.** 1994. Mouse hepatitis virus gene 5b protein is a new virion envelope protein. Virology **202:**1018-1023.

204. **Zhao, X., K. Shaw, and D. Cavanagh.** 1993. Presence of subgenomic mRNAs in virions of coronavirus IBV. Virology **196:**172-178.

205. **Zhou, M., A. K. Williams, S. I. Chung, L. Wang, and E. W. Collisson.** 1996. The infectious bronchitis virus nucleocapsid protein binds RNA sequences in the 3' terminus of the genome. Virology **217:**191-199.

206. **Ziebuhr, J., J. Herold, and S. G. Siddell.** 1995. Characterization of a human coronavirus (strain 229E) 3C-like proteinase activity. J. Virol. **69:**4331-4338.

207. **Ziebuhr, J., E. J. Snijder, and A. E. Gorbalenya.** 2000. Virus-encoded proteinases and proteolytic processing in the Nidovirales. J. Gen. Virol. **81:**853-879.

208. **Ziegler, A. F., B. S. Ladman, P. A. Dunn, A. Schneider, S. Davison, P. G. Miller, H. Lu, D. Weinstock, M. Salem, R. J. Eckroade, and J. Gelb, Jr.** 2002. Nephropathogenic infectious bronchitis in Pennsylvania chickens 1997-2000. Avian Dis. **46:**847-858.

VITA

SOONJEON YOUN

Degree	Institution	Date	Major
Ph.D.	Texas A&M University College Station, Texas		Veterinary Microbiology
D.V.M.	Konkuk University Seoul, Korea	December, 1996	
M.S.	Konkuk University Seoul, Korea	December, 1996	Public Health
B.S.	Konkuk University Seoul, Korea	December, 1994	Veterinary Medicine

Professional Experience

1998-present	Ph.D. graduate student in Veterinary Pathobiology, Texas A&M University
1997-1998	Ph.D. graduate student in Veterinary Medical School, Konkuk University Lecturer, Samyook Univeristy
1996-1997	Veterinarian, Daehan Inti. Inc.
1995-1996	Research Associate, National Veterinary Research & Quarantine Service (NVRQS)
1994-1995	Research Associate, Korean Food and Drug Administration (KFDA)